ISAS - INTERNATIONAL SCHOOL FOR ADVANCED STUDIES

A THESIS SUBMITTED FOR THE DEGREE OF

"DOCTOR PHILOSOPHIAE"

A STUDY OF

THE COSMOLOGICAL QUARK-HADRON TRANSITION

Candidate:

Ornella Pantano

Supervisors:

Prof. S.A. Bonometto

Prof. J.C. Miller

Academic Year 1986/87

TRIESTE

SISSA - SCUOLA INTERNAZIONALE SUPERIORE STUDI AVANZATI

TRIESTE

Strada Costiera 11

A THESIS SUBMITTED FOR THE DEGREE OF

"DOCTOR PHILOSOPHIAE"

A STUDY OF

THE COSMOLOGICAL QUARK-HADRON TRANSITION

Candidate:

Ornella Pantano

Supervisors:

Prof. S.A. Bonometto

Prof. J.C. Miller

Academic Year 1986/87

CONTENTS

PREFACE

In this thesis, several aspects of the cosmological quark-hadron transition are studied in detail. A general introduction discusses the importance of phase transitions in the early universe with particular emphasis on the quark-hadron transition and its possible cosmological consequences.

In the second chapter we first give a brief review of present knowledge of the quark-hadron transition on the basis of lattice results from quantum chromodynamics. These are then used for a general discussion of the possible large scale cosmological effects of the confinement process. In the following discussion it is assumed that the transition is of first order, as suggested by many lattice computations, and that bubbles of the hadronic phase are nucleated in a supercooled quark medium. Lattice results, however, are not accurate enough to give a reliable equation of state for use in hydrodynamical calculations of bubble growth and so we also discuss phenomenological models which are more convenient.

The general relativistic hydrodynamical equations governing the bubble growth are presented in detail in Chapter III. Particular attention is devoted to the characteristic formulation of the hydrodynamical equations and to a correct specification of the junction conditions at the phase interface. For the latter, Israel's method for singular hypersurfaces is used to give a proper treatment of surface effects.

In Chapter IV a short review of classical bubble dynamics is

presented, followed by a description of the characteristic structure of detonation and deflagration solutions. For the deflagration case we point out that it is necessary to specify an extra condition giving the rate of the transition as determined by elementary processes. These considerations are then used for showing some important features of a plane deflagration front.

Chapter V is devoted to discussing the numerical integration of the coupled system of hydrodynamical equations, junction conditions and the transition rate equation which together govern the dynamics of bubble growth. Some results of the computations are also described.

Some possible effects of long range conduction mechanisms are analysed in Chapter VI. In particular, we discuss the ratio between the hydrodynamical and neutrino fluxes and its relevance for possible baryon concentration. There is then an analysis of how the transition would have proceeded on a large scale if the neutrino flux were the dominant mechanism for transfering energy from the quark phase to the hadron phase.

Finally in the Conclusion we summarize some main points and discuss some of their wider implications.

ACKNOWLEDGEMENTS

I would like to thank Prof. Silvio Bonometto for introducing me to the cosmological aspects of phase transitions and for his continuing interest and advice.

I am also very grateful to Prof. John Miller for guiding me in the study of relativistic hydrodynamics and for his continuous encouragement in these difficult years.

Conversations with my collegues have made important contributions to the work described in this thesis. I would like to thank, in particular, Vincenzo Antonuccio, Marisa Bonini, Mark Dubal, Antonio Lanza, Sabino Matarrese and Osvaldo Moreschi.

I would also like to thank Prof. Dennis Sciama both for his help and advice and also for his rôle in creating pleasant and stimulating conditions in which to work at SISSA.

Financial support from SISSA during these years is gratefully acknowledged.

CHAPTER I

INTRODUCTION

In the last decade the subject of phase transitions in the early universe has attracted a lot of interest which has mainly been related to the new theories developed in trying to unify known particle interactions. It is characteristic of these theories that symmetry breaking, which eventually produces the observed particle interactions, usually occurs at energies which are unattainable in the laboratory. On the other hand, the standard model of cosmology suggests that the corresponding temperatures were reached shortly after the big bang. The early universe appears to be the only possible place where most of the higher order symmetries could ever have been manifest and where the associated symmetry breakings could have occurred.

Of particular interest is the possibility that one or more of these symmetry changes was a first order phase transition. Such transitions normally proceed by the formation and growth of bubbles of the new phase (which corresponds to the minimum of free energy for the system). The inhomogeneities connected with the coexistence of the two phases may have produced perturbations or structures which could survive after the completion of the transition and affect the subsequent evolution of the universe (Brandenberger (1985), Bonometto and Masiero (1986)).

A first order phase transition is characterized by the presence of a finite difference in energy density between the two

phases, the emission or absorption of latent heat as matter is converted and the existence of associated metastable superheated or supercooled states. Qualitatively, first order cosmological phase transitions concerning symmetry breaking would be closely similar to boiling in a superheated fluid (Gunton et al. (1983)). The state containing false vacuum corresponds to the superheated fluid phase and that with true vacuum to the vapour phase. Boiling bubble nucleation can be initiated by thermal fluctuations, acoustic disturbances, the influence of impurities or the effect of imperfections on the surface of a containing vessel (Hetsroni (1982). Of these, the first three may be relevant for cosmological transitions (Linde (1977), Guth and Weinberg (1981), Hogan (1983)). For vacuum phase transitions at zero temperature, bubbles of the true vacuum state can be nucleated by quantum fluctuations (Voloshin et al. (1975), Coleman (1977)). In the thermal nucleation picture, bubbles of the new phase are continually being formed within the old metastable phase but the only ones which survive are those large enough so that the energy deficit of material inside the bubble can compensate for the work done in creating the phase separation surface (Landau and Lifshitz (1959), Lifshitz and Pitaevskii (1981)).

For clarity, the dynamics of a first order phase transition may be divided into several stages. First we are concerned with bubble nucleation mechanisms, which determine the degree of supercooling undergone by the system, and next, with the growth of an isolated bubble in a metastable medium. Coleman (1977) has shown that at zero temperature the acceleration of the bubble wall would be very rapid and the velocity would quickly approach the speed of light. At early times, however, the universe was not at

zero temperature and, in fact, the bubble surface would expand as either a deflagration or a detonation front depending on the degree of supercooling (Steinhardt (1982), Berezin et al. (1983a,b), Gyulassy et al. (1984)). The next stage concerns bubble collisions and coalescence and here it is important to determine how the energy stored in the bubble wall is released and how quickly it is thermalized (Berezin et al. (1983c), Hawking et al. (1982)). Eventually the metastable phase is present only in disconnected regions which then shrink until probably only the new stable phase remains. The way in which the transition proceeds through these stages and even whether or not it will ever be completed, depends on the particular phase change and on the conditions in the universe at the corresponding temperature (Guth and Weinberg (1981), Witten (1984)).

The last of the possible phase transitions which have been proposed for the very early universe (at least, within the standard "hot" model) concerns the confinement of quarks and gluons whithin colour singlet states (hadrons). According to the present theory of strong interactions (quantum chromodynamics - QCD), hadrons are composed of more fundamental particles, quarks, which are characterized by a new quantum number called colour. Quarks interact through a colour field whose quanta, gluons, themselves carry colour charges. An important feature of the interaction is that the potential rises linearly with distance for separations greater than about one fermi and, under normal circumstances this gives rise to permanent confinement of quarks within hadrons since an infinite amount of energy would be required to isolated a colour charge completely. However, at short distances the interaction becomes weaker, vanishing

asymptotically as the separation between particles tends to zero. For matter compressed to sufficiently high density, individual hadrons would lose their identity and a quark-gluon plasma would be formed (see Müller (1985)).

In the early universe, if we accept the standard model, the conditions for the existence of a quark-gluon plasma were satisfied before about ten microseconds after the big bang. As the universe continued to expand and cool, strongly interacting matter would then have changed to the hadronic state. The quark-hadron transition is the only one of the early universe transitions which is likely to be recreated under laboratory conditions within the forseeable future (see Van Hove (1986)). It marks a watershed in the history of the universe since it is the beginning of the present era in which matter appears in states which can be studied now in laboratory experiments or in processes which can occur naturally.

Whether this transition is continuous or a first order phase transition is not yet completely clear. QCD lattice calculations (Cleymans et al. (1986a), Svetiski (1986), etc.) strongly suggest the possibility of having a first order phase transition at least for certain ranges of quark masses but, because of the difficulties of the calculation, a definitive answer is not yet available.

In the cosmological context, different consequences can arise depending on the order of the transition. In the case of a continuous transition the most important cosmological effect is a temporary delay in the general cosmic cooling (Bonometto and Pantano (1984), Bonometto and Sakellariadou (1984)).

If, on the other hand, the confinement occurred by a first

order phase transition various sorts of inhomogeneity may have been produced as well. These could be created in many ways. DeGrand and Kajantie (1984) considered the possibility that shocks were formed during the transition and they found that turbulent structures produced as a result of shock collisions might survive diffusive dissipation until the end of the transition if the initial supercooling was larger than 6%. Kajantie and Kurki-Suonio (1986) also considered shock collisions and possible consequent reheating of the metastable medium. Another possibility is that a dark matter component may have been produced in the form of black holes or other condensed objects (probably with planetary masses). Either these objects or shock waves arising from the transition could have been starting points for processes subsequently leading to galaxy formation (Crawford and Schramm (1982), Carr and Silk (1983)).

Witten (1984) showed that in the case of a phase transition occurring without any large departure from equilibrium, baryon number concentration might occur. Baryon number is carried by almost massless particles in the high temperature phase but by massive particles in the low temperature phase and therefore, in conditions of chemical equilibrium, one expects a higher baryon number density in the quark phase. In the final part of the transition, up to 99% of the total baryon number may have been contained within the shrinking quark regions. If as the universe continued to expand, these regions lost energy primarily by processes, such as neutrino radiation, which do not deplete their baryon number, then it is possible that they might have formed dense "nuggets" of strange quark matter (matter with equal number of up, down and strange quarks) which could have survived without

being converted into the hadron phase. Witten predicted that the masses of the nuggets formed could be in the range 10^9-10^{18}g (baryon number A of 10^{33}-10^{42}) and suggested that they might be a baryonic dark matter component. However Alcock and Farhi (1986) found that any nuggets with $A \leq 10^{52}$ would evaporate completely before nucleosynthesis, leaving concentrated baryon clouds. A more recent analysis by Madsen et al. (1986) reduced the limit to $A \leq 10^{46}$ but this is still much larger than the maximum value suggested by Witten.

Even if quark nuggets are ruled out, it is reasonable to expect some baryon concentration around the points where the last remnants of the quark phase finally evaporated. Bound objects with planetary mass might have been formed out of these concentrantions (Iso et al.(1986)) and nucleosynthesis could also have been affected if diffusion was not able to homogenise the baryon medium before then (Bonometto et al.(1985), Applegate and Hogan (1985)).

The standard model of primordial nucleosynthesis, which assumes a homogeneous medium, is in good agreement with the observed abundances of light elements if $0.01 \leq \Omega_b \leq 0.2$, where $\Omega_b=\rho_b/\rho_c$ is the ratio between the present baryon density ρ_b and the critical density necessary for closing the universe (Boesgaard and Steigman (1985)). This result seems to exclude the possibility that a sufficient amount of dark matter to provide the closure density could be in baryonic form. Observations seem to show a rather high degree of homogeneity in light element abundances. However, these observations refer to regions which at the epoch of nucleosynthesis would have contained many horizon volumes and even more nucleon diffusion volumes. Therefore, they

do not exclude, a priori the possibility that baryon inhomogeneities were present at the nucleation epoch and that nucleosynthesis products were homogenized later on the scale which we now observe. Sale and Mathews (1986) showed that computed light element aboundances still agree with observations for $\Omega_b \simeq 0.4$ if one allows isothermal baryon fluctuations at nuclesynthesis. By making the additional assumption that regions of high baryon density are then included in cold dark matter (planetary-type objects, brown dwarfs or black holes), the constraints from nucleosynthesis can be satisfied for Ω_b as large as 1.

Alcock et al. (1987) and Applegate et al. (1987) have independently calculated primordial nucleosynthesis taking into account possible consequences of the quark-hadron transition. They considered baryon fluctuations and also inhomogeneities in the neutron-proton ratio arising because of the different diffusion of neutrons and protons through the radiative plasma. Both analyses suggest that baryon fluctuations might make the observed light element abundances consistent with a larger value of Ω_b. For $\Omega_b \sim 1$, however, they found an overproduction of ^{7}Li compared with the standard model. Applegate et al. also noticed a slight increase in ^{4}He and a decrease in deuterium. The studies disagree on the estimates of heavy element aboundances with Applegate et al. finding values higher than the observed ones, while Alcock et al. found values in agreement with the results of the standard model. These discrepances are probably due to the approximations used and might be eliminated when an improved knowledge of the initial fluctuations allows more detailed calculations.

In view of the important possible consequences for structure

formation and nucleosynthesis, a full-scale hydrodynamical calculation needs to be made for the first order case, to investigate how the transition proceeds under various assumptions about the basic input parameters. This is one of the main objectives of the present work. The initial supercooling will have to be left as a free parameter and suitable phenomenogical models used for describing the two phases until the lattice calculations are able to provide a more complete treatment of the transition.

Throughout the thesis we use units for which $c = \hbar = k = 1$.

CHAPTER II

STRONGLY INTERACTING MATTER AT HIGH TEMPERATURE.

In recent years QCD has gained increasing acceptance as the fundamental theory of strong interactions (see Marciano and Pagels (1978)) and within this framework it is possible to explain the characteristics of hadrons revealed in experiments. High energy scattering of leptons on hadrons in the laboratory shows that hadrons are composite particles whose constituents, called in the first place partons, are point-like particles with spin 1/2 and with non-integer electric charge. Partons have been identified in QCD with quarks, particles introduced by Gell-Mann (1962) in an attempt to clarify the rich hadronic spectrum revealed by high energy experiments.

Today there is experimental evidence for the existence of five different flavours of quark called up (u), down (d), strange (s), charm (c) and bottom (b) and symmetry considerations suggest the existence of a sixth flavour called top (t). Some of the properties of quarks are summarized in Table 1. Quark masses cannot be measured directly since most of the hadron mass comes from the binding energy of quarks; the values written in Table 1 refer to the bare quark masses as calculated by current algebra

Table 1.

Flavour	up	down	strange	charm	bottom	top
Electric charge	+2/3	-1/3	-1/3	+2/3	-1/3	+2/3
Current mass	5MeV	10MeV	150MeV	1.5MeV	5MeV	40MeV

methods. The charges are expressed in units of the proton charge.

The existence of hadrons formed by three apparently identical quarks and the ratio between hadron production and muon pair production in e^+e^- collisions indicate that quarks must be characterized by a further internal quantum number and this is called colour. It is probably more correct to talk about "colour charge" since it plays a rôle similar to that of electric charge in quantum electrodynamics (QED). Like electric charge, colour charge is exactly conserved and acts as the source of a force field. However, there is a fundamental difference between the two kinds of charge which is that, whereas electric charge is a one-dimensional quantity, there are three different colour degrees of freedom. This implies a very different behaviour of the strong interaction as compared with the electromagnetic one in spite of their analogies.

In this chapter, after a brief introduction to the thermodynamical relations which we are going to use later, we give a general introduction to the main properties of QCD and review the results obtained by perturbative methods and by numerical calculations. Next an application of lattice QCD results in cosmology is presented. Finally, we proceed to a two phase description of strongly interacting matter with the presentation of phenomenological models suitable for use in the hydrodynamical treatment of a first order confinement transition. For the quark-gluon phase, we discuss the effect of perturbative corrections within the bag model. For the hadron phase, the thermodynamics of a system of extended hadrons is discussed in detail.

2.1 Thermodynamic relations

The thermodynamic functions of a system governed by a Hamiltonian $\hat{H}$ can be derived from the grand partition function defined as

$$Z = Tr\left[\exp\left\{-\beta\left(\hat{H}-\Sigma_i\mu_i\hat{N}_i\right)\right\}\right] \tag{2.1}$$

where $\beta=1/T$ is the reciprocal of the temperature and μ_i is the chemical potential conjugate to the conserved charge $\hat{N}_i$ (e.g. the total baryon number). From the grand partition function it is possible to calculate the expectation value of an observable $\hat{O}$ by the relation

$$\langle O\rangle = Z^{-1}\, Tr\left[\hat{O}\exp\left\{-\beta\left(\hat{H}-\Sigma_i\mu_i\hat{N}_i\right)\right\}\right] \tag{2.2}$$

From equation (2.2) it can immediately be seen that the mean value of the energy density e and the charge density n_i are given respectively by

$$e = \frac{\langle H\rangle}{V} = \frac{T^2}{V}\frac{\partial}{\partial T}(\ln Z) + \Sigma_i\mu_i n_i \tag{2.3}$$

$$n_i = \frac{\langle N_i\rangle}{V} = \frac{T}{V}\frac{\partial}{\partial\mu_i}(\ln Z) \tag{2.4}$$

A well-known result from statistical mechanics relates the grand partition function to the thermodynamical potential $\Omega(T,V,\mu_i)$ by

$$\Omega = -T\ln Z \tag{2.5}$$

We also have the thermodynamic relations

$$d\Omega = -SdT - pdV - \Sigma_i N_i d\mu_i \tag{2.6}$$

and

$$\Omega = E - TS - \Sigma_i N_i\mu_i = -pV \tag{2.7}$$

where E is the total energy of the system, S is the total entropy, V is the total volume and p is the pressure. Combining equations (2.6) and (2.7) with (2.5) we have

$$s = \frac{S}{V} = \frac{1}{V}\frac{\partial}{\partial T}(\ln Z) \tag{2.8}$$

$$p = \frac{T \ln Z}{V} \tag{2.9}$$

For $\mu_i=0$, the energy density can be expressed in terms of the pressure as (see equations (2.3) and (2.9))

$$e = T^2 \frac{\partial}{\partial T}\left(\frac{p}{T}\right) \tag{2.10}$$

2.2 Quantum chromodynamics

2.2.1 *The gauge field theory of strong interactions.*

QCD is constructed as a gauge field theory in which quarks are represented by a spinor matter field ψ_α^f with colour index α (α=1,2,3) which corresponds to the three possible colour states (f indicates the quark flavour). If we think of colour as forming a three dimensional abstract space, QCD is required to be invariant under local SU(3) transformations in this space. This invariance is obtained by introducing eight distinct gauge fields F_i^A (A=1,..,8), called gluon fields, whose quanta are massless vector bosons (gluons). These fields mediate the strong interaction between quarks but the gluons themselves are also coloured particles and so they self-interact. The Lagrangian density of QCD is given by

$$L = \Sigma_f \bar{\psi}_\alpha^f \left[\gamma^i \left(i\delta_{\alpha\beta}\partial_i + \frac{1}{2}g\tau^A_{\alpha\beta}F_{iA}\right) - m_f\delta_{\alpha\beta}\right]\psi_\beta^f - \frac{1}{4} G^A_{ij}G^{ij}_A \tag{2.11}$$

where g is the coupling constant, m_f is the quark mass and

$$G^A_{ij} = \partial_i F^A_j - \partial_j F^A_i + g\, f^A_{BC} F^B_i F^C_j \qquad (2.12)$$

τ^A are the eight generators of the SU(3) colour gauge group normalized so that $\tau^A \tau^B = 2\delta^{AB}$ and f_{ABC} are the structure constants of SU(3) defined by $[\tau^A, \tau^B] = 2if^{AB}_C \tau^C$. A term $(-\mu \Sigma_f \bar{\psi}_f \psi_f)$ must be added to (2.11) if the net baryon number is different from zero. The coupling constant g is dimensionless and hence the theory is invariant under scale transformations and only the ratios between physical quantities can be predicted.

In QCD hadrons are colour-neutral bound states of quarks and quark-antiquark pairs. The non-abelian character of the theory (the symmetry group is SU(3)) which leads to self-interaction of gauge bosons, produces a confining potential which, at large separation, is proportional to the distance between quarks (r). This prevents quarks appearing as isolated particles. On the other hand, perturbative expansions together with renormalization group techniques show that for $r \to 0$, the effective coupling constant tends to zero (asymptotic freedom) so that quarks and gluons then behave like non-interacting particles.

Once the Lagrangian is given, the analysis of the thermodynamic properties of QCD at finite temperature and density is, at least in principle, a well defined problem. The grand partition function is written in the path integral formulation as

$$Z = \int [\, d\bar{\psi}\,][\, d\psi\,][\, dF_i\,]\; e^{-S} \qquad (2.13)$$

where $[\ ]$ denotes the sum over all of the possible configurations of the system and S is the Euclidean QCD action

$$S = \int_0^\beta d\tau \int d^3x\; L_E(\bar{\psi}, \psi, F_i) \qquad (2.14)$$

where L_E is the Euclidean Lagrangian density obtained from (2.11) by making a Wick rotation of the time, $t \to i\tau$. If the fields satisfy the periodicity conditions

$$F_i(x,0) = F_i(x,\beta)$$

$$\psi(x,0) = -\psi(x,\beta) \qquad \bar{\psi}(x,0) = \bar{\psi}(x,\beta) \tag{2.15}$$

it follows that β is equal to the reciprocal of the temperature. All of the thermodynamical quantities can then be derived from equation (2.13) using the relations presented in Section 2.1. However, in practice the calculation of observables in QCD encounters two main obstacles. Perturbative calculations (i.e. power expansions of Z in terms of the coupling constant g) lead to the usual divergences of quantum field theory and therefore the theory has to be renormalized in order to obtain finite results. Moreover, it is not possible to study the behaviour of the system with perturbative methods over the whole range from confinement to asymptotic freedom because in the strong coupling region this would require the evaluation of the whole infinite series of terms of the perturbative expansion.

2.2.2 *Perturbative QCD at high temperature.*

Here the results obtained from perturbative QCD at high temperature are reviewed mainly with a view to their use in the equation of state for the quark-gluon plasma phase. We refer here to the results presented by Toimela (1985) who extended the previous calculations by Kalashnikov and Klimov (1979) and Kapusta (1979), including terms up to $O(g^4 \ln g)$ in the coupling constant. In the ultra-relativistic regime (m_f=0)the pressure is equal to

$$p = \left[\left(N^2-1+ 7N\ N_f/4\right)T^4 + 15N\ N_f\left(T^2\theta^2+\theta^2\right)\right]\ \pi^2/45$$

$$-\left(N^2-1\right)\ \left[\left(N+5N/4\right)T^4+ 9N_f\left(T^2\theta^2+\theta^2\right)\right]\ g/144$$

$$+\left(N^2-1\right)\ \left[\left(2N+N_f\right)T^2/6 + N_f\theta^2\right]^{3/2} g^3T/12\pi$$

$$+ N\left(N^2-1\right)\left[\left(2N+N_f\right)T^2/6 + N_f\theta^2\right]T^2g^4\ln g/(32\pi^2) \qquad (2.16)$$

where N_f denotes the number of quark flavours which are relativistic at the temperature under consideration, N is the dimension of the gauge symmetry group SU(N) and $\theta^2=\mu^2/(2\pi^2)$. Although in the early universe the net baryon number density was, in fact, different from zero we can nevertheless neglect its contribution to the equation of state in many cases. Specifying equation (2.16) for $\mu=0$, $N_f=2$, N=3 and introducing the running coupling costant $\alpha_s=g^2/(4\pi^2)$ we obtain

$$p = \pi^2T^4\left[\frac{37}{90} - \frac{11}{9}\left(\frac{\alpha_s}{\pi}\right) + \frac{128}{9\sqrt{3}}\left(\frac{\alpha_s}{\pi}\right)^{\frac{3}{2}} + 8\left(\frac{\alpha_s}{\pi}\right)^2\ln\left(\frac{\alpha_s}{\pi}\right) + O(\alpha_s^2)\right] \qquad (2.17)$$

From the renormalization group equations (Caswell (1974)) we have in the high temperature limit:

$$\frac{\alpha_s(T)}{\pi} = \frac{g^2(T)}{4\pi^2} = \frac{6}{(11N-2N_f)\ln(T/\Lambda_{QCD})} \qquad (2.18)$$

where Λ_{QCD} is a dimensional parameter which fixes the scale of QCD and whose value has to be determined independently by reference to some physical quantity such as, for example, the proton mass. Λ_{QCD} is estimated to be in the range 300-500 MeV (Müller (1985)). From equation (2.18), it is evident that as the temperature increases the effective coupling strength decreases, vanishing for

$T \to \infty$ (asymptotic freedom).

The energy density can be calculated from equation (2.17) using relation (2.10) giving

$$e = 3\pi^2 T^4\left[\frac{37}{90} - \frac{11}{9}\left(\frac{\alpha_s}{\pi}\right) + \frac{128}{9\sqrt{3}}\left(\frac{\alpha_s}{\pi}\right)^{\frac{3}{2}} + 8\left(\frac{\alpha_s}{\pi}\right)^2 \ln\left(\frac{\alpha_s}{\pi}\right)\right] +$$

$$\pi^2 T^4\left\{\frac{29}{6}\left(\frac{\alpha_s}{\pi}\right)^2\left[\frac{11}{9} - \frac{64}{3\sqrt{3}}\left(\frac{\alpha_s}{\pi}\right)^{\frac{1}{2}} - 16\left(\frac{\alpha_s}{\pi}\right)\ln\left(\frac{\alpha_s}{\pi}\right)\right]\right\} + O(\alpha_s^3) \qquad (2.19)$$

From equations (2.17) and (2.19) it is easy to obtain the sound velocity in the quark-gluon plasma

$$v_s^2 = \left.\frac{\partial p}{\partial e}\right|_s = \frac{\alpha+\beta}{3\alpha+7\beta} \qquad (2.20)$$

with

$$\alpha = \frac{37}{90} - \left(\frac{\alpha_s}{\pi}\right)\left[\frac{11}{9} - \frac{128}{9\sqrt{3}}\left(\frac{\alpha_s}{\pi}\right)^{\frac{1}{2}} - 8\left(\frac{\alpha_s}{\pi}\right)\ln\left(\frac{\alpha_s}{\pi}\right)\right]$$

$$\beta = \frac{29}{6}\left(\frac{\alpha_s}{\pi}\right)^2\left[\frac{11}{9} - \frac{64}{3\sqrt{3}}\left(\frac{\alpha_s}{\pi}\right)^{\frac{1}{2}} - 16\left(\frac{\alpha_s}{\pi}\right)\ln\left(\frac{\alpha_s}{\pi}\right)\right]$$

Neglecting terms of order higher than $O(\alpha^3)$ we obtain

$$v_s^2 = \frac{\alpha+\beta}{3\alpha}\left[1 - \frac{7\beta}{3\alpha}\right] \simeq \frac{1}{3} - \frac{4\beta}{9\alpha} \qquad (2.21)$$

and expressing v_s^2 in terms of the sound speed in a gas of ultrarelativistic free particles ($v_s^2=1/3$), we finally have

$$3v_s^2 = 1 - \frac{195}{37}\left(\frac{\alpha_s}{\pi}\right)^2\left[\frac{11}{9} - \frac{64}{3\sqrt{3}}\left(\frac{\alpha_s}{\pi}\right)^{\frac{1}{2}} - 16\left(\frac{\alpha_s}{\pi}\right)\ln\left(\frac{\alpha_s}{\pi}\right)\right] + O(\alpha^3) \qquad (2.22)$$

From equation (2.17) we can also derive an expression for p in terms of e. At zero order in α_s we have the following relation for e (from equation (2.19)):

$$\ln\left(\frac{e}{e_o}\right) = 4 \ln\left(\frac{T}{\Lambda_{QCD}}\right) \qquad (2.23)$$

with $e_o = e(\Lambda_{QCD})$. Thus α_s can be written as

$$\frac{\alpha_s}{\pi} = \frac{6}{29\ \ln(T/\Lambda_{QCD})} = \frac{24}{29\ \ln(e/e_o)} \tag{2.24}$$

and finally

$$p = \frac{e}{3}\left\{1 - \frac{30}{37}\left[\frac{576}{174}\frac{1}{\ln^2(e/e_o)}\left[\frac{11}{9} - \frac{64\sqrt{8}}{3\sqrt{29}}\frac{1}{\ln^{1/2}(e/e_o)} - \frac{384}{29}\frac{\ln\ln(e/e_o)}{\ln(e/e_o)}\right]\right] + O\left[\frac{1}{\ln^3(e/e_o)}\right]\right\} \tag{2.25}$$

In section 2.3 we will see how non-perturbative effects may be introduced near the confinement region.

2.2.3 *Lattice QCD at finite temperatures.*

In the last few years, numerical methods have been increasingly widely used for studying QCD (see, for example, Cleymans et al. (1986a)). The procedure is to evaluate the partition function (2.13) on a large but finite lattice where points are separated by a common spacing a, so that the possible momenta range between 1/a and 1/Na, where Na is the linear lattice size. The results then have no infrared and ultraviolet divergences. If N_τ and N_s are the number of lattice sites in the τ and space directions respectively, then the volume is $V = N_s^3 a$ and the reciprocal temperature is $1/T = N_\tau a$. The spinorial quark fields ψ and $\bar{\psi}$ are defined at each of the $N_\tau N_s$ lattice sites. In order to ensure the gauge invariance of the formulation, the gauge fields F_i^A must, however, be defined on the links between adjacent lattice points.

Physical observables must, of course, be independent of the the choice of the lattice and this is guaranteed by the following relation betweeen the lattice spacing a and the coupling g

obtained from the renormalization group theory:

$$a\Lambda_L = \exp\left\{-\frac{4\pi^2}{33-2N_f}\left(\frac{6}{g^2}\right) + \frac{459-57N_f}{(33-2N_f)^2}\ln\left[\frac{8\pi^2}{33-2N_f}\left(\frac{6}{g^2}\right)\right]\right\} \qquad (2.26)$$

where Λ_L is a dimensional parameter which characterizes the interaction scale. All physical quantities calculated by computer simulation techniques are then given in terms of Λ_L. Their values in physical units are obtained at the end by fixing the arbitrary lattice scale Λ_L with the calculation of some experimentally known quantity such as the proton mass.

The main objectives that lattice QCD tries to achieve are the following: (i) to give a complete description of strongly interacting matter in the range of temperatures and densities which cannot be analysed by perturbative methods and to decide whether or not the confinement process is a first order phase transition with true discontinuities in characteristic parameters at a clearly defined critical temperature; (ii) to determine the transition temperature and its dependence on the chemical potential (in other words, to find out how the transition temperature changes for increasing baryon number density); (iii) to see whether or not confinement is related to the breaking of chiral symmetry. This symmetry is a quasi-exact symmetry of QCD which is restored at high temperatures in the limit of zero mass for quarks with the flavours up, down and possibly strange. At low temperature, the dynamical breaking of this symmetry corresponds to a finite value of the mass term $\langle\bar{\psi}\psi\rangle$ which becomes zero at high temperature when the symmetry is restored.

At present, the calculations are most accurate for pure gauge theory (quarkless QCD), and for this, the existence of a first order phase transition connected with confinement has been

demonstrated both analytically (Borg and Seiler (1983)) and numerically (Çelic et al. (1983), Kogut et al. (1985), Gottlieb et al. (1985), Christ and Terrano (1986)). The order parameter of the transition is the thermal Wilson loop <L> ($\propto e^{-F/T}$) which is associated with the free energy F of an isolated quark. Its expectation value is zero in the confined phase (F is infinite since a quark can only exist in a colourless bound state) and finite in the deconfined phase (see Figures 1 and 2).

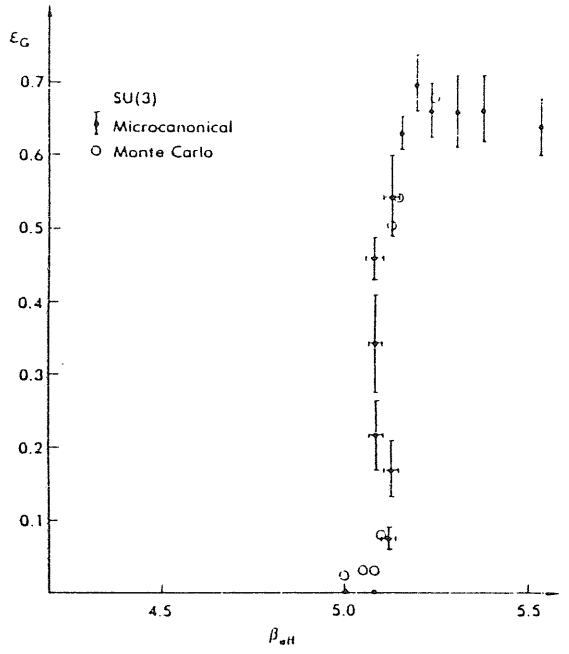

Fig.1 The SU(3) gluonic internal energy density (Kogut et al.(1985)). $\beta_{eff} \sim \ln T$.

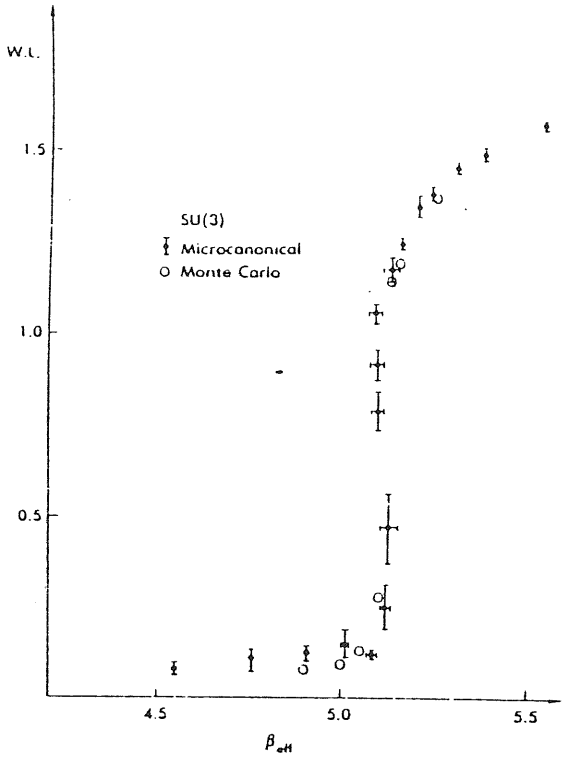

Fig.2. The SU(3) Wilson line order parameter (Kogut et al.(1985)).

The transition temperature T_c is estimated to be in the range (150-230) MeV with the corresponding latent heat being between 1.5 (GeV/fm^3) (Kogut et al.(1983), Çelik et al.(1983), Svetiski and Fucito (1983)) and 2.5(GeV/fm^3) (Gottlieb et al. (1987)). The large uncertainty of the results comes mainly from systematic errors related to the finite volume correction and from the fixing

of the physical value of lattice scale Λ_L.

The situation for full QCD is still quite unclear. The qualitative features near confinement are similar to those for a pure Yang-Mills theory, but the different groups of people involved in these large scale computations claim different answers for the order of the transition. All of the groups agree on the general behaviour shown in Figures 3 and 4. In Figure 3, one can see that the energy density varies rapidly from a value typical of a gas of pions to a value similar to that for a gas of free quarks and gluons. Coinciding with this change there is also an abrupt

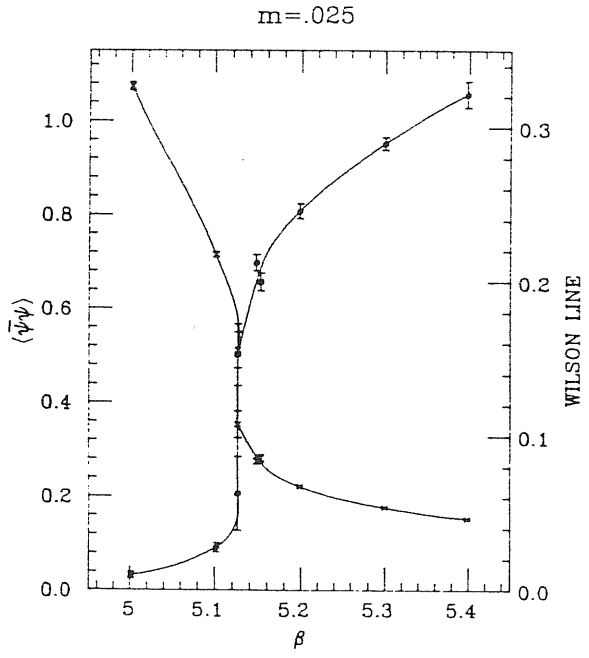

Fig.3. Wilson line (crosses) and $\langle\bar{\psi}\psi\rangle$ (circle) as functions of $\beta=6/g^2$ (Kovacs et al.(1987)).

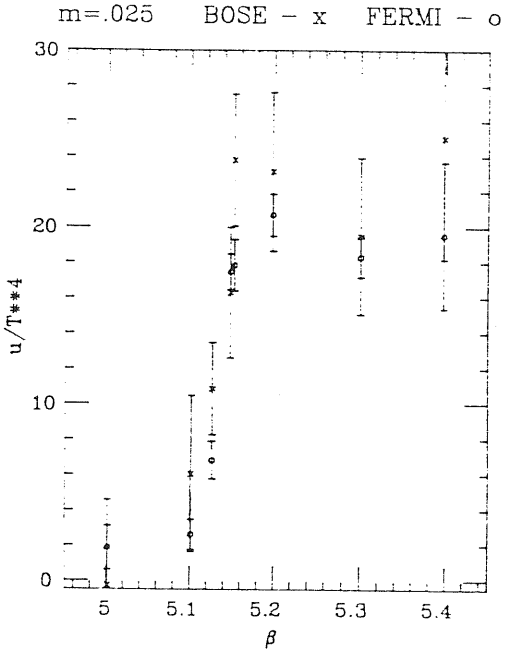

Fig.4. Gluon and fermion energy densities u as function of $\beta=6/g^2$ (Kovacs et al.(1987)).

change in the thermal Wilson loop <L> and in the chiral order parameter $\langle\bar{\psi}\psi\rangle$. The analyses have been performed with algorithms which differ in the range of quark masses considered.

The current overall picture of finite temperature QCD is summarized in Figure 5 which shows the range of quark masses for which a first order phase transition has been claimed. Clear signs of metastability have been found by Çelik et al. (1985) in the limit of high quark masses (the limit $m_f \to \infty$ corresponds to the pure gauge theory where, as we have seen, there is definitely a first order phase transition). In the limit of low quark masses there is probably a first order phase transition for $m_f=0$ but the transition becomes continuous at some value finite of m_f (Fukugita and Ukawa (1986), Fukugita et al. (1987), Gupta et al. (1986), Kovacs et al. (1987), Gavai et al. (1987); for previous results see references therein). The transition temperature is estimated to be about (200±50) MeV.

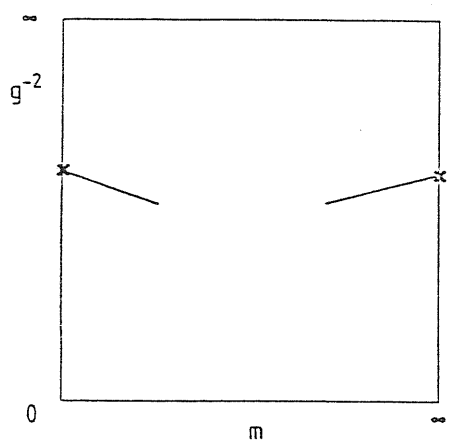

Fig.5 Possible phase diagram for the SU(3) gauge theory with fermions. The crosses indicate the deconfinement transition in the pure gauge sector (m=∞) and the chiral transition at m=0. $g^{-2} \propto \ln T$.

The great difficulties encountered in studying QCD at high temperatures, increase further when a net baryon density is included. In the limit of large quark masses, Berg et al. (1986) have obtained the results shown in Figure 6. The points plotted indicate a rapid variation in $\langle L \rangle$ and $\langle \bar{\psi}\psi \rangle$ but do not necessarily imply a phase transition. Although they should be considered only

as a qualitative description of the true behaviour, it is interesting to notice that the transition temperature decreases with increasing baryon number density.

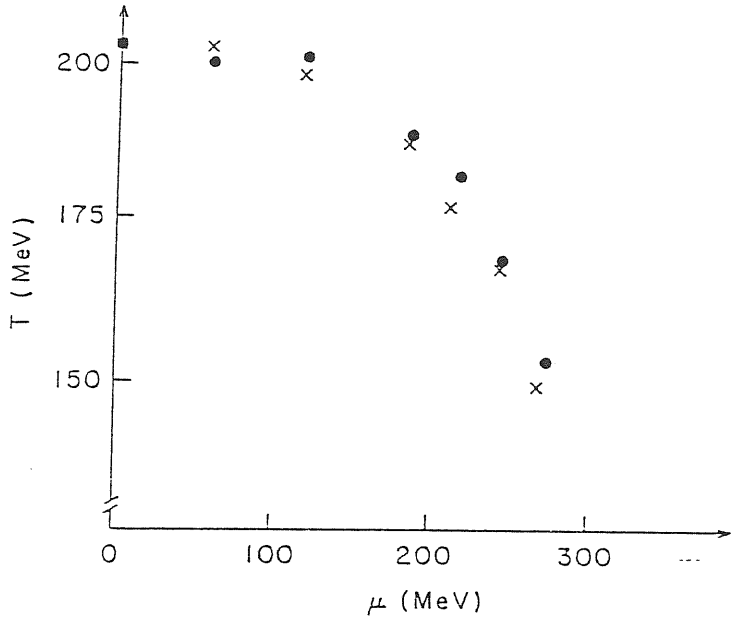

Fig.6 Phase diagram for strongly interacting matter:critical temperature T for deconfinement (x) and for chiral symmetry restoration (o), versus critical baryonic chemical potential μ (Berg et al. (1986)).

In summary we can say that at temperatures larger than 200 MeV, strongly interacting matter is in the quark-gluon plasma state and that the deconfinement process of ordinary hadronic matter, as temperature increases, is characterized by a very rapid variation in the energy density and other thermodynamical quantities. The transition is likely to be first order in the case of quark masses tending to zero or for very large masses but the general situation is not yet completely clear. Because all of these calculations require large amounts of computer time and memory, we will probably have to wait for the next generation of supercomputers before there will be a definitive answer (Toussaint (1987)).

2.3 Large scale analysis of confinement processes using lattice QCD results.

The first attempt to use lattice QCD results in cosmology was made by Bonometto and Pantano (1984) who considered the case where the transition occurs smoothly and continuously without supercooling. The aim was to check which kinds of deviation from the evolution of a simple radiation dominated universe would be produced by the confinement processes under these circumstances.

According to the standard model the universe is assumed to be homogeneous and isotropic for temperatures well above 200 MeV so that it can be described by the Friedmann-Robertson-Walker (FRW) metric

$$ds^2 = dt^2 - a^2(t)\left[\frac{dr^2}{1-k^2r^2} + r^2d\vartheta^2 + r^2\sin^2\vartheta d\phi^2\right] \qquad (2.29)$$

where r is a comoving radial coordinate, t is the proper time of a comoving observer, a(t) is the cosmic scale factor and k is a constant which takes the values +1, 0 and -1 for closed, flat and open universes respectively. The time evolution of the scale factor a can be calculated from the Einstein equations which for the metric (2.29) give

$$\left(\frac{\dot{a}}{a}\right)^2 = \frac{8\pi G}{3} e + k/a^2 \qquad (2.30)$$

$$-\frac{\ddot{a}}{a} = \frac{4\pi G}{3}(e+p) \qquad (2.31)$$

where G is the gravitational constant. We have also assumed that there are no dissipative or viscous phenomena. If the system evolves through equilibrium states, the entropy S per unit comoving volume is conserved (see,for example, Weinberg (1972)), i.e.

$$S = a^3(t)\ \frac{(e+p)}{T} = \text{constant} \qquad (2.32)$$

In the case of a universe dominated by radiation-like particles

$$e = 3p = \left(\frac{\pi^2}{30}\right) g\ T^4 \qquad (2.33)$$

where the degeneracy factor g is equal to $n_b + \frac{7}{8}n_f$, with n_b and n_f being the number of boson and fermion degrees of freedom respectively. For constant g, equation (2.32) implies

$$aT = \text{constant} \qquad (2.34)$$

Consider now the confinement period with the assumption that the transition from the quark-gluon plasma state to the hadron state is continuous, although very rapid, and that the hypotheses of homogeneity and isotropy continue to hold at least for scales larger than the strong interaction length scale. In this work, equation of state used for strongly interacting matter was derived from the lattice calculations of Montvay and Pietarinen (1982). Although improved lattice calculations have appeared more recently, the qualitative behaviour of the results has not changed and so the conclusions presented hereafter are still reasonable. The energy contribution of radiation-like particles (photons, neutrinos, relativistic leptons) is given by equation (2.33) with $g=g_r=14.25$. From equation (2.32) we have

$$\left[E_s + \Phi_s + \frac{4}{3}\left(\frac{\pi^2}{30}\right) g_r \right] (aT)^3 = \frac{4}{3}\left(\frac{\pi^2}{30}\right)\left(g_r+g_s\right)(a\ T\ )_\infty^3 \qquad (2.35)$$

where the suscript s refers to the strongly interacting matter and $E=e/T^4$ and $\Phi=p/T^4$ are derived from the lattice results. The subscript ∞ refers to temperatures well above 200 MeV where strongly interacting matter behaves as a gas of free quarks and gluons (with $g_s=37$ if two quark flavours are essentially massless

at the temperature under consideration; g_s=47.5 for three massless flavours).

The behaviour of $(aTS^{-1/3})$ is shown in Figure 7 for the temperature range $(80\text{-}800)\Lambda_L$. It can be seen that the evolution

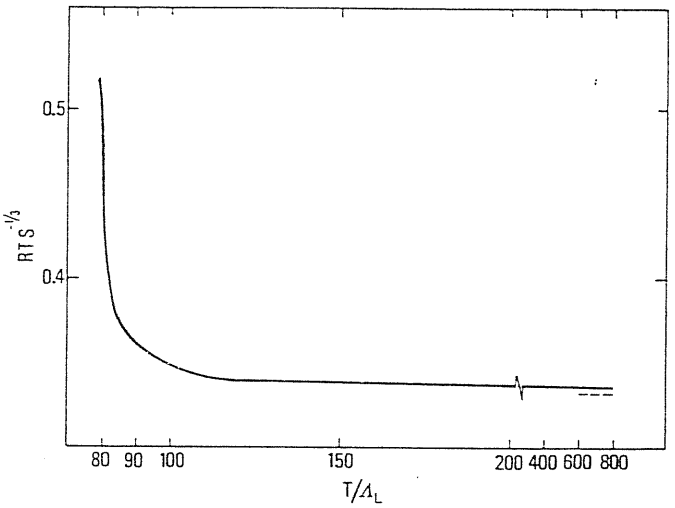

Fig.7. The deviation of $aTS^{-1/3}$ from its behaviuor in a radiation dominated universe is shown as function of T.

deviates from that of a simple radiation-dominated universe as T approaches $100\Lambda_L$ and that the temperature then temporarily stabilizes at a value of roughly $80\Lambda_L$ ($\Lambda_L \simeq 2.0\pm0.6$ MeV). During the confinement period, quarks and gluons are transformed into leptons and photons as can be seen in Figure 8 which shows the fraction of the total entropy per comoving volume which is carried by the leptons and photons. The binding energy of quarks and gluons is released as confinement proceeds and this prevents further cooling of the universe despite its continued expansion.

Bonometto and Sakellariadou (1984) used the same data to derive expressions for a(t) and T(t) during the confinement. They found that the plateau of temperature would probably last for ~ 10^{-5}s which is comparable with the Hubble time $t_H = H^{-1} = (a/\dot{a})$ at

the beginning of the confinement. However, no significant change was found in the behaviour of a(t).

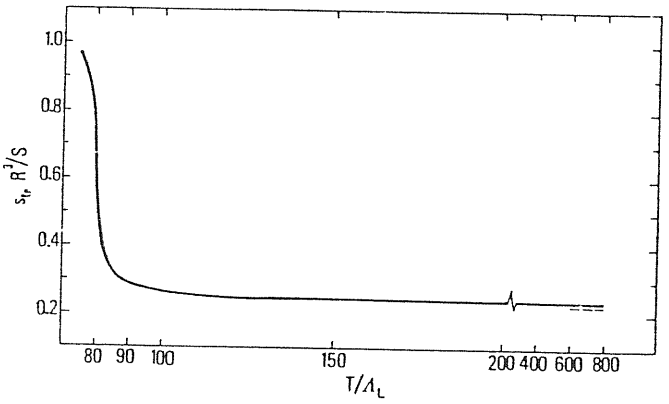

Fig.8. The fraction of the total entropy which is carried by leptons and photons is plotted. The sharp increase corresponds to the onset of the confinement.

If the transition is not continuous and the system, instead, undergoes a first order phase transition for which the energy density has a true discontinuity at a critical temperature T_c, then the situation becomes more complicated. In the case in which the transition takes place without supercooling and it is possible to neglect density fluctuations related to nucleation of the new phase, the analysis of a first order phase transition can be made assuming that the system remains in equilibrium at the critical temperature T_c and pressure $p_c=p(T_c)$. For an isothermal and isobaric transition, equation (2.32) is still satisfied and the Einstein equations can be integrated analytically (Bonometto and Matarrese (1983), Lodenquai and Dixit (1983)). Under these assumptions the length of the transition appears very short ($\sim 10^{-7}$s) compared with the length of the temperature plateau. This comparison suggests that the effect of confinement forces is

already significant for some time before the actual phase transition starts. It is clear that it is not only important to know the order of the transition but also to know the detailed behaviour of strongly interacting matter at temperatures near T_c. At present, lattice QCD data are not very accurate and so, for hydrodynamical calculations, it seems best to use simpler phenomenological models which aim to reproduce the most important features of strong interactions. These allow one to make some predictions about the effects of the transition both in the early universe and in laboratory heavy ion collisions (Van Hove (1986)).

2.4 Phenomenological models for strongly interacting matter near the confinement transition.

2.4.1 *Quark phase: the MIT bag model.*

The main properties of QCD are (i) asymptotic freedom: at short distances the coupling constant goes to zero, (ii) confinement of quarks within hadrons for energy densities lower than ~500 MeV fm^{-3} (the energy density of nuclear matter is ~150 MeV fm^{-3}). These properties are included in the "bag" model (Chodos et al. (1974)) by considering quarks confined inside a "bag" within which the strong interaction is either neglected or treated by perturbation theory. This corresponds to assuming that the vacuum inside the bag is different from the "true" vacuum outside, with the "perturbative vacuum" inside the bag being characterized by a finite energy density B. This corresponds to adding a term $\ln Z_{vac} = BV/T$ to the partition function given by perturbation theory. A negative contribution (-B) then appears in the expressions (2.16) and (2.17) for the pressure and a positive

contribution (+B) must be included in the energy density expression (2.19). Figure 9 shows the behaviour of p and e for three different values of B proposed in the literature. N_f has been chosen equal to two and Λ_{QCD} set equal to 100 MeV. We can see that the temperature at which p=0, increases with increasing values of B, as one expects, since B essentially determines the temperature at which non-perturbative effects become important. In the plot corresponding to $B^{1/4}$=145 MeV the pressure reaches a minimum and then starts to diverge as T is further reduced; this behaviour is due to perturbative corrections of order higher than α_s. The fact that the non-perturbative contribution (-B) is not able to compensate for perturbative corrections suggests that the value $B^{1/4}$=145MeV is too small to give a realistic description of confinements effects. Actually, current analysis of the hadronic spectrum suggests values for $B^{1/4}$ in the higher part of the proposed range, in agreement with the above considerations. Hereafter we will use the value $B^{1/4}$=200 MeV.

$B^{1/4}$=235 MeV

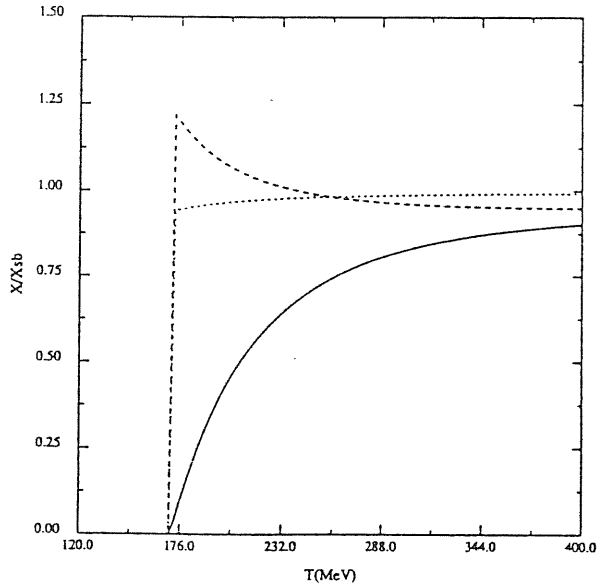

Fig.9. Pressure (——),energy density (--) and sound velocity (..) are plotted as functions of T in units of the Stefan-Boltzmann limiting values for a free gas of massless quarks and gluons. The calculation is stopped when p=0. Three different for $B^{1/4}$ are considered and Λ_{QCD} is set equal to 100MeV.

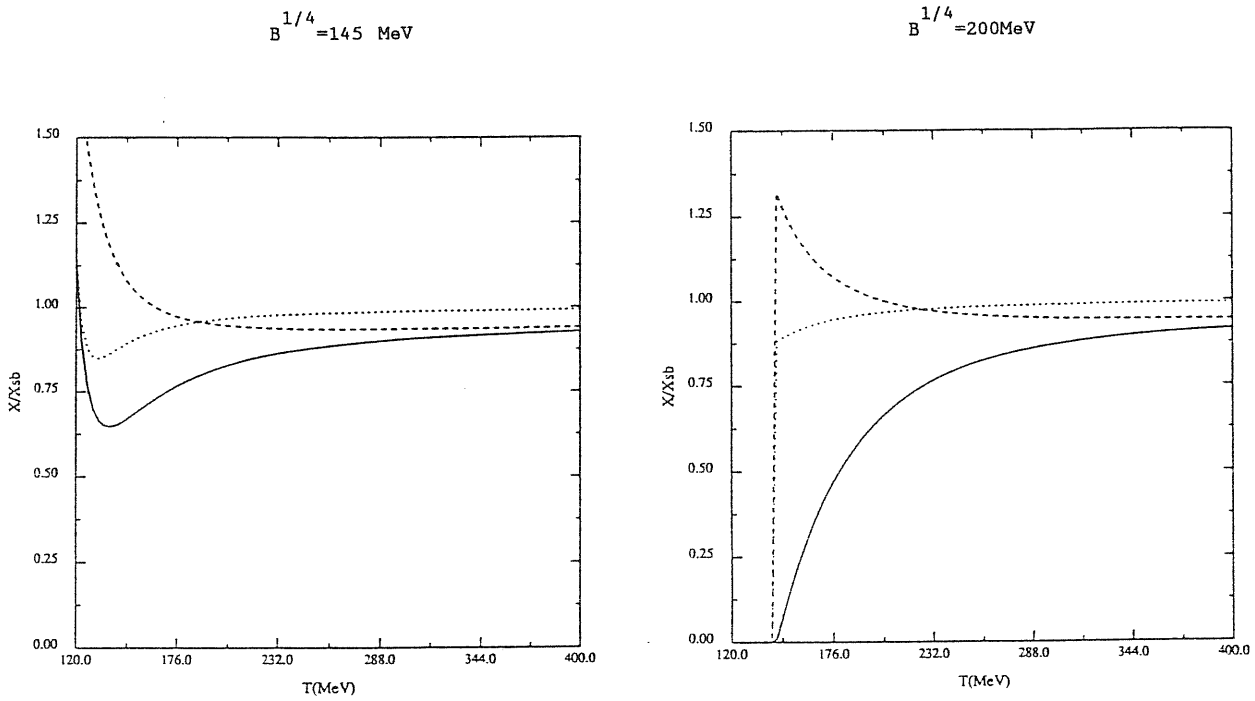

Figure 9 also shows the temperature dependence of the sound speed in the quark-gluon plasma according to equation (2.22). All of the quantities have been plotted in units of their value in a free relativistic gas of quarks and gluons.

In the limit μ=0 and α_s=0 we obtain the bag equation of state for high temperature and zero baryon number in its simplest form (i.e. free quarks inside the bag):

$$p_q = \frac{37}{90}\pi^2 T^4 - B \qquad (2.36)$$

$$e_q = 3p_q + 4B = \frac{37}{30}\pi^2 T^4 + B \qquad (2.37)$$

2.4.2 *Hadron phase: finite volume models*

Just below the critical temperature, pions are the only hadronic species present in large numbers since they are the only species whose mass is likely to be lower than T_c (m_π=137 MeV). In a first approximation, the hadronic phase can then be described as

an ideal gas of relativistic pions with the equation of state being given by:

$$p_h = \frac{\pi^2}{30} T^4 \qquad (2.38)$$

$$e_h = 3p_h = \frac{\pi^2}{10} T^4 \qquad (2.39)$$

The critical temperature T_c of the phase transition is the temperature for which the pressure of the two phases is the same (i.e. $p_h(T_c)=p_q(T_c)$). By using equation (2.36) for the quark-gluon plasma and (2.38) for the hadron phase one obtains T_c= 144 MeV (N_f=2, $B^{1/4}$=200). Including perturbative corrections (see equation (2.22)) increases the value of T_c to 148 MeV.

However, describing the hadron phase as an ideal gas of pions is obviously not completely correct. Pions are not point-like particles and if we compare their size ($\sim 1/m_\pi$) with their mean separation d_π we can see that these are already comparable at $T \sim m_\pi$ ($d_\pi \simeq 1.7\ T^{-1}$). Moreover, pions are not the only hadrons present and although the number density of higher mass hadrons is depleted by a Boltzman factor $e^{-m/T}$ the spectrum of hadronic resonances is such that a divergent behaviour arises in the thermodynamical quantities at a critical temperature T_H if we sum the contributions from the whole spectrum (Hagedorn (1965)). However, if finite volume corrections are also taken into account the divergences do not arise and the total energy density is limited by the total volume available. Finite volume corrections were considered by Karsch and Satz (1980) in the case of a system consisting only of pions and Bonometto (1983) included the contribution of protons and neutrons for the case where μ is not zero. A wider hadronic spectrum, including a continuous part as in the Hagedorn model was analysed by Kapusta and Olive (1982) and

Kapusta (1982).

Here we will discuss the thermodynamics of a system of extended hadrons in its most general form without making any assumption about the nature of the hadronic spectrum. The method followed is similar to the one presented by Hagedorn (1983) (see also Hagedorn (1985)) except that there a pressure *ensemble* was considered by using, as a thermodynamical potential, the function $\Pi=\Pi(T,\mu,p)$ obtained from (2.7) by the Legendre transformation

$$\Pi(T,\mu,p) = \Omega(T,\mu,V) - pV \tag{2.40}$$

With this choice, he found a singularity in the energy density which he then interpreted as a sign of a phase transition to a quark-gluon plasma. The analysis is made by keeping the pressure constant while the total volume of the system is allowed to vary. As these conditions are not suitable for cosmological applications in which the total volume of a comoving region is given and the pressure varies, we have calculated the thermodynamical quantities by considering $\Omega(T,\mu,V)$ as the thermodynamical potential. In our case the appearence of divergences is prevented by fixing the total volume.

The finite extension of the hadrons is treated as in the Van der Waals analysis and their strong interactions are simulated by using the hadronic mass spectrum $\tau(m^2,b)$, where $\tau(m^2,b)dm^2$ is the number of different types of hadrons with baryon number b and squared mass between m^2 and m^2+dm^2. In the expression for $\tau(m^2,b)$ all allowed bound states and resonances are considered, and so the interacting hadron gas formally reduces to a mixture of infinitely many ideal gases.

The grand partition function for a system having variable total baryon number, volume V and temperature T is

$$Z(\mu,V,T) = \sum_{-\infty}^{\infty}{}_{b} \; e^{\beta\mu b} Q_b(\lambda,V,T) \tag{2.41}$$

where μ is the chemical potential conjugate to the baryon number and Q_b is the partition function for a system with total baryon number b:

$$Q_b(V,T) = \int d^4P \; \exp\left\{\beta_i P^i\right\} \sigma(P,b,V) \tag{2.42}$$

where $\sigma(P,b,V)$ is the density of states for a system enclosed in a volume V and having four-momentum P and total baryon number b (Hagedorn and Rafelski (1981)). β^i is the reciprocal of the temperature four-vector and it is defined by the condition that in the rest frame of the system $\beta_i P^i = E/T$ (Touscheck (1968)) and the density of the states $\sigma(P,V,T)$ is given by

$$\sigma(P,V,T) = \sum_{o}^{N_{max}} \frac{1}{N!} \int \delta^4\left(P - \sum_{1\alpha}^{N} p_\alpha\right) \sum_{\{b_\alpha\}} \delta_k\left(b - \sum_{1\alpha}^{N} b_\alpha\right)$$

$$\prod_{1\alpha}^{N} \left[\frac{2\Delta_i P^i_\alpha}{(2\pi)^3}\right] \tau(p_\alpha^2, b_\alpha) \; d^4p_\alpha \tag{2.43}$$

The maximum number of particles N_{max} is determined either by the finite mass of the particles compared with the total four-momentum P or by their finite volume compared with the available volume V. As the number of particles is not fixed, $\sigma(P,V,T)$ corresponds to the *ensemble* formed by systems with different numbers of particles N, but with the same total momentum P and same total baryon number b (the two last conditions are guaranteed by the two δ-functions present in equation (2.43)). The factor 1/N! must be introduced because the integration with respect to the coordinates of each particle is made separately, with the integration extending over the whole volume V, and so the result must be divided by N! which is the number of possible permutations of the

N *clusters*. The summation $\sum_{\{b_\alpha\}}$ is made over all possible combinations of N particles each carrying a baryon number b_α. The result of the integration with respect to the coordinates is expressed by the term $\Delta^i = V^i - \sum_{1\alpha}^{N} V^i_\alpha$ which is the covariant generalization of the non-relativistic available volume $\Delta = V - \sum_{1\alpha}^{N} V_\alpha$ (V_α is the volume of the particle labelled by α). According to the Van der Waals treatment, the density of states of extended particles in the volume V is identical to that of point particles in the available volume Δ. For hard core particles, a factor 4 must be introduced in front of ΣV_α ($=2^{d-1}$), d being the dimension of the space).

We can introduce into the integral (44) the identity

$$\tau(p_\alpha^2, b_\alpha) = \int \delta_o(p_\alpha^2 - m_\alpha^2)\ \tau(m_\alpha^2, b_\alpha)\ \theta(p_\alpha^o)\ dm_\alpha^2 \qquad (2.44)$$

where θ is the unit step function. Then in the rest frame of the system we have

$$\int \frac{2\Delta_i p_\alpha^i}{(2\pi)^3}\ \delta_o(p_\alpha^2 - m_\alpha^2)\ \tau(m_\alpha^2, b_\alpha)\ \theta(p_\alpha^o)\ dm_\alpha^2\ d^4p_\alpha$$

$$= \int \frac{\Delta}{(2\pi)^3}\ \tau(m_\alpha^2, b_\alpha)\ dm_\alpha^2\ d^3p_\alpha \qquad (2.45)$$

where we have performed the integration with respect to the time component of the four momentum. The grand partition function (2.41) then becomes

$$Z = \int d^4P\ e^{-\beta_i P^i} \sum_{o}^{N_{max}} \left[\frac{1}{N!} \int \delta^4(P - \sum_{1\alpha}^{N} p_\alpha) \sum_{-\infty}^{\infty} e^{\beta\mu b} \sum_{\{b_\alpha\}} \delta_k(b - \sum_{1\alpha}^{N} b_\alpha) \right.$$

$$\left. \prod_{1\alpha}^{N} \left(\frac{\Delta_\alpha}{(2\pi)^3}\ \tau(m_\alpha^2, b_\alpha)\ dm_\alpha^2\ d^3p_\alpha \right) \right] \qquad (2.46)$$

Making the integration in P and the sum over $\{b_\alpha\}$ we obtain first

$$Z = \sum_{o}^{N_{max}} \frac{1}{N!} \sum_{(b_\alpha)} \int \prod_{1\alpha}^{N} \left[\frac{\Delta_\alpha}{(2\pi)^3} \tau(m_\alpha^2, b_\alpha) e^{-\beta(\epsilon_\alpha - \mu b_\alpha)} \, dm_\alpha^2 \, d^3p_\alpha \right] \tag{2.47}$$

and then

$$Z = \sum_{o}^{N_{max}} \frac{1}{N!(2\pi)^{3N}} \prod_{1\alpha}^{N} \left[\sum_{-\infty}^{\infty} b \int \Delta_\alpha \, \tau(m_\alpha^2, b) \, \phi(m_\alpha, T) \, e^{\beta\mu b} \, dm_\alpha^2 \right] \tag{2.48}$$

with

$$\phi(m,T) = \int e^{-\beta\epsilon} \, d^3p = 4\pi \int p^2 e^{-(m^2+p^2)^{1/2}/T} \, dp$$

$$= 4\pi m^2 T \, K_2(m/T) \tag{2.49}$$

where $K_2(m/T)$ is a modified Bessel function. In the limit $m/T \gg 1$ we have $\phi(m,T) \simeq (2\pi mT)^{1/2} e^{-m/T}$.

The available volume Δ can be taken out of the integral in equation (2.48) if the volume of a cluster does not depend on the mass. Assuming that all of the particles have the same volume V_o, then $N_{max} = V/4V_0$ for hard core particles and $N_{max} = V/V_o$ for deformable particles. This assumption seems a good approximation for temperatures below 200 MeV where high mass clusters ($m > 1$GeV) are strongly depleted by the factor $e^{-m/T}$ contained in $\phi(m,T)$.

If we assume that all particles have the same volume and hard core repulsive interactions, the expression for $Z(\mu,V,T)$ becomes

$$Z = \sum_{0}^{V/4V_0} \frac{(V-4NV_o)^N}{N!(2\pi)^{3N}} \left[\sum_{-\infty}^{\infty} b \int \tau(m^2, b) \, \phi(m,T) \, e^{\beta\mu b} \, dm^2 \right]^N \tag{2.50}$$

Let

$$C = V/V_o \qquad \text{with} \qquad V_o \simeq \frac{4}{3} \pi m_\pi^3 \tag{2.51}$$

and

$$X(\mu,T) = \frac{4V_o}{(2\pi)^3} \sum_{-\infty}^{\infty} b \int \tau(m^2,b)\ \phi(m,T)\ e^{\beta\mu b}\ dm^2 \qquad (2.52)$$

Then the grand partition function is

$$Z(\mu,V,T) = \sum_{0}^{C} {}_N \frac{(1-N/C)^N}{N!} (CX)^N$$

$$= \sum_{0}^{C} {}_N G_N(X,C) \qquad (2.53)$$

Let $G_{\bar{N}}$ be the largest term of the sum, then

$$G_{\bar{N}}(X,C) \leq Z(\mu,V,T) \leq C\ G_{\bar{N}}(X,C) \qquad (2.54)$$

If we take logarithms and divide each term by C, then in the thermodynamic limit ($C\to\infty$) we have

$$\lim_{C\to\infty} \frac{1}{C} \ln Z = \lim_{C\to\infty} \frac{1}{C} G_{\bar{N}}(X,C) \qquad (2.55)$$

Using the Stirling approximation $N! \simeq (2\pi N)^{1/2}(N/C)^N$, G_N may be written as

$$G_N(X,C) = (2\pi N)^{-1/2} \exp\left\{N+\ln X-\ln(N/C)+\ln(1-N/C)\right\} \qquad (2.56)$$

and the condition for the maximum is

$$\ln X = \ln\left[\bar{N}/(C-\bar{N})\right] + \bar{N}/(C-\bar{N}) \qquad (2.57)$$

which is equivalent to

$$X = b(X)\ \exp(b(X)) \qquad \text{with} \quad b(X)=\bar{N}/(C-\bar{N}) \qquad (2.58)$$

Then

$$\frac{1}{C} \ln G_{\bar{N}}(X,C) = b(X) + \frac{1}{C} \ln \frac{1}{\sqrt{2\pi N}} \qquad (2.59)$$

and in the thermodynamic limit we have

$$\lim_{C\to\infty} \frac{1}{C} \ln Z = b(X) \tag{2.60}$$

It is now possible to calculate all of the thermodynamical quantities using the relations presented in Section 2.1. In the thermodynamic limit, the pressure is given by

$$p(\mu,T) = \lim_{V\to\infty}\left(\frac{T}{V}\ln Z\right) = \frac{T}{4V_o}\left(\frac{1}{C}\ln Z\right)$$

$$= \frac{T}{4V_o}\, b(X) \tag{2.61}$$

The energy density e is given by equation (2.3). We calculate first the term $(\partial \ln Z/\partial T)$:

$$\frac{\partial \ln Z}{\partial T} = -\,(1/T^2)\,\frac{\partial \ln Z}{\partial X}\,\frac{\partial X}{\partial \beta} =$$

$$= -\,(1/T^2)\;\frac{C}{[1+b(X)]}\, e^{-b(X)}\,\frac{4V_o}{(2\pi)^3}$$

$$\sum_{\infty}^{\infty} b \int \tau(m^2,b)\left[\mu b\;\phi(m,T) - \theta(m,T)\right] e^{\beta\mu b}\, dm^2 \tag{2.62}$$

with

$$\theta(m,T) = \int \epsilon(m)\; e^{-\beta\epsilon(m)}\, d^3p$$

$$= 4\pi T^4\left[3\left(\frac{m}{T}\right)^2 K_2(m/T) + \left(\frac{m}{T}\right)^3 K_1(m/T)\right] \tag{2.63}$$

Then we compute $(\partial \ln Z/\partial \mu)$

$$\frac{\partial \ln Z}{\partial \mu} = \frac{\partial \ln Z}{\partial X}\,\frac{\partial X}{\partial \mu} =$$

$$= \frac{1}{T}\,\frac{C}{[1+b(X)]}\, e^{-b(X)}\frac{4V_o}{(2\pi)^3}\sum_{\infty}^{\infty} b^{\mu b}\int \tau(m^2,b)\;\phi(m,T)\; dm^2 \tag{2.64}$$

From equation (2.3) and expressions (2.62) and (2.64) we obtain

$$e = \frac{1}{(2\pi)^3[1+b(X)]e^{b(X)}} \sum_{-\infty}^{\infty} b \int \tau(m^2,b)\ \theta(m,T)\ e^{\beta\mu b}\ dm^2 \qquad (2.65)$$

Finally from relation (2.4) and equation (2.64) we compute the baryon number density n:

$$n = \frac{1}{(2\pi)^3[1+b(X)]e^{b(X)}} \sum_{-\infty}^{\infty} b\ b \int \tau(m^2,b)\ \phi(m,T)\ e^{\beta\mu b}\ dm^2 \qquad (2.66)$$

These expressions for the pressure, energy density and baryon number density have been obtained without making any assumptions about the hadronic spectrum. If only pions are considered, $\tau(m^2,b)$ reduces to

$$\tau(m^2,b) = g_\pi\ \delta(m-m_\pi)\ \delta_k(b,0) \qquad (2.67)$$

where $g_\pi(=3)$ is the degeneracy factor of the pions. Then

$$X = \frac{4V_o}{(2\pi)^3}\ g_\pi \phi(m_\pi,T) \qquad \text{with} \quad \phi(m_\pi,T)=4\pi m^2 T K_2(m_\pi/T) \qquad (2.68)$$

$$p_\pi = \frac{T}{4V_o}\ b(X) \qquad (2.69)$$

and

$$e_\pi = \frac{4\pi T^4}{(2\pi)^3[1+b(X)]e^{b(X)}} \left[3\left(\frac{m_\pi}{T}\right)^2 K_2(m_\pi/T)+\left(\frac{m_\pi}{T}\right)^3 K_1(m_\pi/T)\right] \qquad (2.70)$$

These expressions were originally found by Karsch and Satz (1980).

A general expression for the mass spectrum can be obtained from the "bootstrap" equation (Hagedorn (1965), Frautschi (1971)) In this approach some elementary hadronic particles are given as inputs, and then one considers all of the possible resonances and bound states which can be formed with these and their products. The mass spectrum obtained consist of a discrete part and a continuous part. Following Kapusta and Olive (1982) the

expression for $\tau(m,b)$ is

$$\tau(m,b) = \sum_{1}^{k}{}_{\alpha}\, g_{\alpha}\, \delta_{b,b(\alpha)}\, \delta(m-m_{\alpha}) + c\, \theta(m-m_{o})\, T_{H}^{5/2}\, m^{-7/2}$$

$$\exp\left\{ \frac{m}{T_{H}} - \frac{7\pi^{2} T_{H} b^{2}}{30m} \right\} \qquad (2.71)$$

$$g_{\alpha} = (2I_{\alpha}+1)\,(2J_{\alpha}+1) \qquad (2.72)$$

where I_{α} and J_{α} is the isospin the angular momentum of the particle labelled with α, T_{H} is the Hagedorn temperature and m_{o} is the mass at which the continuous spectrum is assumed to start. The coefficient c is determined experimentally and values obtained for it range between 4 and 40.

CHAPTER III

RELATIVISTIC BUBBLE EXPANSION

In many astrophysical situations we are faced with the necessity of calculating the dynamics of spherical shells. First order phase transitons (Guth and Weinberg (1981)), void expansion (Maeda and Sato (1983)) and cosmological detonation waves (Bertschinger (1985)) are all examples of this.

A lot of work has been done on the nucleation and growth of "true" vacuum bubbles in a metastable "false" vacuum (Voloshin et al. (1975), Coleman (1977), Linde (1977), etc.). Coleman found that at zero temperature the expansion velocity of "true" vacuum bubbles soon approaches the light velocity since all of the energy released in the transition goes into accelerating the bubble wall. However, when gravitatonal effects are taken into account, bubble dynamics may change considerably (Coleman and De Luccia (1980)). Steinhardt (1982) showed that high temperature corrections also make Coleman's result inapplicable and that the bubble wall behaves more like a relativistic detonation wave. His analysis was made for a planar surface, neglecting surface tension. Surface effects were introduced by Berezin et al. (1983a) by using Israel's method for singular hypersurfaces (Israel (1966)). This method has been applied by several authors for studying the expansion of a single bubble either in a Minkowski background (Berezin et al. (1983b), Lake (1984)), in a De Sitter space-time (Maeda (1986)) or in a FRW universe (Laguna-Castillo and Matzner

(1986)). Many of these studies are concerned with the inflationary scenario; however, one should be aware that the Israel's formalism can be applied to bubble growth during inflation only when when the "thin wall" approximation is valid (in other words, when the quantum tunelling is direcly between the false and the true vacuum states - see also Blau et al. (1987)). In all of the previous literature in which bubble evolution is described by time-like hypersurfaces, the metrics for the space-time of regions inside and outside the bubble are given a priori and then the interface dynamics is determined consistently with this choice. Recently Sato (1986) has also analysed the kinds of junction between Minkowski, Schwarzscild and DeSitter space-times which are allowed on the basis of a positive energy condition for the shell.

However, the kind of procedure used in the above work is not completely correct because the Einstein equations are coupled with the interface conditions and they ought to be solved self-consistentely. The aim in this chapter is to present the complete set of hydrodynamical and interface equations valid for a spherically symmetric system in which a phase transition, combustion or void expansion is occuring.

We review, first of all, the relativistic hydrodynamical equations for a spherically symmetric system and then we present a derivation of the characteristic form of the hydrodynamical equations. After this, junction conditions at the interface are discussed. The Gauss-Codazzi method is used for deriving energy-momentum conservation equations at the bubble wall and these are then compared with the relativistic Rankine-Hugoniot junction conditions for a shock. Finally, thermal nucleation

theory is reviewed.

3.1 Coordinate frames and metric components.

The most general metric exhibiting spherical symmetry is:

$$ds^2 = -\alpha^2(dx^0)^2 - 2\alpha\beta dx^0 dx^1 + \gamma^2(dx^1)^2 + R^2 d\Omega^2 \qquad (3.1)$$

$$\text{with} \qquad d\Omega^2 = d\vartheta^2 + \sin\vartheta^2 d\phi^2$$

where α, β, γ and R are functions of x^0 and x^1 only. It is always possible to define a new time coordinate $\bar{x}^0$, by $\bar{\alpha}d\bar{x}^0 = \alpha dx^0 - \beta dx^1$, such that the metric becomes orthogonal.

We use a Lagragian (comoving) coordinate system in which the spatial coordinates are kept constant along the world line of each fluid element. Let t and μ be the time and radial coordinates respectively, then the metric is

$$ds^2 = -a^2 dt^2 + b^2 d\mu^2 + R^2 d\Omega^2 \qquad (3.2)$$

The metric component $R(t,\mu)$ is often referred to as the "Schwarzschild circumference coordinate" since the proper circumference at time t of a sphere characterized by the radial coordinate μ is

$$\int ds = \int g_{\vartheta\vartheta}^{1/2} d\vartheta = 2\pi R(\mu,t) \qquad (3.3)$$

In the newtonian and special relativistic limits, R represents the Eulerian radial coordinate at time t of a shell of fluid labelled by the comoving coordinate μ.

The four velocity of the fluid in our Lagrangian frame is

$$u^i = a^{-1}(1,0,0,0) \tag{3.4}$$

where the normalization factor is determined by the condition

$$u^i u_i = -1 \tag{3.5}$$

In order to see how disturbances propagate in the fluid, it is convenient to introduce also a suitable analogue of the classical Eulerian coordinate frame. The geometrical interpretation of R suggests choosing it as the radial coordinate for the new frame which is referred to as theSchwarzschild frame. The metric is

$$ds^2 = -A^2 dT^2 + B^2 dR^2 + R^2 d\Omega^2 \tag{3.6}$$

where A and B are functions of R and T only. The radial component of the fluid four-velocity is denoted by u and from the normalization condition (3.5) we have:

$$u^i = (A^{-1}(1+B^2u^2)^{1/2}, u, 0, 0) \tag{3.7}$$

The transformation rules for the metric components give the following relations between the two coordinate frames:

$$\frac{1}{A^2} = \frac{T_t^2}{a^2} + \frac{T_\mu^2}{b^2} \tag{3.8}$$

$$\frac{1}{B^2} = -\frac{R_t^2}{a^2} + \frac{R_\mu^2}{b^2} \tag{3.9}$$

$$\frac{T_t R_t}{a^2} - \frac{T_\mu R_\mu}{b^2} = 0 \tag{3.10}$$

where the subscripts indicate conventional partial derivative,

while for the four-velocity components we have

$$u = \frac{R_t}{a} \tag{3.11}$$

$$\frac{\left(1+B^2u^2\right)^{1/2}}{A} = \frac{T_t}{a} \tag{3.12}$$

We also introduce a quantity Γ defined as

$$\Gamma = \frac{R_\mu}{b} \tag{3.13}$$

and then, using equations (3.11) and (3.13), we can rewrite equation (3.9) as

$$\frac{1}{B^2} = \Gamma^2 - u^2 \tag{3.14}$$

From relations (3.8) and (3.10) we get

$$\frac{T_t}{a} = \frac{\Gamma B}{A} \qquad \text{and} \qquad \frac{T_\mu}{b} = \frac{uB}{A} \tag{3.15}$$

3.2 Hydrodynamical equations for a perfect fluid medium with spherical symmetry.

In the absence of dissipation and conduction, the stress-energy tensor of a fluid has the form:

$$T^{ij} = (e + p)\, u^i u^j + p g^{ij} \tag{3.16}$$

Where the source of gravitational field is the fluid itself, the metric is determined by the Einstein equations

$$R_{ij} - \frac{1}{2}\, g_{ij} R = -\, 8\pi G\, T_{ij} \tag{3.17}$$

where $R_{ij} = R^l{}_{ijl}$ is the Ricci tensor defined in terms of the

Riemann curvature tensor R^{i}_{jkl} and $R = g^{ij}R_{ij}$ is the scalar curvature.

For the spherically symmetric metric (3.3), the Einstein equations reduce to

$$4\pi G e R^2 R_\mu = \frac{1}{2}\left[R + \frac{R R_t^2}{a^2} - \frac{R R_\mu}{b^2} \right]_\mu \tag{3.18}$$

$$4\pi G p R^2 R_t = -\frac{1}{2}\left[R + \frac{R R_t}{a^2} - \frac{R R_\mu}{b^2} \right]_t \tag{3.19}$$

$$4\pi G(e+p)R^3 = \left[R + \frac{R R_t^2}{a^2} - \frac{R R_\mu}{b^2} \right] + \frac{R^3}{ab}\left[\left(\frac{a_\mu}{b}\right)_\mu - \left(\frac{b_t}{a}\right)_t \right] \tag{3.20}$$

$$\frac{a_\mu}{a} R_t + \frac{b_t}{b} R_\mu - R_{\mu t} = 0 \tag{3.21}$$

The local conservation laws for energy and momentum are expressed by:

$$T^{ij}{}_{;j} = 0 \tag{3.22}$$

where the semicolon denotes covariant derivatives associated with the metric g_{ij}.

The comoving coordinates are not yet uniquely determined and we still need to fix the scale of the radial and time coordinates. The comoving radial coordinate μ can be fixed by identifying it with the proper volume V_o of the sphere contained within the shell labelled by μ at an initial time t_o when the medium is uniform. This is

$$V_o = \int_0^\mu 4\pi\, b_o R_o^2 \, d\mu \tag{3.23}$$

For a thin shell

$$\Delta V_o = 4\pi\, b_o R_o^2\, \Delta\mu \tag{3.24}$$

At the initial time we set

$$\Delta\mu = \Delta V_o \tag{3.25}$$

then

$$b_o = \frac{1}{4\pi R_o^2} \tag{3.26}$$

As the system evolves, material is compressed or rarefied and then the proper volume of a shell of fluid becomes

$$\Delta V = 4\pi b R^2\, \Delta\mu \tag{3.27}$$

If we introduce the compression factor ρ defined as

$$\rho = \frac{\Delta V_o}{\Delta V} \tag{3.28}$$

then from equations (3.25) and (3.27) it follows that

$$b = \frac{1}{4\pi\rho R^2} \tag{3.29}$$

Equations (3.18)-(3.21) and (3.29) are not sufficient for completely determining the system. We need one more equation and this is the equation of state of the fluid. In chapter II we have discussed the equations of state that can be used for describing the quark and hadron phases. In particular, equations (2.36)-(2.39) describe the two phases for zero net baryon number density.

We can rewrite equations (3.18)-(3.21) in a form analogous to the classical one. In order to do this we follow the procedure described by May and White (1967) and Misner (1968). Our set of equations differs slightly from theirs because we use the total energy density as a fluid variable instead of the specific internal energy.

First, we write explicitly the energy-momentum conservation law (3.22)

$$T_0{}^j{}_{;j} = 0 \qquad e_t + \left(b_t/b + 2R_t/R\right)\left(e+p\right) = 0 \tag{3.30}$$

$$T_1{}^j{}_{;j} = 0 \qquad a_\mu/a + p_\mu/\left(e+p\right) = 0 \tag{3.31}$$

Combining equations (3.29) and (3.30) gives

$$e_t = w\,\rho_t \tag{3.32}$$

where $w = (e+p)/\rho$ is the specific enthalpy of the fluid. From equations (3.21), (3.24) and relation (3.11) we have

$$\frac{\left(\rho R^2\right)_t}{\rho R^2} = -\frac{a_\mu}{R_\mu} \tag{3.33}$$

and the constraint (3.31) can be written as

$$\frac{\left(aw\right)_\mu}{aw} = \frac{\left(e_\mu - w\rho_\mu\right)}{\rho w} \tag{3.34}$$

using the first law of thermodynamics.

From equations (3.18) and (3.19) we see that it is convenient to define a mass function m such that

$$m_\mu = 4\pi e R^2 R_\mu \tag{3.35}$$

$$m_t = -4\pi p R^2 R_t \tag{3.36}$$

We can integrate equation (3.18) and by using relations (3.11), (3.13) and (3.32) we obtain the constraint equation:

$$\Gamma^2 = 1+u^2-2Gm/R \tag{3.37}$$

with

$$m(\mu,t) = \int_0^{\mu} 4\pi e R^2 R_{\mu}\, d\mu \tag{3.38}$$

In the newtonian limit, $\Gamma=1$, while in the special relativistic case it reduces to the Lorentz contraction factor $\Gamma=(1+u^2)^{1/2}$. Since equation (3.37) includes the relativistic corrections due to both kinetic energy and gravitational potential energy, we can consider Γ as the general relativistic analogue of the Lorentz contraction factor. Finally after some manipulations in which we use equations (3.11), (3.13), (3.21), (3.22) and (3.37), equation (3.19) is written as

$$u_t = -a\left[\frac{\Gamma p_{\mu}}{b(e+p)} + \frac{Gm}{R^2} + 4\pi G p R \right] \tag{3.39}$$

Equations (3.11), (3.13), (3.29), (3.32)-(3.37) and (3.39) together with the equations of state comprise the set of partial differential equations which describes the evolution of our system once initial and boundary conditions have been specified. The initial and outer boundary conditions will be discussed in detail in Chapter V where we present the numerical integration scheme for the hydrodynamical equations while the junction conditions at the phase interface are presented in Section 3.4. The boundary conditions at the centre $\mu=0$ are $u=0$, $R=0$ and $m=0$. At the origin we also put $\Gamma=1$, which is the requirement of local flatness; we have already imposed this in the integration of equation (3.18).

The special relativistic form of these equations can be obtained by setting $G=0$ and the plane symmetric form is then obtained by letting $\Delta\mu/(4\pi R^2) \rightarrow \Delta\mu$, $\rho R^2 \rightarrow \rho$, neglecting the equation in m and putting $b=1/\rho$.

3.3 The characteristic form of the hydrodynamical equations.

3.3.1 *General formalism.*

When we deal with a quasi-linear hyperbolic system of partial differential equations it is often more convenient to rewrite them in a "characteristic form". In other words, we look for a linear combination of the evolution equations such that the new system can be written as a set of ordinary differential equations along particular directions in the independent variable space, called characteristic directions.

Let us review briefly the method for obtaining characteristic equations (see Jeffrey 1980). A general quasi-linear system of hyperbolic equations with two independent variables may be written in a compact form as

$$\frac{\partial Z}{\partial t} + A \frac{\partial Z}{\partial x} + C = 0 \qquad (3.40)$$

where Z is a column vector of n dependent variables, $A = A(Z,x,t)$ is an $n \times n$ matrix and $C=C(Z,x,t)$ is a column vector not containing derivatives.

Let l_i be the left eigenvectors of A given by

$$l_i A = \lambda_i l_i \qquad (3.41)$$

where λ_i are the n eigenvalues of A. The characteristic equations corresponding to system (3.40) are then

$$l_i \frac{\partial Z}{\partial t} + \lambda_i l_i \frac{\partial Z}{\partial x} + l_i C = 0 \qquad (3.42)$$

which gives

$$l_i dZ + l_i C \, dt = 0 \qquad (3.43)$$

along

$$dx/dt = \lambda_i \tag{3.44}$$

Equation (3.44) identifies the characteristic direction along which the corresponding equation (3.43) holds.

The characteristic form of the hydrodynamical equations has been used for numerical calculations in newtonian theory (e.g. Hoskin (1965), Henshaw (1987)) and in special relativity (McKee and Colgate (1973)), mainly in connection with the exact treatment of shock discontinuities. In general relativity, Bicknell and Henriksen (1979) have used characteristic methods for studying adiabatic gravitational collapse

3.3.2 *Characteristic equations for relativistic hydrodynamics.*

In order to write in characteristic form the set of hydrodynamical equations presented in Section 3.2, it is convenient, for the moment, to limit our considerations to equations (3.32), (3.33) and (3.39). The subsequent extension to the whole system is straightforward.

Let us first rewrite equation (3.33) in an alternative form using relations (3.11) and (3.13):

$$\rho_t + \left(4\pi\rho^2 R^2 a/\Gamma\right) u_\mu + 2au\rho/R = 0 \tag{3.45}$$

We then substitute it into equation (3.32) to get

$$p_t + wc_s^2 \left(4\pi\rho^2 R^2 a/\Gamma\, u_\mu + 2au\rho/R \right) = 0 \tag{3.46}$$

where we have introduced the local sound speed $c_s = (\partial p/\partial e)^{1/2}$, with the partial derivative being evaluated at constant specific entropy. The compact form (3.40) then corresponds in our case to

$$Z = \begin{pmatrix} u \\ p \\ \rho \end{pmatrix} \qquad A = \begin{pmatrix} 0 & \frac{a\Gamma}{b(e+p)} & 0 \\ \frac{a(e+p)c_s^2}{b\Gamma} & 0 & 0 \\ \frac{a\rho}{b\Gamma} & 0 & 0 \end{pmatrix}$$

$$C = \begin{pmatrix} \alpha \\ \beta\rho c_s^2 \\ \beta\rho \end{pmatrix} \tag{3.47}$$

where

$$\alpha = aG\left(m/R^2 + 4\pi pR\right) \qquad \text{and} \qquad \beta = 2au/R \tag{3.48}$$

The eigenvalue equation for the matrix A is

$$\lambda\left(\lambda^2 - a^2c_s^2/b^2\right) = 0 \tag{3.49}$$

which gives the eigenvalues

$$\lambda_0 = 0 \tag{3.50}$$

$$\lambda_{\pm} = \pm 4\pi\rho R^2 c_s a \tag{3.51}$$

The corresponding eigenvectors (defined up to a multiplicative constant) are

$$l_0 = \left(0, -\frac{1}{wc_s^2}, 1\right) \tag{3.52}$$

$$l_{\pm} = \left(\pm 1, \frac{\Gamma}{\rho w c_s}, 0\right) \tag{3.53}$$

For i=0, which corresponds to the directions of fluid streamlines, we obtain from (3.42) and (3.44)

$$dp = wc_s^2 d\rho \qquad \text{along} \qquad d\mu = 0 \tag{3.54}$$

The curve given by $d\mu=0$ is called the advective characteristic.

For $i=\pm$, we obtain after some manipulations

$$\left(u_t \pm 4\pi\rho R^2 c_s a u_\mu\right) \pm \frac{\Gamma}{\rho w c_s}\left(p_t \pm 4\pi\rho R^2 c_s a p_\mu\right) \pm 2au\Gamma c_s/R + aG\left(m/R^2 + 4\pi pR\right) = 0 \qquad (3.55)$$

which gives

$$du \pm \frac{\Gamma}{\rho w c_s} dp + \left[\pm 2au\Gamma c_s/R + aG\left(m/R^2 + 4\pi pR\right)\right] dt = 0 \qquad (3.56)$$

along

$$d\mu = \pm 4\pi\rho R^2 c_s a\, dt \qquad (3.57)$$

The two curves defined by equations (3.57) are called the forward and backward characteristics, respectively. These are the world lines of disturbances moving with the local sound speed relative to the fluid. In fact, we can rewrite equations (3.57) as

$$\frac{d\mu}{4\pi\rho R^2 a\, dt} = \pm c_s \qquad (3.58)$$

where the left-hand side is the ratio between the proper distance ($bd\mu=1/(4\pi\rho R^2)$) and the proper time (adt) as measured by an observer comoving with the fluid. Equations (3.56) are referred to as the forward and backward characteristic equations.

Equations (3.54) and (3.56) do not form a complete the set as we still need the characteristic equations for R, m and a. It can immediately be seen that R and m can also be calculated along the advective characteristic as equations (3.11) and (3.36) involve only time derivatives. The corresponding characteristic equations are

$$dR = au\, dt \tag{3.59}$$

$$dm = -4\pi pR^2 dt \tag{3.60}$$

The expression (3.34) for a, however, is a constraint equation on each time slice t. In terms of characteristics, it has to be integrated along dt=0.

3.4 Junction conditions.

In this section we discuss the formulation of suitable relativistic junction conditions at surfaces of discontinuity. We are concerned with discontinuity surfaces whenever a system significantly changes its properties over a distance negligible compared with the characteristic dimensions of the problem. The time evolution of the discontinuity is described in the four-dimensional space-time V by a time-like three-dimensional hypersurface Σ which divides V in two regions V^+ and V^-.

We can distinguish between two types of discontinuity surface. The first are surface layers, which are namely surfaces representing the transition region between two different types of medium (for example, two different phases). These are characterized by a δ-discontinuity in the density. The second type includes all boundary surfaces, shock waves and contact discontinuities, characterized by a finite jump in the density. The relativistic junction conditions for the latter type of surface have been discussed in detail by Lichnerowicz (1955) and many others authors but the form which they used can be applied only in particular coordinate systems, called admissible

coordinates (Synge 1960). A general method for treating both kinds of discontinuity has been presented by Israel (1966) and we follow his formalism for imposing conservation of energy and momentum across the interface.

3.4.1 *Metric junction conditions.*

Before going into the details of Israel's method we want to discuss the junction conditions for the metric. Because of our particular choice of coordinates, some of the metric components are not continuous at the interface. The junction conditions can easily be found by observing that the space-time interval between two events on the hypersurface Σ is an invariant quantity so that

$$-a_+^2 dt^2 + b_+^2 d\mu^2 + R_+^2 d\Omega^2 = -a_-^2 dt^2 + b_-^2 d\mu^2 + R_-^2 d\Omega^2 \qquad (3.61)$$

where the subscripts $\pm$ refer to quantities defined on the two sides of Σ bordering $V^{\pm}$ respectively. We define two types of bracket, $\{A\}^{\pm}$ and $[A]^{\pm}$ such that for every variable defined in the two submanifolds we have

$$\{ A \}^{\pm} = A^+ + A^- \qquad [A]^{\pm} = A^+ - A^- \qquad (3.62)$$

R must be continuous across Σ as $4\pi R^2$ gives the proper area of the shell at a fixed time t. Therefore equation (3.61) may be divided into

$$[R]^{\pm} = 0 \qquad (3.63)$$

and

$$\left[a^2 - b^2 \dot{\mu}_s^2\right]^{\pm} = 0 \qquad (3.64)$$

where μ_s is the value of μ at the interface and $\dot{\mu}_s = d\mu_s/dt$.

From the continuity of R at all times it follows that (dR_s/dt) is also continuous across the interface. This provides another junction condition equation

$$\left[au + b\dot{\mu}_s\Gamma \right]^{\pm} = 0 \tag{3.65}$$

Analogously we can find the junction conditions for the Schwarzschild frame which are again equation (3.63) and

$$\left[A^2 - B^2S^2\right]^{\pm} = 0 \tag{3.66}$$

where

$$S = \frac{dR_s}{dT} = \frac{R_t + \dot{\mu}_s R_\mu}{T_t + \dot{\mu}_s T_\mu} \tag{3.67}$$

Using equations (3.11), (3.13) and (3.15) we obtain

$$S = A\sqrt{\Gamma^2 - u^2}\ \frac{au + b\dot{\mu}_s\Gamma}{a\Gamma + ub\dot{\mu}_s} \tag{3.68}$$

From equations (3.14) and (3.37) it can be seen that in the case of a boundary surface, for which there is no contribution to the mass function m from the discontinuity surface (i.e. $m^+ = m^-$), equation (3.66) reduces to

$$\left[A \right]^{\pm} = 0 \qquad \left[B \right]^{\pm} = 0 \tag{3.69}$$

However, equations (3.69) do not hold if Σ represents a surface layer.

3.4.2 *Energy-momentum conservation conditions.*

We now introduce the Gauss-Codazzi method (Israel (1966),

Maeda (1986), etc.) which we use to compute the junction conditions for the fluid flow. Our presentation closely follows that of Maeda. The hypersurface Σ is completely described in terms of its intrinsic metric

$$h_{ij} = g_{ij} - n_i n_j \tag{3.70}$$

and the extrinsic curvature K_{ij} defined as

$$K_{ij} = h^{l}{}_{i} h^{m}{}_{j}\, n_{(l;m)} \tag{3.65}$$

where n_i is the unit space-like vector orthogonal to Σ and $n_{(l;m)} = n_{l;m} + n_{m;l}$. Whereas the intrinsic properties of the hypersurface are described by h_{ij}, the extrinsic curvature tells us the way in which it "bends" in the four-dimensional space-time.

From the Gauss-Codazzi equations, we have

$$^{(3)}R + K_{ij}K^{ij} - K^2 = -2G_{ij}n^i n^j \tag{3.72}$$

$$K_i{}^{j}{}_{\|j} - K_{\|i} = G_{lm}\, h_i^l\, n^m \tag{3.73}$$

where $K = g^{ij}K_{ij}$, $G_{ij} = R_{ij} - \frac{1}{2} g_{ij}R$ is the Einstein tensor in the four dimensional space-time, $^{(3)}R$ is the scalar curvature of the three geometry h_{ij} and $\|$ denotes the intrinsic covariant derivatives associated with h_{ij}.

Let K^{+}_{ij} and K^{-}_{ij} be the extrinsic curvature of Σ associated with its embedding in V^{+} and V^{-} respectively. If $K^{+}_{ij} \neq K^{-}_{ij}$, Σ represents the time history of a surface layer, while, if $K^{+}_{ij} = K^{-}_{ij}$, it refers to a boundary surface. In our problem we may be concerned with both kinds of hypersurface since the confinement region can be described as a surface layer and shocks may form during the bubble growth.

We introduce now the two quantities $\tilde{K}_{ij}$ and S_{ij} defined as

$$\left[K_{ij} \right]^{\pm} = -8\pi G \left(S_{ij} - \frac{1}{2} h_{ij} S \right) \tag{3.74}$$

$$\left\{ K_{ij} \right\}^{\pm} = 2 \tilde{K}_{ij} \tag{3.75}$$

where $S = g^{ij} S_{ij}$. The symmetric tensor S_{ij} defined in equation (3.74) is called surface energy-momentum tensor. In fact, it is possible to show that

$$S_{ij} = \lim_{\epsilon \to 0} \int_{-\epsilon}^{\epsilon} T_{lm} h_i^{\ l} h_j^{\ m} \, dx \tag{3.76}$$

where x is a Gaussian coordinate in the n_i direction and x=0 on Σ. From equations (3.17) and (3.72)-(3.73) one obtains

$$^{(3)}R + \tilde{K}_{ij} \tilde{K}^{ij} - \tilde{K}^2 = -16\pi^2 G^2 \left(S_{ij} S^{ij} - \frac{S^2}{2} \right) - 8\pi G \left\{ T^{ij} n_i n_j \right\}^{\pm} \tag{3.77}$$

$$\tilde{K}_{ij} S^{ij} = \left[T^{ij} n_i n_j \right]^{\pm} \tag{3.78}$$

$$\tilde{K}^i_{\ j \| i} - \tilde{K}_{\| j} = 4\pi G \left\{ T^{lm} n_l h_{jm} \right\}^{\pm} \tag{3.79}$$

$$S_i^{\ j}{}_{\| j} = - \left[T^{lm} n_l h_{im} \right]^{\pm} \tag{3.80}$$

In highly symmetric systems, equations (3.78) and (3.80) are sufficient to completely describe the evolution of the surface layer once they have been coupled to the Einstein equations in $V^{\pm}$. Equations (3.77) and (3.79) need to be solved only if it one wants to know the form of the fictitious background space $\tilde{V}$ in which Σ is a regular surface with extrinsic curvature $\tilde{K}_{ij}$.

We will restrict our attention to matter which behaves as a

perfect fluid so that S_{ij} and T_{ij} take the form:

$$T^{\pm}_{ij} = \left(e^{\pm} + p^{\pm} \right) u^{\pm}_i u^{\pm}_j + p^{\pm} g^{\pm}_{ij} \tag{3.81}$$

$$S_{ij} = \left(\sigma + \alpha \right) v_i v_j + \alpha h_{ij} \tag{3.82}$$

where σ and α are the surface energy density and the (negative) two-dimensional surface pressure($-\alpha$ is the surface tension); $p^{\pm}$, $e^{\pm}$ and $u^{\pm}$ are the pressure, energy density and four-velocity in $V^{\pm}$ and v^i is a unit time-like vector tangent to Σ. In a spherical or planar system there are two space-like Killing vectors $e^i_{(A)}$ (A=2,3) and these together with v^i and n_i form an orthonormal tetrad system on Σ. Projecting equation (3.80) along each of the tetrad directions gives

$$\left[\left(\sigma+\alpha \right) v^i \right]_{\|i} - v^i \alpha_{\|i} = \left[\left(p+e \right) \left(u^i n_i \right) \left(u^l v_l \right) \right] \tag{3.83}$$

$$\left(\sigma+\alpha \right) n_j v^i v^j{}_{\|i} = 0 \tag{3.84}$$

$$\left(\sigma+\alpha \right) v_i e^i_{(A)} v^j{}_{\|i} = 0 \tag{3.85}$$

where all of the fluid quantities are calculated at the hypersurface. From the symmetry, it also follows that

$$v^i v_{\|i} = 0, \tag{3.86}$$

so that the last two equations are trivial and we are left with only equation (3.83) which represents the conservation of energy across Σ. From this point on, we will consider only spherical symmetry.

Using condition (3.86) it can be shown that the acceleration vector is given by

$$\frac{Dv^i}{d\tau} = - n^i v^l v^m n_{l;m} \tag{3.87}$$

where τ is the proper time of an observer moving with the singular surface. Then, using equations (3.70) and (3.71), it follows that the left hand side of equation (3.78) can be written as

$$S^{ij}\tilde{K}_{ij} = \left[\sigma v^i v^j + \alpha e^i_{(A)} e^{j(A)}\right] \tilde{K}_{ij} \tag{3.88}$$

$$= - \frac{\sigma}{2} \left\{ n_i \frac{Dv^i}{d\tau} \right\}^{\pm} + \alpha e^{i(A)} e^j_{(A)} \tilde{K}_{ij} \tag{3.89}$$

For a spherically symmetric orthogonal metric (such as (3.2))

$$e^{i(A)} e^j_{(A)} K_{ij} = n^i \left[\ln R\right]_{,i} \tag{3.90}$$

and so finally equation (3.78) reduces to

$$\left\{ - \frac{\sigma}{2} n_i \frac{Dv^i}{d\tau} + \alpha n^i \left[\ln R\right]_{,i} \right\}^{\pm} = \left[\left[p+e\right] \left[u^i n_i\right] + p \right]^{\pm} \tag{3.91}$$

Equations (3.83) and (3.91) govern the motion of a surface layer in a spherically symmetric system. However, in order to use them, we first rewrite them explicitly in terms of our chosen metric (3.2). First of all we calculate the expressions for the tangent and normal vectors to Σ. The hypersurface equation is

$$F = \mu - \mu_s(t) = 0 \tag{3.92}$$

and the unit normal is given by

$$n_i = N \frac{\partial F}{\partial x^i} = N \left(-\dot{\mu}_s, 1, 0, 0\right) \tag{3.93}$$

where N is a normalization constant calculated by the condition $n_i n^i = 1$. It follows that

$$N = b\gamma \qquad \text{with} \qquad \gamma = a\frac{dt}{d\tau} = \frac{a}{(a^2 - b^2 \dot{\mu}_s^2)^{1/2}} \tag{3.94}$$

The tangent vector to the hypersurface is given by

$$v^i = \frac{dx^i}{d\tau}\bigg|_\Sigma = \frac{\gamma}{a}\left(1, \dot{\mu}_s, 0, 0\right) \tag{3.95}$$

The intrinsic metric of Σ is

$$ds^2_\Sigma = -d\tau^2 + R^2(\tau)d\Omega^2 \tag{3.96}$$

and, using this,

$$\left[(\sigma+\alpha)v^i\right]_{\|i} = \frac{1}{\sqrt{-h}}\left[(\sigma+\alpha)\sqrt{-h}\ v^i\right]_{,i}$$

$$= \frac{1}{R^2}\frac{d}{d\tau}\left[(\sigma+\alpha)R^2\right] \tag{3.97}$$

where $h = \det(h_{ij}) = R^2\sin\vartheta$. Using equations (3.93), (3.95) and (3.97), the energy conservation equation (3.83) becomes

$$\frac{d}{d\tau}\left(\sigma R^2\right) + \alpha\frac{dR^2}{d\tau} = \left[(e+p)R^2 b\dot{\mu}_s\gamma^2/a\right]^{\pm} \tag{3.98}$$

Next, we consider the rewriting of equation (91). Using relations (3.11), (3.13), (3.93), (3.95) and (3.96) we have

$$n_i\frac{R^{,i}}{R} = \gamma b\left(\frac{\dot{\mu}_s^2}{a^2}\frac{R_t}{R} + \frac{1}{b^2}\frac{R_\mu}{R}\right)$$

$$= \gamma b\left(\frac{\dot{\mu}_s^2 u}{aR} + \frac{\Gamma}{bR}\right) \tag{3.99}$$

$$n_i\frac{Dv^i}{d\tau} = \frac{b}{\gamma}\left[\frac{d^2\mu_s}{d\tau^2} + \frac{2b_t\gamma}{ab}\frac{d\mu_s}{d\tau} + \left(\frac{a_\mu}{a} + \frac{b_\mu}{b}\right)\left(\frac{d\mu_s}{d\tau}\right)^2 + \frac{a_\mu}{ab^2}\right]$$

$$= \frac{1}{a}\left[\frac{1}{b}\frac{d}{dt}\left(\frac{b^2\dot{\mu}_s}{c}\right) + \frac{f_\mu}{b}\right] \tag{3.100}$$

$$\left(e+p\right)\left(u^i n_i\right)^2 + p = \frac{1}{f^2}\left(eb^2\dot{\mu}_s^2 + pa^2\right) \tag{3.101}$$

where $f = a/\gamma = \left(a^2 - b^2\dot{\mu}_s^2\right)^{1/2}$. Because of the continuity of f across Σ we can finally write equation (3.91) as

$$\left[e^2\dot{\mu}_s^2 + pa^2 \right]^{\pm} = f^2\left\{ -\frac{\sigma}{2a}\left[\frac{1}{b}\frac{d}{dt}\left(\frac{b^2\dot{\mu}_s}{c} \right) + \frac{f}{b}\mu \right] + \frac{\alpha}{fR}\left(ub\dot{\mu}_s + a\Gamma \right) \right\}^{\pm} \tag{3.102}$$

For a surface layer the mass function receives a non-zero increment at the interface. From equations (3.35) and (3.36) we have:

$$\frac{d}{dt} m\Big|_{\Sigma} = m_t + \dot{\mu}_s m_\mu$$

$$= 4\pi R^2 \left(b\dot{\mu}_s \Gamma e - apu \right) \tag{3.103}$$

Therefore $[m]^{\pm}$ satisfies the following differential equation

$$\frac{d}{dt}\left[m \right]^{\pm} = 4\pi R^2 \left[b\dot{\mu}_s \Gamma e - apu \right]^{\pm} \tag{3.104}$$

For a sufficiently small bubble, space-time may be considered as locally flat and so one can use the newtonian expression $[m]^{\pm} = 4\pi R^2\sigma$ as an initial condition for equation (104).

For boundary surfaces, the surface energy momentum tensor is identically zero and $K_{ij}^{+} = K_{ij}^{-}$. Therefore we can immediately compute the junction conditions across a shock front by setting $\alpha = \sigma = [m]^{\pm} = 0$. Equations (3.98) and (3.104) reduce to the well known relativistic Rankine-Hugoniot relations (May and White (1967):

$$\left[aw \right]^{\pm} = 0 \tag{3.105}$$

and

$$\left[b\dot{\mu}_s \Gamma e - apu \right]^{\pm} = 0 \tag{3.106}$$

In deriving equation (3.105), the metric junction condition (3.64) has been used.

3.5 Nucleation theory during first order phase transitions.

3.5.1 *Thermodynamics of the transition region.*

It is usually convenient to describe the transition region as a discontinuity although we know that the physical properties of the system in fact change rapidly but continuously across a thin region separating the two phases. The discontinuity may then be characterized by excess functions which represent the variation of quantities across the transition region away from their values in the bulk phases. Figure 1(a) shows clearly that the calculation of a surface excess function depends on the location of the hypothetical dividing surface between the homogeneous bulk "liquid", with density ρ_L, and homogeneous bulk "vapour", with density ρ_V. The two locations A and B yield different excess values, the former being essentially the excess with respect to the liquid, while the latter yields the excess with respect to the vapour. Following the argument presented by Gibbs (1928), it is convenient to choose the position of the separation surface so that the superficial excess of matter vanishes, i.e.

$$\int_{-\infty}^{0} \left(\rho(z)-\rho_L\right) dz = \int_{0}^{\infty} \left(\rho(z)-\rho_V\right) dz \qquad (3.107)$$

where $\rho(z)$ is the real matter density across the transition region and ρ_L and ρ_V represent the constant matter density in the liquid and vapour phases respectively (each of which is assumed to be homogeneous away from the interface). The origin of the z-axis

has been located at the interface (see Figure 1(b)).

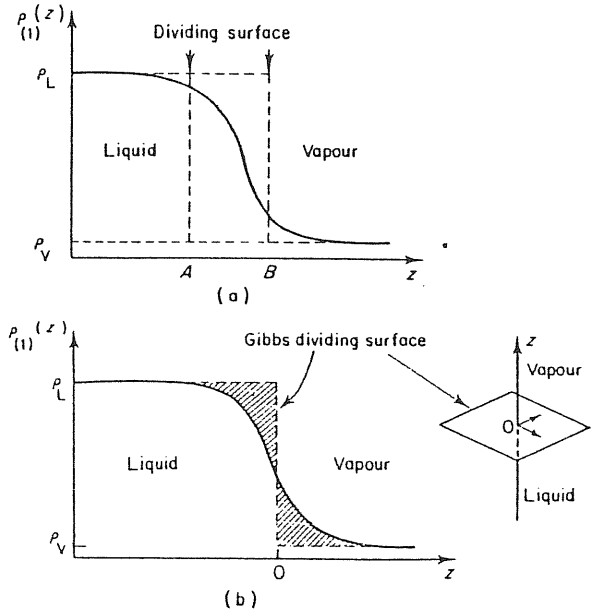

Fig 1 (a) Density profile of the transition region from the liquid to the vapour phase. A and B are two possible choices of positioning the hypothetical transition surface.

(b) The Gibbs location of the dividing surface is chosen such that there is zero surface excess density of matter, the the dashed areas being equal (Croxton (1980)).

Consider for simplicity a plane surface of area A separating the two homogeneous phases. The free energy of the system $F=f(T,V,A,N_V,N_L)$ is now a function also of A. N_V and N_L denote the number of particles in the vapour and liquid phases, respectively. The infinitesimal change in F due to small changes in temperature, volume, area and composition is given by

$$dF= - SdT- PdV + \gamma dA + \sum_{i=L,V} \mu_i dN_i \qquad (3.108)$$

where the entropy S, pressure p, surface tension γ and chemical potential μ_i associated to the ith particle component, are given by

$$S = -\left(\frac{\partial F}{\partial T}\right)_{V,A,N_V,N_L} \qquad p = -\left(\frac{\partial F}{\partial V}\right)_{T,A,N_V,N_L}$$

$$\gamma = -\left(\frac{\partial F}{\partial A}\right)_{V,T,N_V,N_L} \qquad \mu_{L(V)} = -\left(\frac{\partial F}{\partial N_{L(V)}}\right)_{V,T,A,N_{V(L)}} \tag{3.109}$$

Since F is a homogeneous function of first degree in V, A and the composition, it may be written as

$$F = -PV + \gamma A + \sum_{i=L,V} \mu_i N_i \tag{3.110}$$

Following the convention of Gibbs, we assume that there is no particle function excess, $\left(\text{i.e. } \sum_{i=L,V} \mu_i dN_{i|s}\right)$, associated with the surface and therefore the surface part of the free energy is

$$F_s = \gamma A \tag{3.111}$$

The new function of state of the system γ (surface tension) completely describes the interface and represents the gain in the free energy of the system (at constant temperature, volume and composition) for unit increase of the interface area A. If we assume that the bulk properties of the two phases remain unmodified by the increase of surface area, then the change in free energy can be expressed in terms of the surface quantities only:

$$dF_s = -S_s dT + \gamma dA \tag{3.112}$$

From equation (3.111) we also have

$$dF_s = \gamma dA + A d\gamma \tag{3.113}$$

and then combining equations (3.112) and (3.113) gives:

$$S_s = -A \frac{d\gamma}{dT} \tag{3.114}$$

The thermodynamical relation between the internal energy (U) and the free energy of the surface gives

$$F_s = U_s - TS_s \tag{3.115}$$

and the surface energy per unit area (σ_s) is then

$$\sigma_s = \gamma - T\frac{d\gamma}{dT} \tag{3.116}$$

The surface excess entropy per unit area is a measure of the disorder of the interface region relative to that of the bulk liquid phase. If the bulk liquid properties extend unmodified up to the discontinuity surface, then $S_s=0$. From equation (3.115) we see that a minimization of the free energy favours a broadening of the transition zone due to the S_s term. The internal energy contribution favours a sharpening of the transition region with surface particles residing in the energetically most favourable region of the attractive surface field of the bulk fluid. The surface entropy term is likely to be negligible in a strongly first order transition where atoms are more strictly bound to the liquid bulk phase.

Surface tension acts as a tangential negative pressure at the phase interface and so the equilibrium pressures in the two bulk phases can no longer be equal in the presence of a curved interface. For discussing the equilibrium state of a spherical bubble it is convenient to introduce the thermodynamical potential Ω defined by

$$\Omega = F - \sum_i \mu_i N_i = -PV + \gamma A \tag{3.117}$$

with

$$d\Omega = -SdT - PdV + \gamma dA - \sum_i \mu_i dN_i \tag{3.118}$$

The conditions of thermal and chemical equilibrium between

the two phases are

$$T_1 = T_2$$

$$\mu_1(p_1,T) = \mu_2(p_2,T) = \mu(T) \tag{3.119}$$

(where the subscript 1 refers to the interior phase and 2 refers to the surrounding medium). The equilibrium radius of the bubble corresponds to the minimum of Ω at a fixed total volume for the two phases combined, keeping μ and T constant. Since

$$\Omega = -p_1V_1 - p_2V_2 + \gamma A \tag{3.120}$$

the minimum of Ω corresponds to

$$r_c = \frac{2\gamma}{p_1 - p_2} \tag{3.121}$$

Figure 2 shows the behaviour of pressure as a function of temperature for a first order quark-hadron transition. The critical temperature T_c is the temperature at which the the two phases have the same pressure and the dashed line refers to the

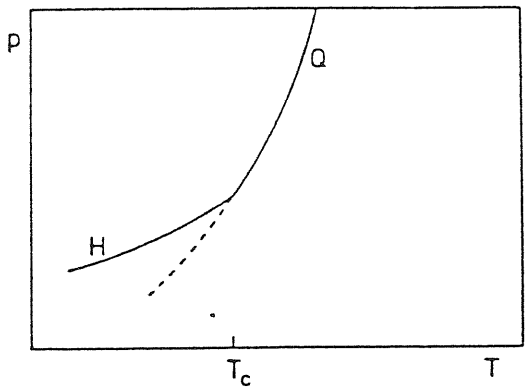

Fig. 2. The behaviour of the total pressure as a function of temperature near to T_c.

metastable supercooled quark phase. In order for a hadron bubble to exist in equilibrium with the quark medium at a common temperature it is necessary to have $p_h > p_q$ and clearly this is only possible at temperatures below T_c.

5.5.2 *Thermal bubble nucleation.*

According to thermal fluctuation theory (Landau and Lifshitz (1980)) the probability f of a fluctuation producing a bubble nucleus is proportional to $\exp(-R_{min}/T)$ where R_{min} is the minimum work needed to form the nucleus. This work is given by the variation of Ω at constant T and μ. Before nucleus formation $\Omega = - p_2 (V_1+V_2)$ while after the nucleation process $\Omega = - p_1V_1 - p_2V_2 + \gamma A$. Thus

$$R_{min} = - (p_1 - p_2)V_1 + \gamma A \qquad (3.122)$$

For a spherical nucleus of critical radius (3.121) we have

$$f(T) \propto \exp \left\{ \frac{16\pi\gamma^3}{3T(p_1-p_2)^2} \right\} \qquad (3.123)$$

Bubbles formed smaller than the critical radius immediately shrink and disappear while the probability of forming larger bubbles decreases exponentially with increasing size. It is therefore only bubbles formed at the critical size which are of interest.

For applying equation (3.123) to the quark-hadron transition we first of all need an expression for the surface tension γ. Following Witten (1984) we approximate γ by

$$\gamma = \gamma_0 T_c^3 \qquad (3.124)$$

where T_c is the critical temperature, which is related to the

strong interaction length scale, and γ_0 is an adimensional factor whose value has to be derived from the details of strong interactions in the transition region. Because its value is at present uncertain, we plan to check its effect for a range of cases. We also make the assumption that γ_0 is constant which corresponds to assuming that the transition region is very thin and that the surface energy density is equal to the surface tension (see equations (3.115) and (3.116)).

By using equations of state (2.36) and (2.38) for the quark and hadron phases respectively, equation (3.123) becomes:

$$f(T) = f_0 T_c^4 \exp \left\{ \frac{W_0}{\hat{T}(1-\hat{T}^4)^2} \right\} \qquad (3.125)$$

with

$$W_0 = \frac{16\pi\gamma_0^3}{[(g_i - g_f)\pi^2/10]} \qquad (3.126)$$

and $\hat{T}=T/T_c$. The factor in front of the exponential is again related to the strong interaction length scale with f_0 being an adimensional factor which is probably of order unity.

After a bubbles has been nucleated its surface expands as detonation or a deflagration front according to the degree of supercooling at the nucleation epoch. DeGrand and Kajantie (1984) made a highly simplified large scale analysis of the nucleation process which implied that only bubbles nucleated at a particular epoch are important for the overall dynamics of the transition. This analysis gives the following relation between W_0 and T_n (nucleation temperature):

$$T_n \simeq \left[1 - \frac{W_0^{1/2}}{45} \right] T_c \qquad (3.127)$$

This last equation is used in the code, at least as a first

approximation, in order to leave only one initial input parameter for the nucleation state. However the validity of (3.127) still needs to be checked on the basis of a more complete analysis.

CHAPTER IV

BUBBLE DYNAMICS AND COMBUSTION FRONTS

Boiling phenomena connected with classical first order phase transitions have been widely studied and a knowledge of the main results obtained can give a useful background for the discussion of the relativistic problem examined in this thesis. A brief review of classical bubble dynamics is presented in the first section of this chapter with particular emphasis on the important characteristics of each of the stages of bubble growth.

In the literature, both detonations and deflagrations have been discussed in connection with the quark-hadron transition (Van Hove (1983), Barz et.(1985), Seibert (1985,1987), Danielewicz and Ruuskanen (1987), etc.). It seems that, in practice, it is almost certainly deflagration fronts which are relevant here but the literature on these within the cosmological context is rather confused and it seems that the process as considered have not been well understood in general. In the second section of this chapter, we focus attention on the deflagration case and describe some of its interesting properties.

4.1 Classical bubble dynamics

We give here a brief introduction to the classical theory of bubble dynamics in order to provide a background for our later discussion. The extensive literature on this subject, starting

with the fundamental paper by Rayleigh (1917), has been reviewed by Plesset and Prosperetti (1977).

The subject divides naturally between the study of those bubbles whose interiors contain only vapour of the surrounding liquid and those where the internal medium is mainly composed of permanent gas. The first class subdivides further into cases where the surrounding liquid is superheated (boiling bubbles) or cool (cavitation bubbles). For boiling bubbles, the consideration of heat transfer is important whereas for growth of cavitation bubbles, the inertia of the liquid always dominates. We concentrate here on the growth of boiling bubbles.

At the phase interface, one has to consider conservation of mass, momentum and energy as well as the supply of latent heat necessary for continuing the evaporation of liquid into the bubble interior. Also, there is the effect of surface tension. Most studies, consider only the behaviour of a single bubble with spherical symmetry which is a good approximation for many purposes. From a mathematical point of view, the bubble growth problem is of the free-boundary-value type since the position and shape of the interface (which forms the boundary for each of the two separate regions) are not know until the solution has been completed.

Plesset and Zwick (1954) extended the pioneering work by Rayleigh, on cavitation bubble, to study the dynamics of vapour bubbles in a superheated liquid. According to their analysis (and the subsequent later work reviewed by Plesset and Prosperetti) the growth of the bubble proceeds as follows. After its formation, the rate of growth depends on the surface tension and on the thermal conductivity and inertia of the fluid. In the initial stages of the expansion, the pressure and surface tension forces

are nearly in equilibrium and the growth is slow. However, as the bubble radius increases, the effect of the surface tension decreases and the interface motion is accelerated. As the bubble expands, the rate of vapour inflow increases (since it is proportional to the square of the radius) and so a more rapid supply of latent heat is required in order to maintain the evaporation. This produces a substantial cooling in the bubble region which tends to reduce the pressure gradient in the liquid and to slow down the expansion. At this stage, both thermal and inertial effects limit the growth rate but cooling rapidly becomes dominant as the expansion slows down. In the final asymptotic stage, the growth is essentialy controlled by the rate at which heat can be transferred to the bubble wall.

In order to study bubble dynamics, some further simplifications are usually introduced. For small bubble expansion velocities the bubble interior is usually assumed to be uniform, so that the parameters which characterize it are set equal to the corresponding equilibrium values at the interface. Therefore, in the vapour phase the temperature is taken to be equal to the liquid temperature T at the bubble wall and the pressure $p_v(T)$ is set equal to the equilibrium vapour pressure for that temperature. In addition, viscosity and compressibility are neglected both in the vapour and in the liquid. Liquid incompressibility implies that the velocity of the liquid at a distance r from the bubble centre is

$$u(r,t) = \frac{R_s^2}{r^2} \dot{R}_s \qquad (4.1)$$

where R_s is the radius of the bubble boundary and $\dot{R}_s = dR_s/dt$ its velocity at the time t. From the Euler equations integrated between R_s and ∞ we obtain that the boundary obeys the relation

$$R_s\ddot{R}_s + \frac{3}{2}(\dot{R}_s) = \frac{p(R_s)-p_\infty}{\rho} \qquad (4.2)$$

where ρ is the liquid density, p_∞ is the pressure at large distances from the bubble (which is also the pressure everywhere in the liquid at the time of bubble formation) and $p(R_s)$ is the pressure in the liquid adjacent to the interface.

The relationship between the internal and external pressure in given by

$$p(R_s) = p_v(T) - \frac{2\sigma}{R_s} \qquad (4.3)$$

where σ is the surface tension, and inserting this expression into equation (4.2) gives

$$R_s\ddot{R}_s + \frac{3}{2}(\dot{R}_s) = \frac{1}{\rho}\left[p_v(T) - p_\infty - \frac{2\sigma}{R_s}\right] \qquad (4.4)$$

This is a specialized form of the Rayleigh-Plesset equation which is the fundamental equation used in classical studies of bubble dynamics. Further extensions may be made to include the effects of viscosity and mass exchange across the interface (see Prosperetti (1982) for the latter). In the following discussion, we will neglect the small variations of σ and ρ with temperature.

It is convenient to introduce a radius R_o defined by the relation

$$\frac{2\sigma}{R_o} = p_v(T_\infty) - p_\infty \qquad (4.5)$$

where T_∞ is the temperature of the liquid at large distances from the bubble. R_o is the radius of a bubble in equilibrium with its surroundings at a constant temperature T_∞ and it is assumed that the bubble expansion starts from an initial state similar to this. The equilibrium is an unstable one. Denoting by T_b the temperature at which the equilibrium vapour pressure is equal to

p_∞, i.e. $p_v(T_b)=p_\infty$, equation (4.5) implies $T_\infty > T_b$ and $\Delta T = T_\infty - T_b$ is referred to as the liquid superheat. Using equations (4.4) and (4.5), one can obtain

$$\frac{1}{2R_s^2\dot{R}_s}\frac{d}{dt}\left(R_s^3\dot{R}_s\right) = \frac{1}{\rho}\left[p_v(T)-p_v(T_\infty)+\frac{2\sigma}{R_o}\left(1-\frac{R_o}{R_s}\right)\right] \qquad (4.6)$$

and if the cooling effect of evaporation is disregarded so that $p_v(T)=p_v(T_\infty)$, this equation can be integrated to give

$$\dot{R}_s^2 = \left(\frac{R_o}{R_s}\right)^3\dot{R}_o^2 + \frac{4\sigma}{3\rho R_o}\left[1-(R_o/R_s)^3\right] - \frac{2\sigma}{\rho R_s}\left[1-(R_o/R_s)^2\right] \qquad (4.7)$$

which is referred to as the Rayleigh solution. In the limit $R \gg R_o$, this gives

$$\dot{R}_s^2 = \frac{4\sigma}{3\rho R_o} = \frac{2}{3\rho}\left[p_v(T_\infty)-p_\infty\right] \qquad (4.8)$$

which means that the expansion rate tends to a constant limit. However, the cooling effect tends to make the actual motion deviate from the solution given by equation (4.7) and the limit (4.8) can be only reached for high superheats.

The latent heat required in order to maintain liquid evaporation into the bubble is carried to the interface by means of conduction in the liquid and this situation is expressed by the following relation at $r = R_s$

$$-4\pi R_s^2 k_L \frac{\partial T}{\partial r} = L\frac{d}{dt}\left(\frac{4}{3}\pi R_s^2\rho_v\right) \qquad (4.9)$$

where L is the latent heat per unit mass, ρ_v is the vapour density and k_L is the thermal conductivity of the liquid. The temperature structure within the fluid is given by the equation

$$\frac{\partial T}{\partial t} + \frac{R_s^2}{r^2}\dot{R}_s\frac{\partial T}{\partial r} = \frac{D_L}{r^2}\frac{\partial}{\partial r}\left(r^2\frac{\partial T}{\partial r}\right) \qquad (4.10)$$

where D_L is the thermal diffusivity of the liquid, while the

pressure structure may be calculated using the general Bernoulli equation, from which one obtains

$$p(r,t) = p_\infty + \frac{R_s}{r}\left[p(R_s)-p_\infty\right] + \frac{1}{2}\rho\frac{R}{r}\dot{R}_s\left[1-\left(\frac{R_s}{r}\right)^3\right] \qquad (4.11)$$

Equations (4.1), (4.4), (4.9), (4.10) and (4.11) together with suitable initial and boundary conditions give a complete mathematical specification of the problem. At late times, one finds the asymptotic solution $R_s \propto t^{1/2}$.

In this discussion, the thermodynamic state of the vapour in the bubble has been assumed to correspond to conditions of thermodynamic equilibrium at the instantaneous bubble wall temperature. However, under some circumstances, deviations from equilibrium are important (Plesset (1964), Theofanous et al. (1969)). These can be estimated by considering the mass balance at the bubble wall.

$$\frac{d}{dt}\left(\frac{4}{3}\pi R_s^3 \rho_v\right) = 4\pi R^2 W \qquad (4.12)$$

where W is the net mass flux per unit area across the interface. The standard way of calculating W is as follows (see Plesset and Prosperetti (1976) and Theofanous (1969)). It is assumed that the velocities of the vapour molecules follow a Maxwellian velocity distribution and then one can use standard methods (Landau and Lifshitz (1959)) to calculate the mass fluxes away from the interface towards the body of the vapour and from the body of the vapour towards the interface. The difference between these is then the net flux into the bubble. The temperature and density of the incoming material are taken to be the temperature and equilibrium vapour density of the adjacent liquid (T_L, ρ_v^e). Corrections to the pure kinetic theory result (due to surface emission and absorption effects and deviation away from the

Maxwellian distribution) are represented by adjustable accomodation coefficients α and β. The flux formula is then given by

$$W = \left(\frac{R_g}{2\pi} \right)^{1/2} \left[\alpha \rho_v^e T_L^{1/2} - \beta \rho_v T_v^{1/2} \right] \qquad (4.13)$$

where T_v is the temperature of the vapour phase and R_g is the gas constant per unit molecular weight. It is conventional to set $\beta=\alpha$ (although the motivation for this is obscure for the case of dynamical bubble growth) and equation (4.13) then implies that the equilibrium solution ($T_v=T_L$, $\rho_v=\rho_v^e$) corresponds to $\alpha \to \infty$ which is, of course, strictly unphysical. However, the nature of the equilibrium assumption is classified by the following argument (after Plesset (1964)). Suppose that we take $T_v=T_L$, $\beta=\alpha$ and combine equations (4.12) and (4.13) neglecting the term in $d\rho_v/dt$. It is then possible to show that

$$\frac{\rho_v^e - \rho_v}{\rho_v^e} = \frac{M}{\alpha(1/2\pi\gamma)^{1/2} + M} \qquad (4.14)$$

where γ is the adiabatic index of the vapour and M is the dowstream Mach number. Equation (4.14) then implies that the equilibrium assumption is satisfactory provided that the bubble expansion is sufficiently slow. In the general case, however, one needs to solve the dynamical equations coupled with junction conditions across the interface and Theofanous et al. (1969) performed a calculation of this type. Their results for $\alpha=1$ are in good agreement with the equilibrium solution but non-equilibrium corrections become progressively more important as α is reduced (and the measured value of α for water is $\sim 10^{-2}$).

In discussing the classical bubble growth calculations our aim has been to emphasize the various factors involved and the importance of a proper treatment of each of the them. Although

the relativistic case requires a more complicated system of dynamical equations, classical bubble growth is a useful guide for implementing them.

4.2 Analysis of a discontinuity surface using the method of characteristics.

In this section we discuss the conditions under which the system of hydrodynamical equations (3.11), (3.13), (3.29), (3.32)-(3.37) and (3.39) plus the set of juction conditions (3.64), (3.65), (3.98), (3.102) and (3.104) completely determine the evolution of the transition front and the fluid flow in each phase once initial and the boundary conditions have been given (Miller and Pantano (1986)). As the system of hydrodynamical equations under consideration is hyperbolic, it is possible to rewrite them in characteristic form as seen in Section 3.3. All of the evolution equations were there rewritten as ordinary differential equations along the three families of characteristic curves in the μt plane. Physically these directions indicate how disturbances are propagated during the fluid motion (for details see Section 3.3.2). This way of rewriting the evolution equations is particularly useful for discussing causal structure either for continuous flow or in the presence of some discontinuity.

In the case of a continuous flow, suppose that we know the complete solution everywhere on some base time level t and want to calculate the new solution at the point X on a subsequent time level $(t+\Delta t)$ (see Figure 1). In order to find this solution we need to use data at points N, M and H where the forward, backward and advective characteristics, respectively, intersect the base

time level. Equations (3.56) are solved along the forward and backward characteristic directions to give u and p. Then ρ, R and m are calculated from equations (3.54), (3.59) and (3.60) along the advective characteristic while

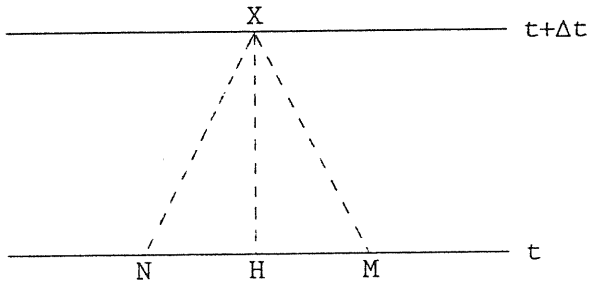

Fig. 1. Illustration of the characteristic solution at a normal point. XH is the advective characteristics while XN and XM are the forward and backward characterics respectively.

a is given by equation (3.34) which must be integrated across each time slice.

Consider now the situation for a phase interface. For stable physical solutions the interface always moves sonically or subsonically relative to the medium behind but, relative to the medium ahead, it may either move supersonically (giving a detonation front) or subsonically (giving a deflagration). In the case of a detonation, pressure and energy density are larger behind the interface than ahead of it while the reverse situation holds for a deflagration (see Courant and Friedrichs (1948), Landau and Lifshitz (1959)). The two cases are examined below.

Figure 2 shows the characteristic curves for points immediately ahead of and behind the interface in the case of a detonation front (notice that the scale is different in the two phases). As the interface is moving supersonically relative to

the medium undergoing the transition, all three characteristic curves may be drawn from the point just ahead of the interface back to the base time level. Then all of the hydrodynamical equations can be solved as well as the a equation whose boundary condition can be fixed in the medium ahead of the interface. This means that the state of the fluid ahead of the interface is completely determined by initial data in the same phase and so is not affected by the presence of the transition front. In the medium behind, only the forward characteristic can be drawn up to the fluid element just behind the interface. However, the junction conditions have to be satisfied across the interface and these together with the forward characteristic equation are

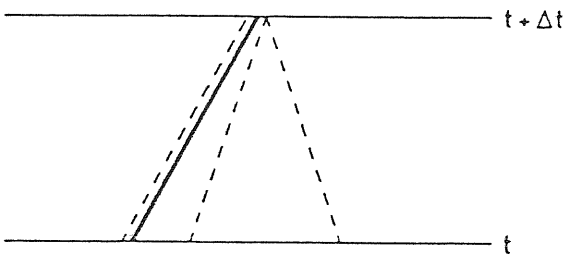

Fig. 2. Characteristic structure of a detonation solution. The heavy line marks the path of the interface.

exactly sufficient to fix completely the velocity of the transition surface and the values of u, p, ρ, a and R just behind it. Actually, the only possible solution for a self-sustaining detonation front is that corresponding to a Chapman-Jouguet process where the velocity of the medium behind relative to the interface is equal to the sound speed (Courant and Friedrichs (1976), Gyulassy et al. (1984)).

For a deflagration (which moves subsonically relative to the

medium ahead), the characteristic structure is as shown in Figure 3. In this case it is not possible to draw a forward characteristic up to the point just ahead of the interface since it would need to have a slope smaller than that of the interface path. This means that the state of the fluid just ahead is not now determined only by initial data in the medium ahead and so it is perturbed by the presence of the transition front. Moreover,

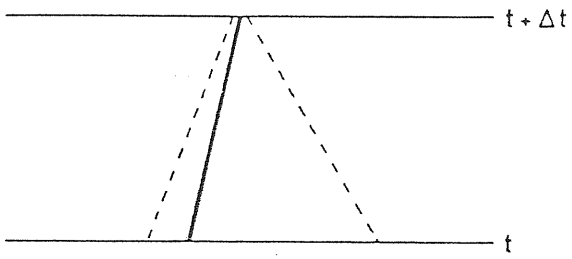

Fig. 3. The characteristic strcture of a deflagration solution.

the absence of the forward characteristic also means that the number of equations is one less than the number of unknowns. In order to close the system an additional equation is required and this should be an expression for the rate at which material is transformed from one phase to the other. Whether the transition front is supersonic or subsonic therefore deeply influences the way in which the transition proceeds: for a detonation, the hydrodynamics forces the rate of flow across the interface, while, for a deflagration, it is the rate of flow which controls the hydrodynamics.

4.3 Hydrodynamics of a deflagration front.

4.3.1 *Transition rate equation.*

For the quark-hadron transition, the front is likely to be a deflagration since a detonation requires much greater supercooling than is expected here (Seibert (1985)). If this is the case then we need an extra condition for closing the system of equations as shown in the previous section. In the literature, this extra condition has usually been provided in one of two ways, either by assuming that the velocity of the hadron medium is always zero (this requirement is connected with the construction of similarity solutions - Gyulassy et al. (1984), Kurki-Suonio (1985), Seibert (1985), Blaizot et al. (1986), etc.), or by fixing the temperature ahead of the interface equal to T_c (Applegate and Hogan (1985), Cleymans et al. (1986b), Kajantie and Kurki-Suonio (1986), etc.).

One expects to have a similarity solution in situations where there is no preferential scale and this is, at least, unclear in the present case. Significant scales include the nucleation scale, the scale defined by the evaporation process, the characteristic scales of strong, electromagnetic and weak interactions and the current Hubble radius. The assumption that the temperature ahead of the interface remains strictly equal to T_c during almost all of the transition (some initial supercooling being accepted for allowing bubble nucleation), seems to be fundamentally inconsistent as we will discuss in the next section. It is likely that the temperature ahead does, in fact, remain close to T_c but the expected small deviations away from this are nevertheless crucial.

From a physical point of view, the extra condition should be obtained by setting the hydrodynamical flux (F_H) across the

interface equal to F_t, the rate at which energy passes from one phase to the other as derived from considerations of the transition process. The imposition of any other condition effectively determines F_t. A simple expression for this quantity is given by

$$F_t = \alpha \left[F(T_q) - F(T_h) \right] \tag{4.15}$$

where $F(T_q)$ represents the thermal flux from the interface (at temperature T_q) into the bubble, $F(T_h)$ is the corresponding flux from the hadronic matter towards the bubble wall and α is an accommodation coefficient which takes account of deviations away from the ideal situation. This expression is analogous to the one discussed in Section 4.1 for the net mass transfer across a vapour-liquid interface in classical bubble dynamics (Theofanous et al.(1969)). It is an idealization to take F_t equal to the thermal flux given by (4.15) since the correct expression would be more complicated and would have to be calculated on the basis of detailed considerations concerning the conversion of quarks into hadrons. Several detailed calculations on the hadronization rate have been made within the context of heavy ion collisions where one considers evaporation from the surface of the quark matter into vacuum (Danos and Rafelski (1983), Banerjee et al. (1983), Müller and Eisenberg (1985)). However these are not directly applicable to the present case where leptons are also present and the evaporation is not into vacuum. In the absence of improved calculations, equation (4.15) provides a fair approximation with the uncertainties being included in the accommodation coefficient α.

Using the equation of state (2.39) for the hadron phase, equation (4.15) becomes

$$F_t = \frac{1}{4}\,\alpha\, g_h \left(\frac{\pi^2}{30}\right)\left(T_q^4 - T_h^4 \right) \qquad (4.16)$$

This has the important feature that for $T_q = T_h$, the hydrodynamical energy flux across the interface is equal to zero. In the limit in which the temperatures in the two phases are close to T_c we can write:

$$F_t = \alpha\, g_h \left(\frac{\pi^2}{30}\right) T_c^4 \left(\frac{\Delta T}{T_c}\right) \qquad (4.17)$$

with $\Delta T = T_q - T_h$. This expression is not in agreement with the result claimed by Applegate and Hogan (1985) that $F_H \propto (\Delta T/T_c)^{1/2}$. They obtained this using the junction conditions together with the assumption $T_q = T_c$ apparently not realising that, far from being an innocuous approximation, this is a drastic assumption which determines the solution in a non-physical way. It is a fundamental feature of deflagration solutions that the energy flux is not determined by the hydrodynamics but must be given by an additional separate condition. While the formula (4.17) is approximate and subject to modification, we expect that the true relationship is still likely to give $F_t \propto (\Delta T/T_c)$.

4.3.2 *Plane deflagration transition fronts.*

We want now to examine which kinds of constraint the transition rate expression puts on the hydrodynamics of a deflagration transition front. The analysis presented here is for the case of a plane interface in the special relativistic limit. However, the conclusions drawn can be extended to a spherical transition front at least when the radius is large and the gravitational corrections are small.

In the rest frame of the interface, energy-momentum

conservation across the front simply reduces to the continuity of the T^{01} and T^{11} components of the stress-energy tensor (3.16), namely

$$(e_h+p_h)\gamma_h^2 v_h = (e_q+p_q)\gamma_q^2 v_q \tag{4.18}$$

$$p_h + (e_h+p_h)\gamma_h^2 v_h^2 = p_q + (e_q+p_q)\gamma_q^2 v_q^2 \tag{4.19}$$

where the subscripts h and q refer as usual to the hadron and quark phases respectively, v is the fluid three velocity in the rest frame of the interface and $\gamma=(1-v^2)^{-1/2}$. Combining equations (4.18) and (4.19) one obtains the following expressions for the velocities v_h and v_q:

$$v_h^2 = \frac{(p_q-p_h)(e_q+p_h)}{(e_q-e_h)(e_h+p_q)} \tag{4.20}$$

$$v_q^2 = \frac{(p_q-p_h)(e_h+p_q)}{(e_q-e_h)(e_q+p_h)} \tag{4.21}$$

Using the expressions (2.36) and (2.37) for the quark phase and (2.38) and (2.39) for the hadron phase one gets

$$v_h^2 = \frac{1}{3}\frac{(e_q-e_h-4B)(3e_q+e_h)}{(e_q-e_h)(e_h+e_q-4B)} \tag{4.22}$$

$$v_q^2 = \frac{1}{3}\frac{(e_q-e_h-4B)(3e_h+e_q-4B)}{(e_q-e_h)(3e_q+e_h)} \tag{4.23}$$

The energy flux in the hadron phase measured in the rest frame of the interface, is equal to

$$\begin{aligned} F_H &= (e_h+p_h)\gamma_h^2 v_h \\ &= \frac{\left[(e_q-e_h)(p_q-p_h)(e_h+p_q)(e_q+p_q)\right]^{1/2}}{e_q-p_q-e_h+p_h} \end{aligned} \tag{4.24}$$

which is, of course, also equal to the corresponding flux in the quark phase. Cleymans et al. (1986b) claimed that the expression (4.24) is sufficient for calculating the energy flux across the interface as a function of T_h since, in their view, the deviation of the quark temperature T_q away from T_c can be neglected. The same comments apply as above. Figures 4-6 show the value of F_H given by (4.24) (solid line) and the value of F_t given by (4.16) (dashed line) plotted as functions of T_h for a given value of T_q.

We take $F_H=F_t$ and this gives a relation between the temperatures ahead of and behind the interface. For the equations of state (2.36)-(2.39) this relation is

$$\frac{1}{4}\alpha g_h\left(\frac{\pi^2}{30}\right)\left(T_q^4-T_h^4 \right) = \frac{\left[(e_q-e_h)(e_q-e_h-4B)(3e_h+e_q-4B)(3e_q+e_h)\right]^{1/2}}{2\sqrt{3}\ (e_q-e_h+2B)} \tag{4.25}$$

In the T_h-T_q plane, equation (4.25) gives the curves shown in

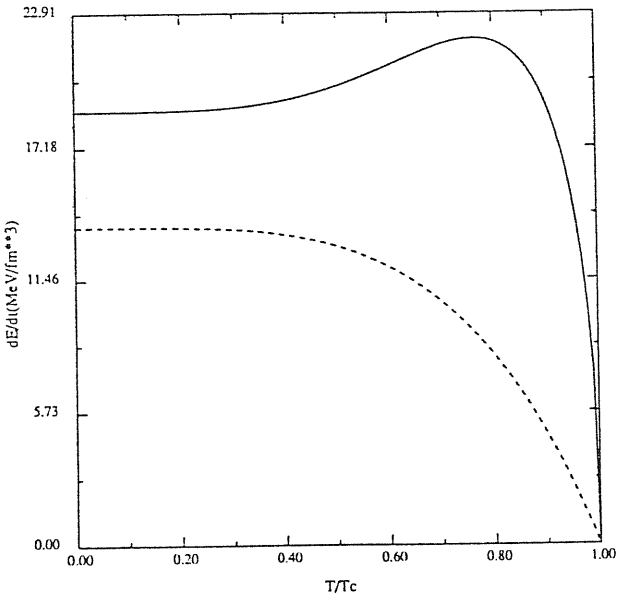

Fig. 4. Behaviour of F_H (continuous line) and F_t (dashed line) as functionS of T_h/T_c for $T_q/T_c=1$.

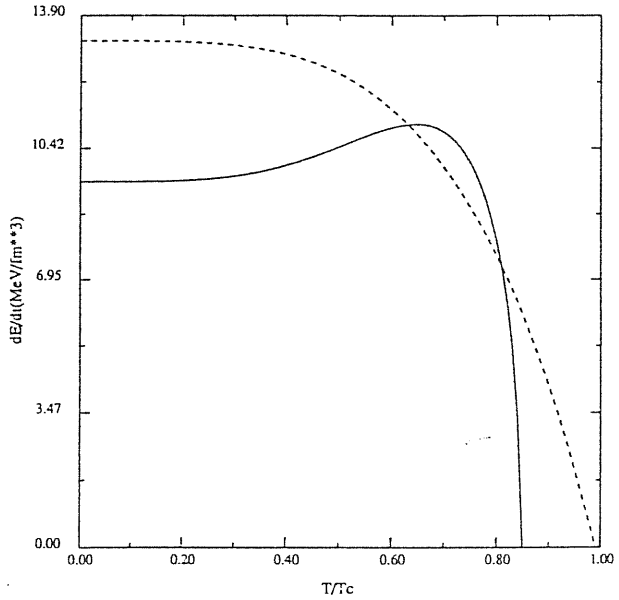

Fig. 5. As in Figure 4 for T_q/T_c=0.990.

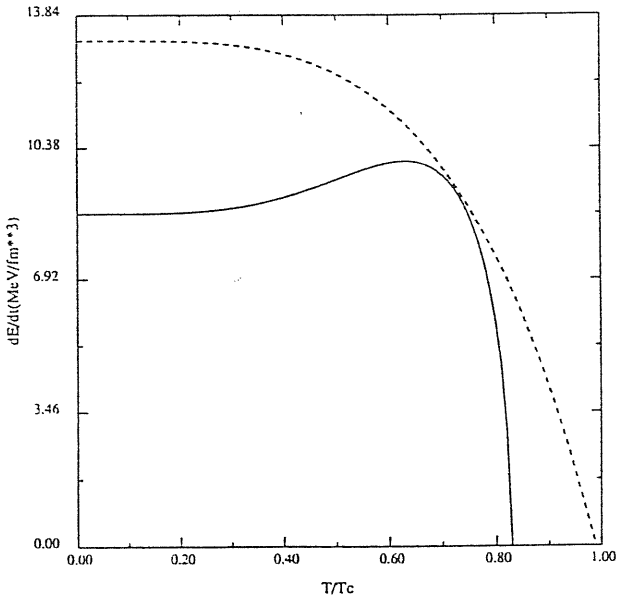

Fig. 6. As in Figure 4 for T_q/T_c=0.989.

Figures 7-8 which are drawn for two different values of the accommodation coefficient α. The points on these curves

correspond to intersection points such as those shown in Figures 4 and 5.

Let us concentrate on Figure 7 which has been obtained for α=1. We can see that for T_q=T_c, T_h also has to be equal to T_c and therefore there is no energy flux across the interface. This fact shows that the transition cannot proceed if T_q=T_c and small deviations from it are important for having any phase transformation at all.

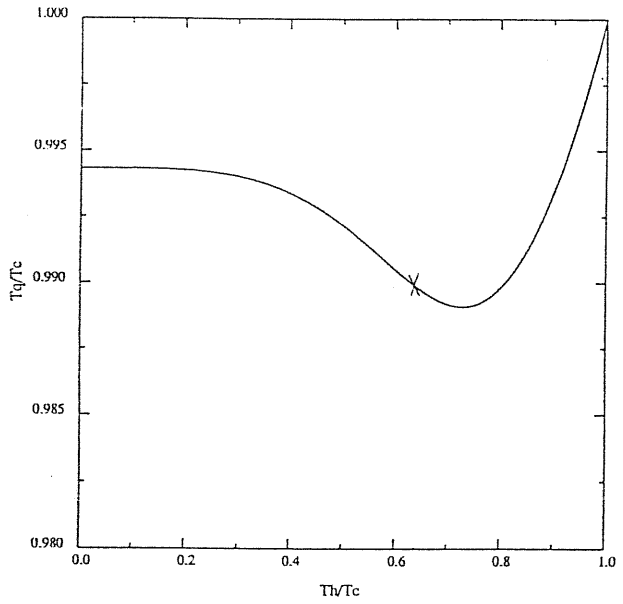

Fig. 7. Relation between T_q and T_h for a plane deflagration Transition front for α=1. The cross indicates a Chapman-Jouguet process.

The second important point illustrated by the plot is that, for α=1, T_q cannot be lower than 0.989 T_c which represents a very small variation from T_c. The minimum for T_q depends on α, as one expects, and it decreases as α decreases (compare Figures 7-9) but even for α as small as 0.6 it is still larger than 0.98 T_c.

The behaviour of the fluid velocities corresponding to the

allowed coupled values of T_q and T_h is the following: both v_h and v_q increase for decreasing values of T_h and in the case of a Chapmann - Jouguet (CJ) process (i.e. v_h equal to the sound speed v_s in the hadron phase) $v_q|_{CJ}$ is as large as 1.2×10^{-2}. The Chapman-Jouguet point is indicated by a cross on the curve $T_q(T_h)$.

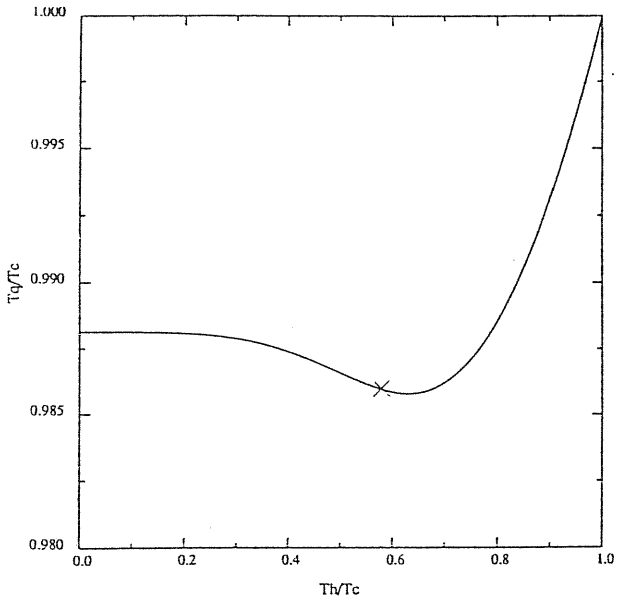

Fig. 8. As in Figure 7 for α=0.6.

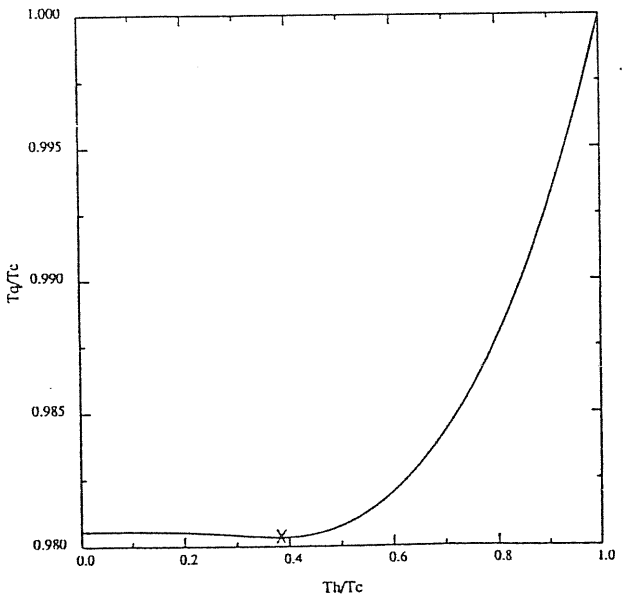

Fig. 9. As in Figure 7 for α=0.1.

For decreasing values of α, $v_q|_{CJ}$ also decreases. Since the part of the $T_q(T_h)$ curve to the left of the CJ point corresponds to strong deflagration fronts ($v_h>v_s$) which are not allowed solutions (see Courant and Friedrichs (1976)), $v_q|_{CJ}$ represents the maximum velocity relative to the medium ahead which can possibly be reached by a deflagration transition front.

On the basis of this analysis we can derive two important conclusions: (i) the temperature in the quark phase must be smaller than the critical temperature T_c in order for the phase transformation to proceed; (ii) only small deviations of T_q away from T_c seem to be allowed, at least for $\alpha>0.6$.

It is interesting to notice that for a range of temperatures T_q above the minimum of the curve $T_q(T_h)$, two possible values of T_h are consistent with the same value of T_q. This could be related to instability phenomena already observed in classical deflagration fronts. In general, instabilities are often related to double valued solutions.

Although our solutions use a simplified expression for F_t, our conclusions, at least on the point concerning the quark phase being below the critical temperature T_c, should be correct even in the case of a more accurate expression for F_t. T_c represents the temperature at which the two phases can coexist in equilibrium and any expression for the transition rate has to give $F_t=0$ for $T_q=T_h=T_c$. In the presence of a curved interface with surface tension, we expect equilibrium to be possible at some slightly lower temperature $T_q=T_h=T_N$ and the phase transformation then proceeds when the equilibrium is perturbed in some way such as, for the cosmological quark-hadron transition, by the general expansion of the universe.

CHAPTER V

COMPUTATIONS OF BUBBLE GROWTH DURING THE QUARK-HADRON PHASE TRANSITION

In this chapter we apply the formalism introduced in Chapter III to the particular system in which we are interested, i.e. to the growth of a bubble during the cosmological quark-hadron transition.

In the literature, this problem has already been discussed under particular assumptions or restrictions. Van Hove (1984) made the assumptions of entropy conservation and of the temperature everywhere returning rapidly to the transition temperature T_c after bubble nucleation. On this basis he found that the bubble expansion velocity would be very low ($\sim 10^{-11}$). Similarity solutions have been studied by Kurki-Suonio (1986) in a discussion of deflagration transition fronts (see also Kajantie and Kurki-Suonio (1987)). As mentioned earlier, there are doubts about whether these methods are applicable here and even if they are, one would still need to clarify why one similarity solution from the infinite family should be preferred to the others (Zel'dovich and Raiser (1967)). Witten (1984), DeGrand and Kajantie (1984) and Iso et al. (1986) made overall conceptual analyses with various simplifying approximations. It is a general result that the bubble expansion velocity increases with the degree of supercooling.

Our aim in this computation is to relax all of the

restrictive conditions imposed in the above papers and to determine the bubble growth velocity and the fluid flow in both phases as a correctly formulated initial value problem. In addition, for the first time, the effect of surface tension on hadron bubble dynamics is also included.

It is important to stress that, although we have restricted our attention to the confinement transition, the method which we present can also be applied for studying bubble growth during earlier cosmological phase transitions. For these the method used until now is, in a certain way, opposite to the one which has been followed in the confinement transition. The space-time is described by different metrics inside and outside the new phase bubble and the motion of the bubble wall (within which there is a surface tension σ), is derived from the junction conditions across the time-like hypersurface separating the two phases (Berezin et al. (1983 b,c), Maeda (1986), Laguna-Castillo and Matzner (1986), for false vacuum bubble see also Blau et al. (1987)).

Our method, instead, provides a numerical solution of the coupled system of hydrodynamical and surface equations and therefore gives the evolution of the system from the nucleation epoch.

The hydrodynamical equations in the two bulk phases are integrated using a largely explicit two step finite difference method (Richtmyer and Morton (1967), May and White (1967), Potter (1973)). Particular care is required in solving the junction conditions at the interface and this is done with the aid of the characteristic form of the hydrodynamical equations. Characteristic equations have previously been used for treating boundary surfaces and shock discontinuities both in newtonian

hydrodynamics (Keller et al. (1960), Hoskin (1963), Henshaw (1987)), and in special relativy (McKee and Colgate (1973)), but here they are applied for the first time to study the evolution of a surface layer. This case is more difficult to handle because a surface layer corresponds to a δ-function singularity of the stress-energy tensor; in other words, the discontinuity surface is characterized by an intrinsic tension and energy density which make the solution of the junction conditions at the interface much more difficult.

In this chapter we review first the system of hydrodynamical equations and junction conditions which we use in the numerical treatment. Some of the junction conditions are also rewritten in a form more convenient for the numerical calculation. Initial and boundary conditions are then discussed in detail. Following this, we present the numerical integration scheme and, finally, discuss the results obtained for two different transition rates.

5.1 Basic equations

5.1.1 *Hydrodynamical equations in the two bulk phases.*

To clarify the presentation of the numerical scheme, we repeat here the set of hydrodynamical equations, for a spherically symmetric system, derived in chapter III. Their order is the same as that followed in the numerical integration.

$$R_t = au \tag{5.1}$$

$$\frac{(\rho R^2)_t}{\rho R^2} = -\frac{a_\mu}{R_\mu} \tag{5.2}$$

$$e_t = w\,\rho_t \tag{5.3}$$

$$\frac{(aw)_\mu}{aw} = \frac{(e_\mu - w\rho_\mu)}{\rho w} \tag{5.4}$$

$$m_\mu = 4\pi e R^2 R_\mu \tag{5.5}$$

$$\Gamma^2 = 4\pi\rho R^2 R_\mu = 1 + u^2 - 2Gm/R \tag{5.6}$$

$$b = (4\pi\rho R^2)^{-1} \tag{5.7}$$

$$u_t = -a\left[\frac{\Gamma p_\mu}{b(e+p)} + \frac{Gm}{R^2} + 4\pi GpR\right] \tag{5.8}$$

$$p = p(e) \tag{5.9}$$

The mass function m is also calculated by using the alternative equation:

$$m_t = -4\pi p R^2 R_t \tag{5.10}$$

The above set of equations is used for studying the evolution in both bulk phases, each of which is characterized by a different equation of state.

It is useful to derive also an alternative form for the constraint equation (5.4). From the first law of thermodynamics we have:

$$\rho T\, ds = de - w\, d\rho \tag{5.11}$$

where s is the specifis entropy. By using equation (5.3) and the fact that for a perfect fluid the motion is adiabatic (i.e. s_t=0)

we have

$$\rho T\, s_{\mu} = e_{\mu} - w\rho_{\mu} \tag{5.12}$$

which combined with equation (5.4) gives

$$\frac{(aw)_{\mu}}{aw} = \frac{Ts_{\mu}}{w} \tag{5.13}$$

For a one-parameter equation of state, it is possible to integrate equation (5.13); in fact, in this case, s = w/T and then equation (5.13) reduces to

$$aT = \text{const.} \tag{5.14}$$

By using the equations of state (2.36) and (2.37) or (2.38) and (2.39) we have

$$a\,(e+p)^{1/4} = \text{const.} \tag{5.15}$$

Equations (5.15) can be applied as long as the fluid properties are continuous and we do not introduce any dissipative processes. In our case it has to be applied separately in each phase and the constants of integration are different in the two cases but not independent. The metric factor a is set equal to unity at large R thus synchronizing the coordinate time t with time as measured by a FRW fundamentalobserver at infinity. Then we have in the quark phase

$$a = \left(\frac{e_{\infty}+p_{\infty}}{e+p} \right)^{1/4} \tag{5.16}$$

and in the hadron phase

$$a = a_{-} \left(\frac{e_{-}+p_{-}}{e+p} \right)^{1/4} \tag{5.17}$$

where the subscript ∞ refers to distant points that have not yet

felt the effect of the transition and the subscript - refers as usual to quantities just behind the interface obtained by applying the junction conditions.

We convert the previous set of differential equations into difference equations on a finite mesh grid of between 25 and 75 zones depending on the stage of calculations. Each zone corresponds to a spherical shell of matter with shell boundaries identified by a time independent value of μ and indexed by a subscript j. One computational cycle advances the solution from the time level t^n (base time level) to $t^{n+1} = t^n + \Delta t^{n+1/2}$, where $\Delta t^{n+1/2}$ is the time step which is varied according to computational requirements. Truncation errors are minimized by taking $\Delta\mu$=constant and the initial $\Delta\mu$ is chosen such that the interface coincides with a zone boundary at the beginning of the calculation. The equations are written in the system of units mentioned at the beginning and we use the fm as the fundamental unit.

5.1.2 *Calculation of interface quantities.*

The transition front acts as an internal boundary for the system and solutions in the two bulk phases are connected there by the junction conditions discussed in Section 3.4 and the transition rate expression presented in Section 4.3 Actually, in our calculation we do not use the junction equations in the form shown in Section 3.4, but we specify them for the case $\sigma = -\alpha =$ constant. Then equation (3.98) reduces to

$$\left[(e+p)R^2 b\dot{\mu}_s\gamma^2/a\right]^{\pm} = 0 \qquad (5.18)$$

which can be shown to be equivalent to the simpler form

$$\left[\ aw\ \right]^{\pm} = 0 \tag{5.19}$$

using equations (5.7), (3.64) and (3.94). When $\sigma = -\alpha =$ constant it follows that

$$\frac{d}{d\tau}\left(\sigma R^2\right) + \alpha \frac{dR^2}{d\tau} = 0 \tag{5.20}$$

which shows that the increase in total energy of the interface is due only to the work done by the surface tension. There is no flow of energy from the two media to the interface.

Under the same hypothesis, equation (3.102) becomes

$$\left[\ e^2 b^2 \dot{\mu}_s^2 + pa^2\right]^{\pm} = -\frac{\sigma}{2} f^2 \left\{ \frac{1}{ab}\frac{d}{dt}\left[\frac{b^2\dot{\mu}_s}{c}\right] + \frac{f_\mu}{ab} + \frac{2}{fR}\left(ub\dot{\mu}_s + a\Gamma\right)\right\}^{\pm} \tag{5.21}$$

In spherical coordinates the hydrodynamical flux equation (4.15) assumes the form

$$\frac{aw\dot{\mu}_s}{4\pi R_s^2\left(a^2 - b^2\dot{\mu}_s^2\right)} = F_t \tag{5.22}$$

where F_t is the transition rate as given by microscopic considerations. Equation (5.22) can be rearranged to give an explicit expression for $\dot{\mu}_s$:

$$\dot{\mu}_s = 4\pi\rho_+ R_s^2 a_+ \frac{(1+\xi)^{1/2} - 1}{\xi}$$

$$\text{with} \qquad \xi = \frac{2F_t}{(e+p)_+} \tag{5.23}$$

Following the discussion in Section 4.3, we use for F_t the corrected net thermal flux expression and then, for the equations of state which we are considering, we obtain

$$\xi = \frac{\alpha g_h (\pi^2/30)(T_+^4 - T_-^4)}{2(e+p)_+} \tag{5.24}$$

The metric junction condition (3.64) and equation (5.19) are combined so that we obtain

$$x^4 + \left[1 + \left(\frac{b_+\dot{\mu}_s}{a_+}\right)^2\right] x^2 - \left[\frac{(e+p)_+}{(e+p)_-}\left(\frac{b_+\dot{\mu}_s}{a_+}\right)^2\right] = 0 \tag{5.25}$$

$$\rho_- = \rho_+ \times \frac{(e+p)_+}{(e+p)_-} \tag{5.26}$$

with $x = (a_-/a_+)$.

Finally the junction condition (3.65), is written as an explicit expression for u_- where we keep only the negative root since this satisfies the velocity relation for a deflagration front ($v_- > v_+$, v being the fluid velocity in the rest frame of the interface):

$$u_- = \frac{\left\{ a_- A - b_-\dot{\mu}_s \left[A^2 + \left(a_+^2 - b_+^2\dot{\mu}_s\right)\left[1 - \frac{Gm_-}{R_s}\right]\right]^{1/2} \right\}}{\left(a_+^2 - b_+^2\dot{\mu}_s\right)}$$

$$\text{with} \quad A = a_+u_+ + b_+\dot{\mu}_s\Gamma_+ \tag{5.27}$$

Equations (5.19), (5.21), (5.23), (5.25) - (5.27) are the five junction conditions to be imposed at the interface. In Section 3.3, we also mentioned the condition for the mass function m which is not, however, used directly in the code because m is computed on the two sides of the interface in such a way that it satisfies (3.104) automatically.

In order to impose the junction conditions accurately, we need the values of fluid variables immediately ahead of and behind

the interface, while the finite difference scheme gives values only at grid points (or half zones). In addition, the presence of the interface prevents correct centring of the difference equations in the two adjacent zones and, therefore, any extrapolation to the interface points making use of values computed in these particular zones looks quite doubtful. This difficulty may be overcome by using characteristic equations. We have seen in Section 3.4, how information flows along characteristic directions and so it seems natural to use them for calculating the interface quantities which must be inserted into the junction conditions.

The characteristic structure of a deflagration front has already been illustrated in Section 4.2. Here, in Figure 1, we show again the interface path SS' and the characteristic curves from the interface position at t^{n+1} back to the base time level t^n. Mesh points are also shown with j_s being the grid point nearest to the interface.

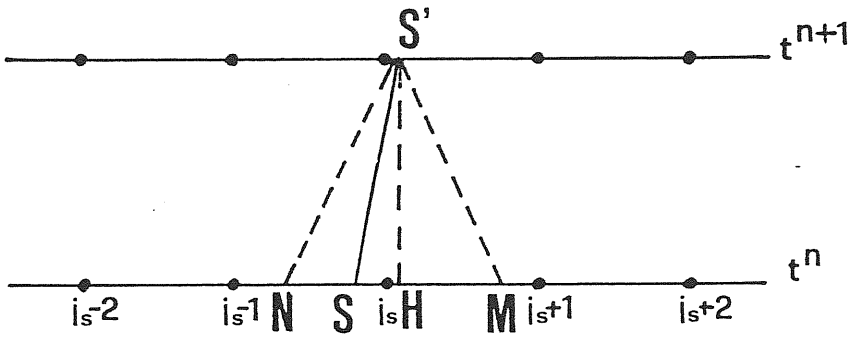

Fig. 1. Motion of the deflagration transition front across the grid. SS' is the interface path and characteristics are shown with dashed lines.

In the fluid ahead, we have the following equations along the advective characteristic HS' (i.e. along $d\mu = 0$):-

$$dR = au\ dt \tag{5.28}$$

$$dm = -4\pi pR^2 au\ dt \tag{5.29}$$

$$d\rho = \frac{1}{wc_s}\ dp \tag{5.30}$$

while along the backward characteristic MS', given by

$$d\mu = -\ 4\pi\rho R^2 c_s a\ dt \tag{5.31}$$

we have:

$$du - \frac{\Gamma}{\rho wc_s}\ dp + \left[-\ 2au\Gamma c_s/R + aG\ \left(m/R^2 + 4\pi pR\right)\right] dt = 0 \tag{5.32}$$

and along the forward characteristic in the fluid behind, given by

$$d\mu = +\ 4\pi\rho R^2 c_s a\ dt \tag{5.33}$$

we have:

$$du + \frac{\Gamma}{\rho wc_s}\ dp + \left[\ 2au\Gamma c_s/R + aG\ \left(m/R^2 + 4\pi pR\right)\right] dt = 0 \tag{5.34}$$

As discussed in the previous chapter, the set of equations (5.4), (5.19), (5.21), (5.23) and (5.25) - (5.34) is sufficient to completely determine the interface variables. Because of its complexity, the system has to be solved by an iterative procedure at several levels.

The quantities which we need to compute at the transition discontinuity are: the position μ_s of the interface, its velocity $\dot{\mu}_s$, the radial coordinate R_s and for each phase the metric component a, the fluid variables e, p, ρ, u and the mass function m.

The outer iteration in the interface calculations concerns the position of the deflagration front at the new time level. In the first loop, μ_s is calculated by using for $\dot{\mu}_s^{n+1/2}$ a value obtained by linear extrapolation from the values at the two previous time levels.

We then proceed to solve the equations for matter on the metastable phase side. As we have already discussed in the previous chapter, the state of the fluid ahead of the interface is not independent of conditions behind it and so, in principle, one should solve the equations for fluid ahead and behind simultaneously with the junction conditions.

The procedure used here is the following:-

a) A value for T_+ is estimated by extrapolation (as for $\dot{\mu}_s$) and then all of the other variables just ahead of the interface may be evaluated in terms of this.

b) e_+ and p_+ are computed from the equation of state and then ρ_+ is calculated using the advective equation (5.30). Thus all of the quantities required for calculating w_+ are known and then the constraint equation (5.4) can be solved for a_+.

c) The advective equation (5.28) is solved for R_s.

d) The position of the foot of the backward characteristic is determined by (5.32) and u_+ is computed using (5.31).

e) Equation (5.29) for the mass function is solved.

The steps c), d) and e) are initially carried out using data at the base time level in one-sided difference formulae. When provisional values at the new time level have been calculated in this way, these can then be used to centre the differences at successive stages of the iterative procedure in which steps b)-d)

are repeated until convergence is obtained.

f) Next Γ_+ and b_+ are found using equations (5.6) and (5.7).

g) A provisional value for e_- is next obtained by an extrapolation similar to that used for $\dot{\mu}_s$.

h) p_- is calculated using the equation of state. Equation (5.5) for m is integrated and the interface velocity is computed from equation (5.23).

i) Equation (5.25) for the a_-/a_+ ratio is solved by the Newton-Raphson method with the initial estimate being a value extrapolated in the usual way. Then ρ_- is calculated from equation (5.26).

j) Equation (5.27) gives u_-.

k) The position of the foot of the forward characteristic is calculated from equation (5.34).

l) The forward characteristic equation (5.33) is used for obtaining successive improved values of e_- by means of a secant iteration looping over steps h) to l). The two initial estimates required for this are given by (i) the extrapolated value introduced at step g) and (ii) a value obtained by an explicit solution of equation (5.33) at the end of the first pass through the loop.

m) Successive improved values of T_+ are obtained from the junction condition equation (5.21) also by using a secant iteration. The two initial estimates required for this are given by (i) an extrapolated value obtained in the usual way (see point a)) and (ii) a small perturbation away from this. The iteration loops from b) to m).

The values of variables at the feet of the characteristic curves (points H, M and N in Figure 1) are calculated by linear interpolation. We choose as interpolation points the position of the interface at the base time level (point S) and the points $j_{s\pm1}$ or $j_{s\pm3/2}$ for zone boundary or mid-zone quantities respectevely.

At this point $\dot{\mu}_s^{n+1/2}$ is calculated by using $\dot{\mu}_s^{n+1}$ as obtained above. If the extrapolated value of $\dot{\mu}_s^{n+1/2}$ was not accurate enough, the interface position can be computed again and then steps b)-m) repeated. Convergence in this case is made faster by considering as initial values in all iterations the ones obtained at the end of the previous secant iteration for T_+. However this outer iteration is not usually necessary since the interface velocity changes in a regular way and the extrapolated value is often a very good estimate of the true $\dot{\mu}_s^{n+1/2}$.

5.1.3 *Shock treatment and artificial viscosity*

In principle we can treat shocks formed during the evolution with the same method as used for the transition surface. Actually, for a shock discontinuity the system of equations to be solved and the iteration scheme would be simpler than in the case discussed above. The metric junction conditions are the same, while energy and momentum conservation are given by equations (3.105) and (3.106). As the shock moves supersonically relative to the medium ahead, the state of the fluid ahead is unperturbed by the presence of the shock. Therefore the characteristic structure is the same as that for a detonation front and the energy flux is completely determined by the dynamics of the system (see Section 4.2).

In our code, however, we have chosen to handle possible shocks by means of an artificial viscosity (cf. Richtmyer and Morton (1965)). The introduction of an artificial bulk viscosity is based on the observation that, although a fluid may be properly described in many circumstances by non-dissipative evolution equations, viscous forces and heat conduction can no longer be neglected in the presence of a sufficiently strong compression.

It is a natural consequence of the non-linearity of the fluid flow equations that the kinetic energy associated with acoustic disturbances tends to be channelled progressively to higher and higher wavenumber modes. In nature, this process is always eventually terminated by the action of dissipative mechanisms which convert this kinetic energy into internal energy of the fluid. When we treat a shock as a discontinuity in the solution of non-dissipative evolution equations, we simply make the idealization that all dissipative and entropy-producing mechanisms operate only within an infinitesimal surface layer.

On a computational mesh, there is an upper limit to the wavenumber that can be reached corresponding to a wavelength of two zones. In the absence of dissipation, energy builds up in oscillations with this wavelength which grow and destroy the solution preventing the calculation of shock behaviour unless a dissipative mechanism is added. This can be provided either by intrinsic diffusion within the difference scheme or by means of an explicitly added artificial viscosity.

Von Neumann and Richtmyer first suggested the introduction of a wavelength dependent artificial viscosity which has a neglegible effect for long wavelength modes and becomes important only for short wavelengths. This spreads shocks over several zones of the

mesh and automatically ensures that the junction conditions are satisfied. A suitable artificial viscosity for use with spherically symmetric relativistic problems is given by (May and White (1967))

$$Q = \begin{cases} k^2 \rho/\Gamma \left(\Delta\mu/R^2\right)^2 \left[\left(R^2 u\right)_\mu\right]^2 & \text{if } \rho_t > 0 \\ 0 & \text{if } \rho_t < 0 \end{cases} \qquad (5.35)$$

Clearly, Q operates only in the case of a compression. The coefficient k^2 is commonly set equal to two.

Although the effect of artificial viscosity is very small outside shock regions, we have noticed that its presence is also important in our calculation when we perturb the initial conditions and the system has to relax to a consistent solution.

5.2 Initial conditions.

5.2.1 *Conditions at the nucleation time.*

We start to study the evolution of the bubble from the moment immediately after its nucleation and so the interface discontinuity is already present at the initial time and the initial data have to satisfy the junction conditions. At this time, the system is taken to be in thermal equilibrium at a temperature T_n with the medium being everywhere uniform within each phase. In the numerical calculation T_n is treated as a parameter whose value is related to the surface tension $\gamma = \gamma_0 T_c^3$ through the relation (3.127). The critical radius of a bubble nucleated at temperature T_n is

$$R_s(T_n) = \frac{2\gamma}{p_h - p_q} \tag{5.36}$$

Throughout Section 5.2 the subscripts h and q will indicate values of the various quantities in the hadron and quark phases respectively at the nucleation time.

Since the temperature is constant, it follows from equation (5.23) that $\dot{\mu}_s = 0$ and from equations (5.25) and (5.27) we then obtain

$$a_+ = a_- \tag{5.37}$$

$$u_+ = u_- \tag{5.38}$$

where the value of a_+ at infinity is fixed by the time synchronisation condition mentioned earlier. Using equations (5.16) and (5.17) we obtain $a = 1$ everywhere. From equation (5.18) we compute the relationship between the compression factors

$$\rho_- = \frac{(e_h + p_h)}{(e_q + p_q)} \rho_+ \tag{5.39}$$

and using the equations of state (2.36) - (2.39) we obtain $\rho_- = (g_h/g_q)\ \rho_+$. The value of ρ is set equal to one everywhere in the homogeneous quark medium immediately before the nucleation of the bubble and we assume that its value at all points of the quark medium is not changed significantly by the bubble formation process. Therefore, immediately afterwards, $\rho_+ = 1$ and this gives $\rho_- = 0.17$.

The velocity field near to the bubble just after nucleation is difficult to estimate precisely but it is safe to say that the values will be small enough to be neglected. Further away, it is reasonable to assume that the velocity field has not been

significantly changed by the nucleation process so that is still given by the solution for a FRW universe in the quark phase.

Equation (5.36) which has been obtained from a classical discussion, also corresponds to the limit of the momentum equation (5.21) for $\dot{\mu}_s = 0$, ρ constant in each phase and $a_{\pm} = 1$. The mass function m is discontinuous at the interface because of the surface energy density contribution, namely

$$[\, m \,]^{\pm} = 4\pi R_s^2 \sigma \tag{5.40}$$

The value of m at all points is obtained by integrating (5.5) on the time slice with the condition (5.40) on the interface. At the nucleation time the relativistic correction to relation (5.40) is very small and can be neglected.

The last quantity which we need to specify is the relativistic Γ factor. According to the standard model, the evolution of the early universe is well approximated by a flat FRW model and therefore immediately before nucleation Γ is equal to one everywhere. The nucleation process cannot change the situation substantially and so we assume that Γ is equal to one everywhere also immediately after nucleation.

The state of the system at the nucleation time can therefore easily be calculated as long as we know T_n but unfortunately these conditions cannot be applied directly as initial conditions for the numerical calculation because the initial evolution is so slow that round-off errors dominate and destroy the solution. Instead, one must perturb the state at the nucleation time and set initial conditions accordingly.

5.2.2 *Perturbation of conditions after nucleation.*

The following physical considerations suggest a way of introducing a perturbation of the conditions after nucleation. We have seen that the bubble is first formed at rest with respect to the metastable medium but, as the universe expands further and cools, the equilibrium condition (5.36) ceases to be satisfied. The pressure inside the bubble becomes greater than the effective pressure outside (surface tension forces also being taken into account) and the bubble expands compressing and reheating the medium ahead. Matter transformation starts at the bubble boundary and the latent heat released goes both into accelerating the interface and into thermal and kinetic energy of the two media. However, as soon as new material undergoes the transition the effective pressure outside becomes greater than the pressure inside as is always the case for a deflagration front.

In the calculation, a small temperature pertubation ΔT is introduced between the two phases such as to have a positive pertubation in the quark phase where material is compressed and a negative one inside the bubble where the medium is expanding. With these perturbed initial conditions we want to reproduce the state of the system after the interface has already started to move. Because we do not expect an explosive initial growth (and this is confirmed by the numerical computations) it is possible, as a first approximation, to think of the evolution from the nucleation state to the perturbed state as a succession of equilibrium states. Of course, this assumption is not completely correct, but we can demonstrate that it corresponds, in equation (5.21), to neglecting the interface acceleration and the second

order term in $(\Delta T/T_n)$. The first of these omissions is probably the more doubtful one but, in any case, the stability properties of the computer code ensure that the solution always relaxes towards the correct one as long as the initial conditions are roughly reasonable and as long as the initial temperature pertubation is not too large $\left[\Delta T/T_n \leq 0.1(T_c-T_n)/T_n \right]$.

Let $\Delta T_+=(T_+-T_n)$ and $\Delta T_-= (\Delta T_+ - \Delta T)$ be the temperature perturbations ahead of and behind the interface. There is then a corresponding variation in R_s equal to

$$\Delta R_s = - \frac{2\sigma}{(p_h-p_q)^2} (\Delta p_- - \Delta p_+) \tag{5.33}$$

Δp_+ and Δp_- can easily be obtained from the known equation of state in each phase.

At first order in ΔT, the rate equation (5.21) reduces to

$$\dot{\mu}_s = 4\pi R_s^2 \alpha \, (e_h/w_q) \, (\Delta T/T_n) \tag{5.34}$$

while the junction condition (5.27) gives

$$u_+ - u_- = (b_- - b_+) \, \dot{\mu}_s \tag{5.35}$$

where we have put $\Gamma_+, \Gamma_- = 1$ and $a_+, a_- = 1$ since the deviations from those values are of second order in $(\Delta T/T_n)$.

Sufficiently far from the bubble, the medium has not yet been affected by the transition and it can still be considered as being at a temperature of approximately T_n and expanding according to the relation for a FRW universe in the quark phase. Here we have implicitly assumed that the time interval necessary for producing the temperature difference ΔT is much smaller than the Hubble time $t_H = H^{-1}$. Material is reheated and accelerated at the transition front from which outgoing compression waves are propagated, but on

the other hand, since the medium sufficiently far from the bubble is unperturbed and homogeneous there should be no incoming waves. This can be convenientely expressed in erms of characteristics. As discussed in chapter III, the hyperbolic system of fluid equations may be written in the characteristic form

$$l_i \frac{\partial Z}{\partial t} + \lambda_i l_i \frac{\partial Z}{\partial \mu} + l_i C = 0 \tag{5.36}$$

and Hedstrom (1979) has proved that when such a system is homogeneous (C=0) the condition for a pure outgoing flow is

$$l_i \frac{\partial Z}{\partial \mu} = 0 \tag{5.37}$$

for each incoming characteristic curve $\lambda_i = d\mu/dt$. However $C \neq 0$ in the present case. Thompson (1987) attempted to extend Hedstrom's result to inhomogeneous systems and his argument proceeds as follows. If it is possible to define a function V such that

$$dV_i = l_i dZ + l_i C dt \tag{5.38}$$

then the system (5.36) becomes

$$\frac{\partial V_i}{\partial t} + \lambda_i \frac{\partial V_i}{\partial \mu} = 0 \tag{5.39}$$

which is a set of wave equations for waves with characteristic velocities λ_i. Each wave amplitude V_i is constant along the curve C_i, in the μt plane, defined by $d\mu/dt = \lambda_i$. The condition that there are no incoming waves is then expressed by

$$\frac{\partial V_i}{\partial t} = 0 \tag{5.40}$$

or

$$l_i \frac{\partial Z}{\partial t} + l_i C = 0 \tag{5.41}$$

for disturbances along the incoming characteristic curves. The problem with this argument is that in general it is not possible to make the definition (5.38) except in the trivial cases where either A and C are constant everywhere or, alternatively, there are no more than two differentials appearing on the right hand side of (5.38). Failing this, the coefficients in (5.38) would have to satisfy Pfaff's condition for the integrability of differential forms in order for the function V to exist but this condition is not met for the fluid equations (see Whitham (1974)). However this fact did not deter Thompson from applying the prescription (5.41) to non-homogeneous systems and, despite the lack of mathematical rigor, it turns out to be surprisingly successful in obtaining the desired objective. We have therefore used it in the absence of anything better, but note that further mathematical investigation would be desirable.

Applying conditions (5.41) to the backward characteristic (see equation (3.50)) we obtain the following relationship between the spatial derivatives of u and e

$$u_\mu = \frac{\Gamma c_s}{\rho w} e_\mu \tag{5.42}$$

When we introduce the initial perturbation we impose condition (5.42) throughout the whole quark phase.

The velocity field is determined on the basis of the following considerations. For small perturbations, the quark medium remains almost incompressible. From equation (5.9) which can be written as

$$\frac{\rho_t}{\rho} = - \frac{a}{R^2} \frac{d}{dR}(uR^2) \tag{5.43}$$

we see that $\rho_t \simeq 0$ corresponds to a solenoidal velocity field

$$uR^2 = \text{constant} = u_+ R_s^2 \tag{5.44}$$

Differentiating equation (5.44) with respect to μ and combining it with (5.42) we obtain

$$\frac{e_\mu}{(e+p)} = - \frac{2u_+ R_s^2 R_\mu}{\Gamma c_s R^3} \tag{5.45}$$

Equation (5.39) can be integrated between R_s and $R \gg R_s$. At the first order in $\Delta T_+/T_n$ we obtain a relation between e and u (taking $\Gamma \simeq 1$):

$$e - e_q = \frac{e_q + p_q}{c_s} u_+ \left(\frac{R_s}{R} \right)^2 \tag{5.46}$$

At first order in $(\Delta T/T)$ the ρ equation (5.2) becomes

$$\rho = \rho_q \left(1 + \frac{e - e_q}{e_q + p_q} \right) \tag{5.47}$$

By substituing equation (5.46) into equation (5.47) one gets

$$\rho = \rho_q \left[1 + \frac{u_+}{c_s} \left(\frac{R_s}{R} \right)^2 \right] \tag{5.48}$$

which shows that the assumption of a solenoidal velocity field is approximately correct as long as the fluid Mach number is small, $(u_+/c_s) \ll 1$.

Relations (5.46) and (5.47) are used both just ahead of the interface and throughout the quark phase. Finally the metric function a is computed by equation (5.16).

Inside the bubble the temperature is assumed constant and this is justified by the fact that the small bubble dimensions allow rapid thermalization of the hadron phase. The advective characteristic is used to calculate ρ everywhere except just behind the interface (i.e. an expression is used which is similar to equation (5.47) but with e_q and p_q being replaced by e_h and

p_h). However, ρ_- is calculated by using the junction conditions since this refers to material transformed into the new phase after nucleation. We know that the phase transformation is not an adiabatic process and therefore we have to take into account entropy production mechanisms.

The relation between a_+ and a_- is obtained by combining equations (5.12) and (5.13) to give

$$x^2 - 1 = \frac{b_+^{2\cdot 2}\mu_s^2}{a_+^2}\left(\frac{1}{\eta^2 x^2} - 1\right) \tag{5.49}$$

where $x=a_-/a_+$ and $\eta = (e_-+p_-)/(e_++p_+)$. For $(\Delta T/T_n) \ll 1$ we can approximate equation (5.49) by

$$a_- = a_+\left[1+ \frac{1}{2} b_+^{2\cdot 2}\mu_s^2(\eta^{-2}-1)\right] \tag{5.50}$$

and then ρ_- is given by

$$\rho_- = \rho_+ x\ \eta \tag{5.51}$$

The values used for u inside the bubble are found by linear interpolation in μ between the centre, where the fluid is at rest, and the interface where it moves with velocity u_-.

Γ is computed everywhere by the approximate expression

$$\Gamma = 1 + \frac{1}{2} u^2 \tag{5.52}$$

and m and R are given by equation (5.5) and (5.6) respectively with the boundary conditions

$$\begin{aligned} m &= 0 \qquad R = 0 \qquad \text{at the centre} \\ m^+ &= m^- + 4\pi R_s^2\sigma \qquad \text{at the interface} \end{aligned} \tag{5.53}$$

In summary, once we have chosen the initial temperature

pertubations ΔT_+ and ΔT_- at the interface and calculated the corresponding value for the energy density and the pressure in the two phases we can compute ΔR_s and $\dot{\mu}_s$ by (5.33) and (5.34) respectively. Then we compute ρ_+ by (5.47), a_+ by (5.16), the a ratio by (5.50), u_+ by (5.46) and u_- by (5.35). The specification of the state of the hadron phase is then completed by using the hypothesis of constant temperature and the interpolation in the velocity field. $\Delta\mu$ is fixed in such a way that the interface coincides with a zone boundary. Next m_+ is calculated from (5.53) and then the set of equations (5.44), (5.45), (5.47), (5.52), (5.5) and (5.16) provide the complete description of the quark phase.

The approximations made in specifying the initial conditions are such that the code needs some time for relaxing the system to a fully consistent solution. For this reason it is important to introduce only a small perturbation so that the relaxation phenomena occur well before the interface motion starts to become relativistic.

5.3 Numerical integration scheme.

5.3.1 *General considerations.*

The method used for integrating the hydrodynamical equations in the two bulk phases is a standard explicit two-step finite-difference scheme (Potter (1973), Richtmyer and Morton (1967), May and White (1968)) which we have modified in the zones near the interface for implementing the solution of the junction conditions. The time and space centring of the various quantities

is the following:

i) The quantities e, p, ρ, w and Γ are calculated at the full time step and at mid zones.

ii) R and the mass function m are calculated at the full time step and zone boundaries.

iii) The metric function a is calculated at the full time step and both at the zone boundaries and at the mid zones.

iv) The fluid velocity u is calculated at the half time step and at the zone boundaries.

v) The artificial viscosity is calculated at the half time step and mid zones.

Temporary auxiliary values of the various quantities necessary for correctly centring the equations are obtained by extrapolation or interpolation. However the choice of points for calculating the different variables is such as to limit the necessity of auxiliary steps. Figure 2 shows which lattice points are used in the time integration of mid-zone quantities (straight line) and of the velocity (dashed line).

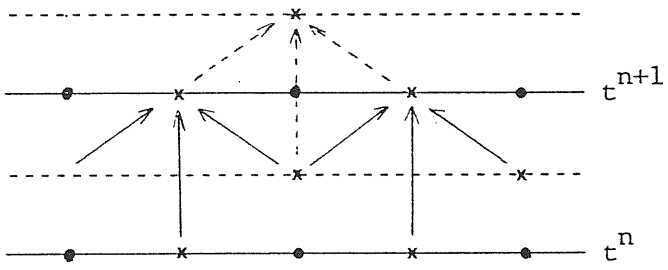

Fig. 2. Two step finite difference scheme.

The time step Δt is adjusted after each cycle so that it satisfies the relativistic generalization of the Courant condition

for numerical stability:

$$\Delta t = k\Delta\mu/4\pi R^2 \rho a c_s \qquad (5.54)$$

where k is a number less than 1 (for which we take the value 0.2). The time step is further limited so that changes in e and ρ are restricted to 2% per cycle. This condition may be relaxed to 10% per cycle if a strong shock is present.

Note that for a deflagration front, which moves subsonically relative to the medium ahead, the Courant condition prevents the interface from crossing more than one zone in a cycle. Actually, by fixing k=0.2, the discontinuity moves forward by less than one fifth of a zone per cycle and this is important for the way in which we perform the solution.

At the centre the boundary conditions are:

$$R=0 \qquad u=0 \qquad m=0 \qquad (5.55)$$

The outer boundary conditions (at $j=j_G$) are discussed in the next section together with the zone adding procedure.

The integration of the set of hydrodynamical equations plus junction conditions proceeds in the following way:

a) R, e and ρ are evolved in each phase; in the hadron phase these quantities are evaluated from the centre (μ=0) up to the grid point (j_s-1) and in the quark phase from the grid point (j_s+1) up to the outer boundary of the grid.

b) The m equation is integrated only up to (j_s-1) in the hadron phase since for completing the calculation in the quark phase we need to solve the interface equations.

c) The a equation is integrated only in the quark phase since its

boundary condition is at ∞ and we need, as for m, to solve the interface equations before completing its calculation on the time slice.

d) Then we solve the interface equations, calculating the interface position and velocity, R_s, and the values of e, p, ρ, u and Γ immediately on either side.

e) Values of quantities at intermidiate points are found by interpolation.

f) Next we complete the integration for a (in the hadron phase) and for m (in the quark phase).

e) The velocity is calculated at the next time level.

f) Finally the time step is set for the next time cycle.

5.3.2 *Boundary conditions and regridding procedure.*

The choice of uniform zoning, made for reducing truncation errors, has as a major consequence the necessity of dealing with time varying boundary conditions. The zone width is set in order to have a satisfactory description of the bubble interior while the total number of zones is mainly limited by computational constraints. However, since the Mach number of the interface relative to the medium ahead is very small, at least in the first stages of bubble growth, disturbances moving with the sound speed relative to the fluid are continuously travelling outside the region in which the numerical calculation is performed. As the bubble grows, the grid needs to be extended to a larger region and this requires the adding of new zones at the grid boundary. This procedure cannot continue indefinitely and the region covered by the numerical computation has to be periodically regridded in

order to keep the number of grid points reasonable.

As the system evolves, the conditions near the outer boundary of the grid change and so in order to give suitable boundary conditions one needs to make some extrapolation from the computed values (see Roache (1976)). In particular, one needs to supply boundary values for the metric functionr a and the velocity u. At infinity a is set equal to unity and its value at $j_{G+1/2}$ can then be calculated using the integral expression (5.16) with extrapolated values for e (which also gives p) and ρ. Then the value of a at j_G can be obtained by space averaging the slowly-varying quantity (aw) between $j_{G-1/2}$ and $j_{G+1/2}$. The integral expression (5.16) holds only for a strictly adiabatic motion and therefore it cannot be applied within the grid since an artificial bulk viscosity has been introduced as part of the numerical scheme.

The calculation of the velocity u at the boundary presents a problem because it is not more possible to correctly centre equation (5.9). However, it has been observed that ρ is almost constant in the quark phase and, as previously mentioned, it follows from this that the velocity field is approximately solenoidal (see also Bachelor (1967)). It is then convenient to calculate u at j_G by extrapolating (uR^2) which is a slowly varying quantity. After many experiments with extrapolation techniques, it seems best in this case to make the extrapolation using an exponential least square fit, while the extrapolation of e and ρ is performed by using a linear least squares fit. Direct extrapolation suffers from the disadvantage of tending to amplify small oscillations whereas least squares extrapolation does the reverse. Making numerical least squares fits at each time-step

would be very computationally expensive but fortunately it is possible to make fits analytically (see Press et al. (1986)) and then use these to derive very simple extrapolation formulae. Fitting a linear function to the last four computed points within the grid gives the formula

$$y_{JG} = \frac{1}{2}\left(2y_{JG-1}+y_{JG-2}-y_{JG-4}\right) \tag{5.55}$$

while fitting an exponentional gives

$$y_{JG} = 2y_{JG-1}\left(\frac{y_{JG-2}}{y_{JG-4}}\right)^{1/2} \tag{5.56}$$

The exponential has the advantage for some applications of giving a negative but increasing gradient without the danger of introducing a minimum.

The method used for assigning values to new zones as they are added, closely follows that for the calculation of a and u at the boundary. The quantities e, ρ and Γ are extrapolated using a linear least squares fit, a , R and m are calculated using equations (5.16), (5.6) and (5.5) and u is obtained by exponential least squares extrapolation of uR^2.

At present, the computation is started with 75 grid zones, five of which are contained within the hadron bubble. When the interface has crossed 10 zones the regridding procedure is applied with a grid expansion factor equal to three, (i.e. the width of a new zone is three times the previous width - see Figure 3). Then, as the bubble expands further a new zone is added at the outer grid boundary each time the interface crosses one fifth of a zone. When the total number of zones is again equal to 75, the regridding is repeated. For avoiding instabilities due to an over-rapid variation of the time step following regridding, an

extra condition is imposed in setting the time step which limits its variation to a maximum of 20% in any cycle.

The criterion used for specifying the various quantities on the new grid is the following :

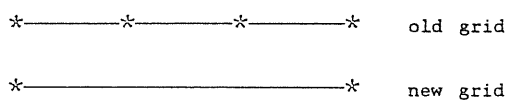

Fig. 3. Regridding

(i) quantities defined at the grid points (such as a, R, m, u) are set equal to the value at the corresponding grid point of the old grid;

(ii) quantities defined in the mid zones are then specified consistently with the constraint equations (5.4)-(5.6).

5.3.3 *Results and discussion.*

There are many experiments which it would be nice to make with the code and also a number of ways in which it could be extended. These things will be the subject of future work. However, the results that have been obtained so far, already show some very interesting consequences.

Figures 4 and 5 show results for a nucleation temperature $T_n=0.98T_c$ with two different values of the accommodation coefficient, $\alpha=1$ and $\alpha=0.6$ respectively. The quantities plotted in each case are the radial component u of the fluid four-velocity, the energy density e and the compression factor ρ. The fm is used here as the fundamental unit. The curve labelled with 0 shows initial values and the other curves show results at

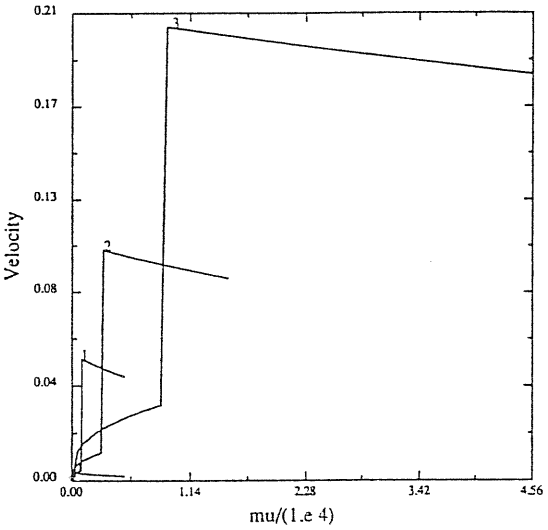

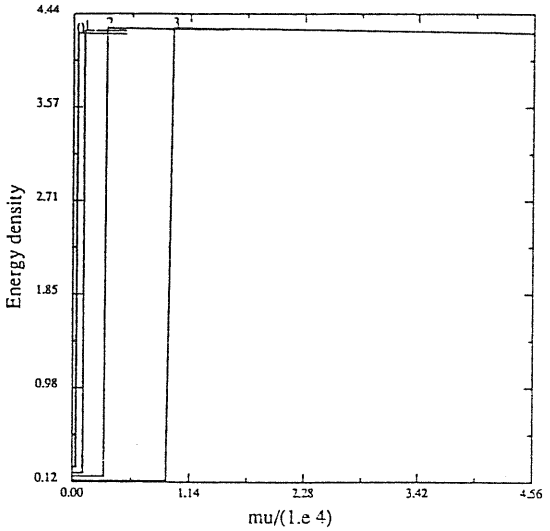

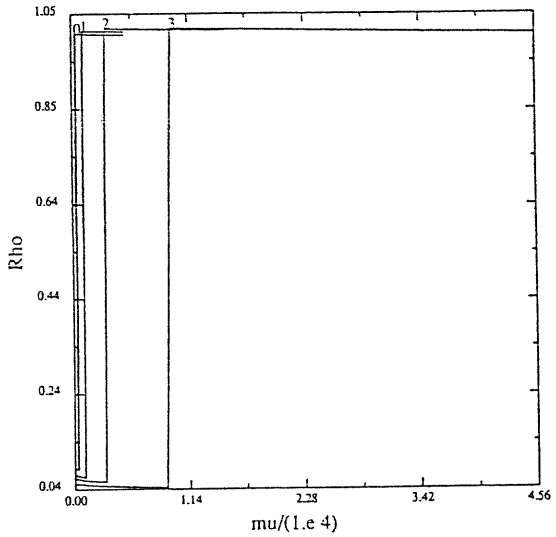

Fig. 4. Plots of the velocity u, energy density e and compression factor ρ against the Lagrangian coordinate μ. The value of α is set equal to one. All of the quantities are measured using the fm as the fundamental unit.

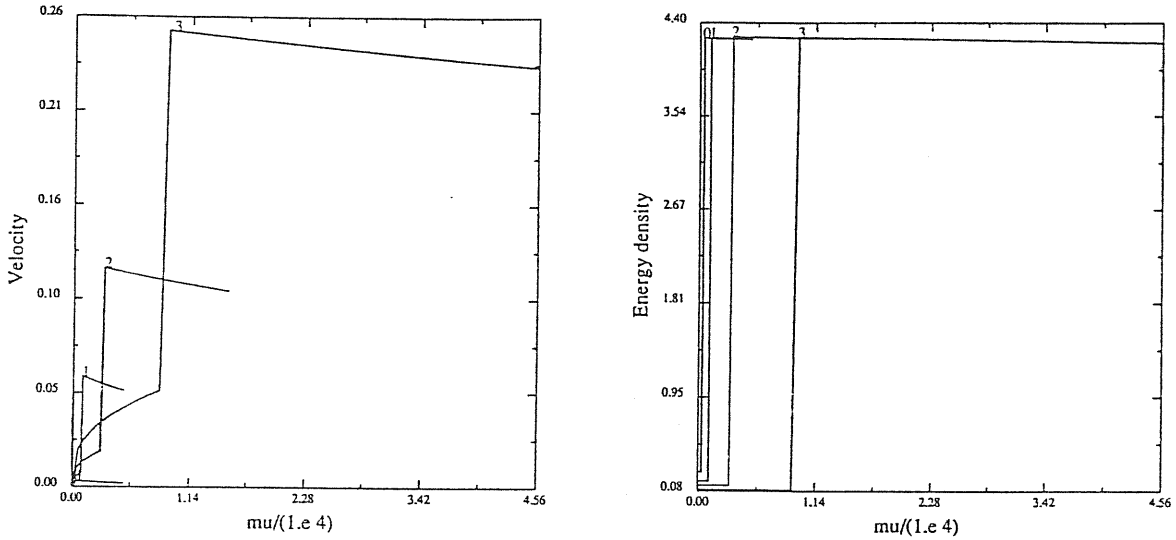

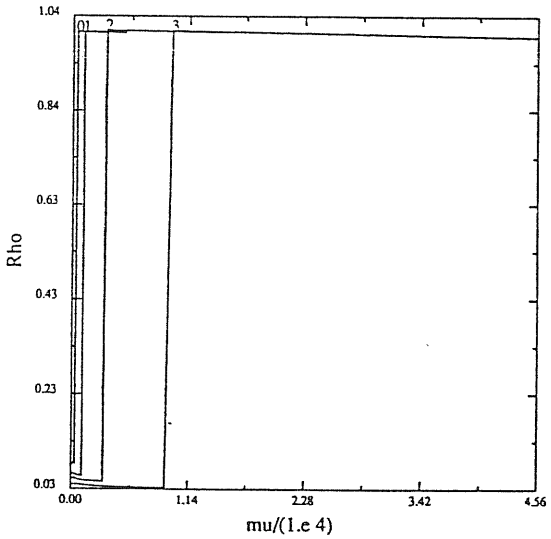

Fig. 5. As in Figure 4 with α equal to 0.6.

Table 1

$\alpha = 1$

curve label	0	1	2	3
t	0.00	1.75×10^{2}	2.75×10^{2}	3.61×10^{2}
R_s	9.98	14.42	23.42	36.50
T_+/T_c	0.982	0.984	0.985	0.986
T_-/T_c	0.980	0.924	0.888	0.833
u_+	3.46×10^{-3}	5.43×10^{-2}	1.04×10^{-1}	2.06×10^{-1}
u_-	2.09×10^{-3}	4.55×10^{-2}	1.25×10^{-2}	3.45×10^{-2}
M	2.09×10^{-4}	5.82×10^{-3}	8.98×10^{-3}	1.29×10^{-2}

Table 2

$\alpha = 0.6$

curve label	0	1	2	3
t	0.00	1.84×10^{2}	2.85×10^{2}	3.72×10^{2}
R_s	9.98	16.17	25.29	40.94
T_+/T_c	0.982	0.982	0.983	0.983
T_-/T_c	0.980	0.887	0.833	0.758
u_+	3.46×10^{-3}	6.08×10^{-2}	1.21×10^{-1}	2.52×10^{-1}
u_-	2.64×10^{-3}	7.72×10^{-2}	2.01×10^{-2}	5.45×10^{-2}
M	1.25×10^{-4}	5.26×10^{-3}	7.64×10^{-3}	1.02×10^{-2}

successive regriddings up to the third.

Let us first examine the curves for the energy density and the compression factor. It can be seen that in the quark phase the values of these quantities change only slightly as the system evolves and that the reheating and compression resulting from the phase transformation are less than 1%. Inside the bubble, the consequences of the transition are more evident and the decrease in temperature in the hadron phase is greater than 10% during the interval considered. This was, in a certain sense, already anticipated by the relation between the temperatures in the two phases found for a plane deflagration front (see Section 4.3), although some care is required in comparing the results obtained in the two cases particularly as those in the spherical case refer to a period in which the effect of surface tension is important. Surface forces act in the direction of increasing the effective pressure pushing inwards on the interior of the bubble which mimics the effect of a higher temperature in the quark phase.

The bulk velocity is increased by two orders of magnitude in the quark phase and by more than one order of magnitude in the hadron phase. It is important to notice that, in disagreement with some previous literature (Gyulassy et al. (1984), Kurki-Suonio (1985), etc.), there is no evidence of shock formation ahead of the deflagration front. Two factors which may contribute to this are the geometrical ($1/R^2$) fall-off factor and the very relativistic sound speed. Another point on which these results are in disagreement with assumptions in the previous literature concerns the velocity field inside the bubble. We have already mentioned that the extra condition required for a deflagration solution has sometimes been fixed by taking the

hadronic medium to be at rest inside the bubble. Here, we can see that the medium inside is, in fact, expanding. Its velocity is lower than that of the fluid ahead of the interface but it is far from vanishing. We can see that most of the latent heat liberated by the transition is going into bulk kinetic energy rather than into thermal energy.

Tables 1 and 2 show comparative results for interface quantities in the two cases. While the effects of changing α are complicatedly non-linear, they may be understood as follows. A lower value for α implies that, for a given temperature difference, there is a lower energy flux. The smaller energy flux tends to give a lower temperature inside the bubble which produces a bigger temperature difference between the phases leading, in turn, to an increased energy flux. The self-consistent balance of these effects produces greater cooling of the hadron medium and higher expansion velocities although the Mach number (M) is reduced.

Two particularly important points for further work will be the extension of the present computation to include long-range radiative processes and enlargement of the region covered by the computational grid. Although the effect of electromagnetic and weak interactions does not influence bubble dynamics significantly at the present stage of the computation, it will no longer be possible to neglect electromagnetically interacting particles when the bubble radius has grown to order 10^3 fm. Neutrino transport, however, becomes significantly only at much larger distances. Although the characteristic method is related to the hyperbolic nature of the equations, it is nevertheless possible to extend it to cases including radiation and viscosity.

Enlarging the region covered by the grid would provide interesting information on how the large scale bulk motion produced by the transition process influences the medium between expanding bubbles. In particular, it should be possible to say whether the occurrence of a shock ahead of the deflagration front can be completely ruled out. It has been expected that any shock would initially form near to the bubble surface and therefore would be seen in the present computation but this could be wrong. Another reason for wanting to move the outer grid boundary far from the bubble surface is to improve the problems connected with having time varying boundary conditions.

For making the enlargement, it is not a good idea simply to add further zones of equal width to the present grid because it would not be possible to increase the region covered very much in this way without prohibitive computational expense. One possibility would be to add zones of exponentially increasing width in to the edge of the present uniform grid in such a way that the join was made smoothly. If each successive new zone were 20% wider than the previous one and 75 new zones were added to the edge of uniform grid also of 75 zones, the region covered would be increased by a factor of 5.8×10^{4}. A drawback of this method is that truncation errors are increased by using a variable mesh size but since the flow is expected to be quite smooth far from the bubble, this may not be a serious difficulty. An alternative would be to use $\log \mu$ as the independent variable and then to have a mesh uniform in this new coordinate. It will be necessary to experiment in order to find the best solution.

CHAPTER VI

THE ROLE OF NEUTRINO CONDUCTION DURING THE TRANSITION

In the previous chapter the hydrodynamics of the quark-hadron transition was studied neglecting thermal conduction and dissipative mechanisms. . However, in addition to strongly interacting matter there are also photons and light leptons (ν_e, ν_μ, ν_τ, $e^{\pm}$, $\mu^{\pm}$) present in each phase and they could play an important rôle in determining how the transition proceeds. Electromagnetic interactions can thermalise the strongly interacting particles with the photons and charged leptons on scales greater then 10^3 fm which is larger than the strong interaction length scale but much smaller than the mean-free-path for neutrinos which only interact weakly with the other particles ($\lambda_\nu \sim 1\text{cm}(140/T_c)^5$). For bubbles having radii large compared with 10^3 fm the strong and electromagnetically interacting components can be taken to behave as a fluid with the neutrinos providing a longer range heat conduction mechanism.

If neutrino conduction were to dominate over hydrodynamical flow, this could cause a concentration of baryon number within shrinking quark regions at the end of the transition, as first pointed out by Witten (1984). Both neutrino conduction and hydrodynamical flow carry energy out of the quark phase but baryon number can only be carried along with the hydrodynamical flow.

In a subsequent paper, Applegate and Hogan (1985) presented a more detailed analysis of flow across a phase interface and

reached the conclusion that if the temperature difference between the two phases (ΔT) remains small then the ratio of the neutrino energy flux (F_ν) to the hydrodynamical energy flux (F_H) is proportional to $(\Delta T/T_c)^{1/2}$. It follows that the hydrodynamic flux would then dominate unless either ΔT became large or the hydrodynamical flow were strongly suppressed for some reason. The second possibility (which they considered unlikely) corresponds to the transition having a very small accommodation coefficient α (see section 4.3.1). Using F_ν/F_H as a parameter, they then gave a detailed discussion of baryon concentration. However their analysis was based on fixing the temperature of the quark phase equal to T_c as the extra condition needed for a deflagration solution.

The plan in this chapter is to discuss the relative importance of hydrodynamic and neutrino flow and to present a revised analysis of baryon concentration at the transition. Then we present an analysis of how the transition would have proceeded on a large scale if the hydrodynamical flow was strongly supressed and the evolution of the transition was controlled by neutrino conduction.

6.1 Neutrino flow and baryon concentration.

6.1.1 *Ratio between the energy fluxes of hydrodynamical flow and neutrino flow.*

In Chapters III and V, only hydrodynamical flow was considered in the evolution equations for the bubble growth. Particles having a long mean-free-path provide an energy conduction mechanism and act in the sense of tending to smooth

discontinuities (see Mihalas and Mihalas (1984)). However, the underlying structure of the solution is not expected to be greatly changed and, in particular, it continues to be necessary to supply an additional expression for F_H as long as the transition front remains subsonic. We have already suggested in Section 4.3 that for a deflagration, in which the development of the hydrodynamical flow is regulated by the details of the transformation process, it is a reasonable approximation to set the hydrodynamical energy flux equal to the corrected net themal flux:

$$F_H = \frac{1}{4} \alpha \, g_h \left(\frac{\pi^2}{30}\right) \left(T_q^4 - T_h^4 \right) \qquad (6.1)$$

Some care is needed over specification of the factor g_h which represents the total number of degrees of freedom for particles which are in thermal equilibrium in the hadron phase within the length scale under consideration. In the first stages of growth of a bubble when its radius is much smaller than the electromagnetic interaction length scale λ_{em}, the fluid equations refer only to the strongly interacting components. However, when the bubble size is much greater than λ_{em}, we can consider charged leptons and photons as being in thermal equilibrium with strongly interacting matter and in this case g_h in equation (6.1) refers to the total degeneracy number for the strongly and electromagnetically interacting particles. The interval in which $r \sim \lambda_{em}$ requires some care, but we can reasonably expect that the effect of charged leptons and photons is of slowing down the interface velocity and smoothing out structures formed in the previous evolution.

In this chapter we will consider the epoch in which neutrino transport is also important, namely for $r \geq \lambda_\nu$. At this stage the fluid description is appropriate for all particles except

neutrinos since $\lambda_\nu \gg \lambda_{em}$.

A temperature difference ΔT between the two phases causes an energy flux carried by neutrinos given by :

$$F_\nu = \frac{1}{4} g_\nu \left(\frac{\pi^2}{30}\right) \left(T_q^4 - T_h^4 \right) \qquad (6.2)$$

where g_ν is the degeneracy factor for neutrinos. In this case T_q and T_h have to be thought of as mean temperatures in each phase over a distance of the order of the neutrino mean-free-path. If each phase is at roughly uniform temperature then the ratio between the neutrino and hydrodynamical energy fluxes is given by:

$$F_\nu/F = g_\nu/(\alpha g_h) \qquad (6.3)$$

and we can see that the remaining temperature dependence is through the α and g_h terms. In g_h the dependence on temperature comes from considering the finite mass of the hadronic particles and the more important finite volume corrections. Both of these effects, but in particular the second one, imply a higher value for F_ν/F_H. The maximum value that α can take is unity which corresponds to a hydrodynamical flux equal to the net thermal flux. Considering only pions in the hadron phase and neglecting mass and volume effects we obtain a rough lower limit for the energy flux ratio of ~ 0.44. Therefore, as long as the bubble radius is larger than the neutrino mean-free-path, neutrino flow and hydrodynamical flow are comparable and the first might become the dominant mechanism of energy transfer if the nature of the emission process from the interface determines that α is small. It is interesting to note that this result is in agreement with that suggested by Witten on the basis of a rather conceptual argument but fundamentally disagrees with the subsequent more sophisticated analysis by Applegate and Hogan.

6.1.2 *Change in the entropy per baryon.*

Now we examine how the previous results change the predicted distribution of entropy per baryon S_b in the last part of the transition during the shrinking of disconnected quark bubbles. We consider the scenario in which the transition occurs under conditions of quasi equilibrium between the two phases. In this case baryons are likely to have already been concentrated in the quark phase in the first part of the transition. The condition of chemical equilibrium between the two phases favours baryons staying in the quark phase as there baryon number is carried by almost zero mass particles while, in the hadron phase, it is carried by massive particles (mainly protons and neutrons - Witten (1984), Bonometto et al. (1985)). It seems that about 99% of the total baryon number would be contained within the quark phase at the time when it becomes disconnected. As a quark bubble evaporates and shrinks, it loses both entropy and baryon number and if the entropy per baryon of the remaining material decreases then the remaining baryon number will become progressively more concentrated. We will now analyse the way in which entropy and baryon number leave the bubble, using always quantities in the quark phase unless otherwise stated.

The entropy flux ϕ_s leaving the quark phase, as measured in the rest frame of the interface, is given by

$$\phi_s = \gamma v s \qquad (6.4)$$

where s is here the entropy density; v is the velocity relative to the interface and $\gamma=(1-v^2)^{-1/2}$. If we express ϕ_s in terms of the energy flux, which is

$$F = (e+p)\gamma^2 v \qquad (6.5)$$

we have

$$\phi_s = \frac{s}{\gamma(e+p)} F \tag{6.6}$$

This relation holds both for neutrinos (ν) and for the particle components carried along with the hydrodynamical flow (H).

Analogously, if baryon number is taken to be strictly carried along with the hydrodynamical flow, then the baryon number flux ϕ_b can be expressed in terms of the hydrodynamical energy flux:

$$\phi_b = \frac{b}{\gamma_H (e+p)_H} F_H \tag{6.7}$$

where b is the baryon number density.

The relative variation of the total entropy S within the bubble compared with the relative variation of the total baryon number B contained within the bubble is given by:

$$\frac{B}{S}\frac{dS}{dB} = \frac{b}{s_H+s_\nu} \frac{(\phi_s)_H+(\phi_s)_\nu}{b} \tag{6.8}$$

Therefore the variation of the entropy per baryon S_b (=S/B) with respect to the fraction N (=B/B_o) of the initial baryon number B_o which is still contained within the contracting bubble is given by

$$\frac{d\ \ln S_b}{d\ \ln N} = \frac{B}{S}\frac{dS}{dB} - 1$$

$$= \frac{s_\nu}{s_H+s_\nu} \left[\frac{\gamma_H (e+p)_H}{\gamma_\nu (e+p)_\nu} \frac{F_\nu}{F_H} - 1 \right] \tag{6.9}$$

This expression does not reduce to the one given by Applegate and Hogan. From equation (6.9) we can immediately see that there would be no baryon concentration if

$$\frac{F_\nu}{F_q} = \frac{\gamma_\nu (e+p)_\nu}{\gamma_q (e+p)_q} \tag{6.10}$$

Neglecting deviations of the γ-factors away from unity, taking the

neutrino temperature equal to that of the quark fluid and using the bag model equation of state and expression (6.3) for the flux ratio, equation (6.4) can be rewritten as

$$\frac{d\ \ln S_b}{d_q \ln N} = \frac{g_\nu}{g_q + g_\nu}\left[\frac{1}{\alpha}\ \frac{g_q}{g_h}\ - 1\right] \tag{6.11}$$

Since $g_q > g_h$ and $\alpha \leq 1$, it follows that some baryon concentration is a generic feature of the transition according to this picture, with the concentration becoming greater as α is reduced. As an example, if we consider two cases of shrinking bubbles with $\alpha=1$ and $\alpha=10^{-1}$ and choose as initial entropy per baryon $S_i=10^{10}$; for the final remaining 10% of the material, S_b is reduced by factors of two and 10^4 respectively. The temperature differences between the two phases do not influence these results and the only further condition which we have introduced is that r remains greater than λ_ν up to the end point of the calculation. We can also notice that the inclusion of a finite volume correction in the equation of state for the hadrons acts in the same direction as smaller α values.

While the reductions in S_b suggested here are not as large as some which have been claimed in the literature, they might nevertheless have some interesting consequences. Also, the picture used here is a very simple one and a more sophisticated treatment of phase transformation at the interface might perhaps lead to greater reductions.

6.2 Progress of the transition if neutrino flow is dominant.

6.2.1 *Basic equations*

We consider here the picture in which the hydrodynamical flux is negligible ($\alpha \to 0$) and the energy flux between the two phases is dominated by neutrino conduction (Bonometto and Pantano (1987)). All components apart from the neutrinos are taken to be in thermal equilibrium within their respective phases. This analysis does not apply to the initial stages of the transition when surface tension is important or to the final stages where surface tension is again important and the effect of baryon concentration needs to be included in the equation of state. If the average distance between the bubble "centres" δ is much smaller than λ_ν, it is a fair approximation to assume a homogeneous distribution of neutrinos described in terms of a constant temperature T_ν.

In the case in which there is no hydrodynamical flux across the interface we have from equation (4.19)

$$p_q(T_q) = p_h(T_h) \tag{6.12}$$

At temperatures below T_c, this implies $T_q > T_h$. Radiative effects, such as neutrino conduction, tend to eliminate the difference in temperature; however, this causes a higher pressure in the hadron phase which tends to make it expand producing again $T_q > T_h$. The two phases could coexist in thermal and mechanical equilibrium only for $T_q = T_h = T_c$ but the general expansion of the universe acts in the direction of decreasing the temperature and perturbing this equilibrium.

We want to calculate the time dependence of the scale factor (a), the fraction of the total volume occupied by the quark phase (y) and the temperatures T_q, T_h and T_ν. We will denote by V_q, V_h

and V_ν the volumes occupied by the various components within a given large volume V_{tot} (the subscripts q and h refer, as usual, to the components in thermal equilibrium within the quark and hadron phases while ν refers to neutrinos). Clearly $V_\nu = V_{tot}$. Provided that the initial bubble nucleation is such that $\delta \ll t_H$, and that local motions are negligible, we can define a mean energy density $\bar{e}$ over scales large compared with δ

$$\bar{e} = e_h(T_h)(V_h/V_{tot}) + e_q(T_q)(V_q/V_{tot}) + e_\nu(T_\nu) \tag{6.13}$$

and an *averaged* scale factor a can be calculated from the Friedmann equation

$$\left(\frac{\dot{a}}{a}\right)^2 = \frac{8\pi G}{3}\bar{e} \tag{6.14}$$

The conservation of energy is expressed by

$$a^3 \frac{d}{dt}\bar{e} = (\bar{e}+p)\frac{d}{dt}a^3 \tag{6.15}$$

where p $(=p_{q(h)}+p_\nu$ in the quark(hadron) phase) is constant everywhere because of the condition (6.12). Equation (6.15) is equivalent to

$$\sum_{i=h,q,\nu}\left[(e_i+p_i)\frac{d}{dt}V_i + V_i\frac{d}{dt}e_i\right] = 0 \tag{6.16}$$

Assuming that neutrino conduction is the only mechanism for entropy transfer, the energy balance in each phase is given by

$$\dot{e}_q + (e_q+p_q)\frac{\dot{V}_q}{V_q} = -(T_q-T_\nu)N_q \tag{6.17}$$

$$\dot{e}_h + (e_h+p_h)\frac{\dot{V}_h}{V_h} = -(T_h-T_\nu)N_h \tag{6.18}$$

where the dot indicates a time derivative and

$$N_{q,h} = f_{q,h}G_w^2(4/3)e_\nu(e_{q,\nu}+p_{q,h}) \tag{6.19}$$

is the average number of ν-collisions per unit volume and time in the quark and hadron regions. The factors $f_{q,h} \simeq 1$ take account of the different relations between energy density and number density in the two phases and of the fact that the average energy transfer per collision is not simply given by the temperature difference. G_W^2 ($=1.3\times10^{-22}\text{MeV}^{-4}$) is the weak interaction constant.

6.2.2. *Expansion law and temperature behaviour.*

The large scale behaviour of the transition is then calculated by solving the system of equations (6.12), (6.15), (6.16)-(6.18). It is convenient to introduce the quantities $E=eT^{-4}$ and $\phi=pT^{-4}$. For the hadron phase the equation of state used is

$$E_h = 3\phi_h = \left(\frac{\pi^2}{30}\right)\left(g_r + 3f_{rid}\right) \tag{6.20}$$

where g_r is the degeneracy factor for the photons and charged leptons, which are in equilibrium with each phase, and $3f_{rid}$ is the effective number of degrees of freedom for the strongly interacting component. The degeneracy factor for pions is equal to 3 and f_{rid} (set equal to 0.1 here) takes account of finite mass and volume effects. Taking E_h/ϕ_h=constant seems reasonable since photons and charged leptons give the dominant contribution to the e_h and p_h.

For the quark phase we use an equation of state given by

$$\phi_q = \left(\frac{\pi^2}{90}\right) g_r + \left(\frac{\pi^2}{90}\right) g_{(q)}\left[1 - \left(\frac{T_r}{T}\right)^n\right] \tag{6.21}$$

$$E_q = \left(\frac{\pi^2}{30}\right) g_r + \left(\frac{\pi^2}{30}\right) g_{(q)}\left[1 - (n/3 - 1)\left(\frac{T_r}{T}\right)^n\right] \tag{6.22}$$

where $g_{(q)}$ is the degeneracy factor for the quark-gluon component,

n is an adjustable parameter and $T_r = T_c\left(1-3f_{rid}/g_{(q)}\right)$. This equation of state is based on a phenomenological model proposed by Bonometto and Sokolowsky (1985) in order to give a suitable analytic expression for fitting lattice data. The case n=4 corresponds to the bag model with bag constant $(\pi^2/90)g_{(q)}T_c^4$. For these calculations, three quark flavours were included giving $g_{(q)}$ = 47.5. The values of the time and scale factor at the beginning of the transition are denoted by t_1 and a_1 respectively and it is convenient to write the temperatures in terms of their relative variations from T_c as follows

$$\nu = \frac{T_\nu - T_c}{T_c} \qquad q = \frac{T_q - T_c}{T_c} \qquad h = \frac{T_h - T_c}{T_c} \tag{6.23}$$

By using relations (6.20)-(6.23) the Friedmann equation (6.14) can be rewritten as

$$a' = \Gamma a \left\{ E_\nu (1+\nu)^4 + E_h (1+h)^4 + \left[E_q (1+q)^4 - E_h (1+h)^4 \right] y \right\}^{1/2} \tag{6.24}$$

where the prime indicates a derivative with respect to (t/t_1) and Γ is given by

$$\Gamma = (8\pi/3)^{1/2} \, (t_1/t_{pl}) \tag{6.25}$$

where t_{pl} is the Planck time. In order to obtain a differential equation for the volume fraction occupied by the quark phase, we rewrite equation (6.15) in the following way:

$$\dot{y} = y \left[3\,\frac{\dot{a}}{a} + \frac{\dot{e}_q}{e_q + p_q} + G_w^2 (T_q - T_\nu)\, f_q \, \frac{4}{3}\, \rho_\nu \right] \tag{6.26}$$

Changing the independent variable to (t/t_1) and using definitions (6.23) we have

$$\eta y' = 3y \left[\eta \frac{a'}{a} + \eta F(h) \frac{h'}{(1+h)} + (q-\nu) f_q \, \frac{4}{3} \, E_\nu (1+\nu)^4 \right] \tag{6.27}$$

where η is defined by

$$\eta = 3(\lambda_c/t_1)(1/G_w^2 T_c^4) \simeq 3\times10^{-5}(m_\pi/T_c)^5(8.3\times10^{-5}s/t_1) \qquad (6.28)$$

λ_c is the Compton wavelength corresponding to T_c and (using equation (6.12)) F(h) $\left(\propto \frac{q'}{h'}\right)$ is given by

$$F(h) = \frac{1}{3}\frac{de_q}{dp_q}\frac{T_h}{T_q}\frac{T'_q}{T'_h} \qquad (6.29)$$

The differential expression for T_ν is derived by combining equation (6.16) with equations (6.17) and (6.18) giving

$$\dot{e}_\nu = -3(e_\nu+p_\nu)\frac{\dot{a}}{a} + G_w^2(T_q-T_\nu)(e_q+p_q)\frac{4}{3}f_q e_\nu y$$

$$- G_w^2(T_\nu-T_h)(e_h+p_h)\frac{4}{3}f_h e_\nu(1-y) \qquad (6.30)$$

and then, after some manipulations,

$$\eta\nu' = -(1+\nu)\left[\eta\frac{a'}{a} - (1+q)^4 y f_q(E_q+\phi_q)(q-\nu) + \right.$$

$$\left.(1+h)^4(1-y)f_h(E_h+\phi_h)(\nu-h)\right] \qquad (6.31)$$

T_h and T_q are related by equation (6.12) and so we only need a differential equation for one of them. Summing equations (6.17) and (6.18) we get

$$3\frac{\dot{a}}{a} + \left[\frac{de_h}{dp_h}\frac{\dot{T}_h}{T_h}(1-y) + \frac{de_q}{dp_q}\frac{\dot{T}_q}{T_q}y\right] +$$

$$\frac{4}{3}e_\nu G_w^2\left[(T_q-T_\nu)f_q y - (T_\nu-T_q)f_h(1-y)\right] = 0 \qquad (6.32)$$

Expressing $\dot{T}_q$ in terms of $\dot{T}_h$ in this equation, one can obtain, after several steps,

$$\eta h' = -(1+h)\left\{\eta\frac{a'}{a} - \frac{4}{3}E_\nu(1+\nu)^4\left[yf_q(q-\nu) + (1-y)f_h(h-\nu)\right]\right\}/$$

$$\left\{(1-y) + F(h)y\right\} \qquad (6.33)$$

The complete system of differential equations for this problem is then given by equations (6.24) for a, (6.27) for y, (6.31) for ν and (6.33) for h. The quantity q can be calculated by using the pressure balance equation (6.12). An analysis of this set of differential equations shows that it is possible to obtain from it a well-approximated analytical solution in spite of the non-linearity. In fact, from equation (6.33) we see that q, h and ν ought to be of the same order as η (see equation (6.28)) and therefore the left hand side is negligible provided that neither y nor (1-y) are less than η. Then, to lowest order, we have

$$(1-y)f_h(h-\nu) = - yf_q(q-\nu) - \eta(a'/a)/(E_\nu+\phi_\nu) \tag{6.34}$$

On the basis of similar arguments and using equation (6.34), equation (6.31) yields

$$yf_q(q-\nu) = \eta\ (a'/a)B \tag{6.35}$$

with

$$B = \frac{E_h+\phi_h+E_\nu+\phi_\nu}{E_q-E_h} \tag{6.36}$$

Substituing equation (6.35) into (6.27), one obtains a relation between y' and a' which can be integrated giving

$$y = (1+B)\ (a_1/a)^3 - B \tag{6.37}$$

Using expression (6.37) in (6.34), the a equation (6.24) can also be integrated and this gives

$$\left(\frac{a}{a_1}\right)^3 = U\sin^2\left[(6\pi\phi_c)^{1/2}(T_c/m_{pl})\frac{(t-t_1)}{\lambda_c} + \arcsin(U^{-1/2})\right] \tag{6.38}$$

with $U=[1+(E_q+E_\nu)/(\phi_q+\phi_\nu)]$ and ϕ_c being the pressure at the critical temperature T_c. This expression is the same as that for a phase transition taking place exactly at T_c (Bonometto and

Matarrese (1983), Lodenquai and Dixit (1983)).

From equations (6.34), (6.35) and (6.12) one can finally derive expressions for the temperatures which are

$$T_q = T_c\left\{1-4\left[\mu(y)+\pi(y)\right] / \left[E_{c,q}/\phi_{c,q}-3\right]\right\} \tag{6.39}$$

$$T_\nu = T_q - T_c\pi(y) \tag{6.40}$$

$$T_h = T_q - T_c\mu(y) \tag{6.41}$$

where

$$\pi(y) = A(y)\left(E_h+E_\nu+\phi_h+\phi_\nu\right) / \left(f_q y\right) \tag{6.42}$$

$$\mu(y) = A(y)\left(E_q+E_\nu+\phi_q+\phi_\nu\right) / \left[f_h(1-y)\right] \tag{6.43}$$

with

$$A(y) = 8\left(2\pi/3\right)^{1/2}\left(T_c/m_{pl}\right)\left(G_w^2T_c^4\right)^{-1}\frac{\bar{E}^{1/2}(y)}{(E_q-E_h)(E_\nu+\phi_\nu)} \tag{6.44}$$

$$\bar{E} = E_h + E_\nu + (E_q-E_h)\,y \tag{6.45}$$

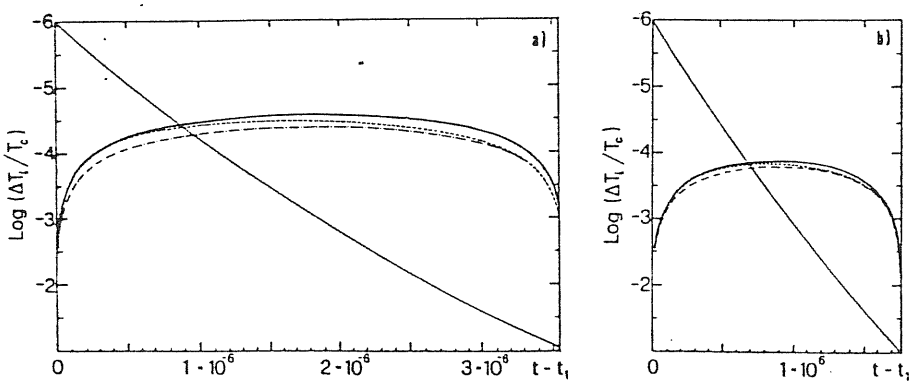

Fig. 1. The temperature behaviour and the quark volume fraction y are plotted. The ordinate scale refers only to the temperatures. Among the three nearby curves, the upper and lower ones refer to the quark and hadron phases respectively while the intermediate one gives the neutrino temperature. The almost diagonal curve, ranging between 1 and 0, gives the time dependence of y. The cases a) and b) refer to quark equations of state with n = 4 and n = 2.7 respectively. T_c = 150 MeV is taken.

The behaviour of the temperatures and of the volume fraction occupied by the the quark phase is shown in Figure 1 for the two cases n=4 and n=2.7. It can be seen that there is only a small amount of supercooling ($\sim 10^{-4}$) during most of the transition if the flux of energy from the quark phase to the hadron phase is due to the long range neutrino transport. Although this result holds only in the absence of a hydrodynamical energy flux, it is nevertheless a further indication that, contrary to the conclusions of Applegate and Hogan, neutrino transport can be important even in the case of small supercooling.

CONCLUSION

In this thesis we have presented results from a detailed study of some aspects of the cosmological quark-hadron transition. As is often the case in astrophysics, this has involved the use of a wide range of ideas and techniques drawn from various branches of physics and mathematics. The transition is particularly interesting becouse its consequences may well affect two of the most important central questions of current work in cosmology: the formation of pregalactic structure and the presence and influence of dark matter. At present there are still considerable uncertainties related to the behaviour of strongly interacting matter during the confinement process but, nevrtheless we think that it is worthwhile to explore the possible consequences of a first order transition with a range of assumptions about the relevant parameters. Much of the previous work in this area has been of a very approximate and conceptual nature and, while this is valuable in the early stages of development of a subject, at some stage more detailed analysis is required. This is particularly true of the hydrodynamical phenomena involved here and, in this thesis, we have tried to lay the basis for such a detailed analysis.

A key point to emerge from this work is that the nature of flow in the neighbourhoud of a deflagration front seems to be different from what has been assumed in most of the previous literature on the transition. Three particularly interesting

consequences have emerged from the present study. Firstly, neutrino flow may be relatively more important than had been supposed, leading to a greater possibility of baryon concentration and subsequent effects on nucleosynthesis. Secondly, most of the energy liberated by the transition seems to go initially into bulk kinetic energy of the quark medium rather than into thermal energy. Contrary to previous statements in the literature, this means that the temperature of the quark medium will not quickly return to T_c after bubble growth has commenced. Thirdly, there is at present no evidence in our calculation for shock formation ahead of the interface as has been widely assumed in the literature. If a shock were to form, this would travel out ahead of the phase interface and the first interaction between neighbouring bubbles would be the meeting of the shocks. This could produce a turbulent medium through which the interface would then propagate more slowly. High velocity bulk motion without shock formation might well cause large hydrodynamical compression of the medium between the bubbles leading to baryon concentration or even formation of compact objects. This needs to be further investigated.

REFERENCES

Alcock,C.R. and Farhi,E., (1986), *Phys. Rev. D* 32,1273.

Alcock,C.R., Fuller,G.M. and Mathews,G.J., (1987), preprint UCRL-95896, *"The quark-hadron phase transition and primordial nucleosynthesis"*.

Applegate,J.H. and Hogan,C.J., (1985), *Phys. Rev. D* 31,3037.

Applegate,J.H. and Hogan,C.J., and Scherrer,R.J., (1987), *Phys. Rev. D* 35,1115.

Banerjee,B., Glendenning,N.K. and Matsui,T., (1983), *Phys. Lett.* 127B,453.

Barz,H.W., Csernai,L.P., Kämpfer,B. and Lukács,B., (1985), *Phys. Rev. D* 32,115.

Batchelor,G. (1967), *An introduction to fluidynamics* (Cambridge University press)

Blaizot,J.P. and Ollitrault,J.Y., (1986), *Nucl. Phys.* A458,745.

Blaizot,J.P. and Ollitrault,J.Y., (1987), Saclay preprint SPhT/87-25 *"The structure of hydrodynamical flows in expanding quark-gluon plasma"*.

Berezin,V.A., Kusmin,V.A. and Thachev,I.I., (1983a), *Phys.Lett.* 120*B*,91.

Berezin,V.A., Kusmin,V.A. and Thachev,I.I., (1983b), *Phys.Lett.* 124*B*,479.

Berezin,V.A., Kusmin,V.A. and Thachev,I.I., (1983c), *Phys.Lett.* 130*B*,23.

Berg,B., Engels,J., Kehl,E., Waltl,B. and Satz,H. (1986), Bielefeld preprint BI-TP 86/05 "Critical behaviour in baryonic matter".

Bertschinger,E., (1985), *Astrophys.J.* 295,1.

Bicknell,G.V. and Henriksen,R.N., (1979), *Astrophys. J.* 232,670.

Blau,S.K., Guendelman,E.I. and Guth,A.H., (1987), *Phys. Rev. D* 35, 1747.

Boesgaard,A.M. and Steigman,G., (1985), *Ann. Rev. Astron. Astrophys.* 23,219.

Bonometto,S.A. (1983), *Il Nuovo Cimento* 74A,325.

Bonometto,S.A., Marchetti,P.A. and Matarrese,S., (1985), *Phys. Lett.* 157*B*,216.

Bonometto,S.A. and Masiero,A., (1986),La *Riv. Nuovo Cimento* 9,1.

Bonometto,S.A. and Matarrese,S., (1983), *Phys. Lett.* 113B,77.

Bonometto,S.A. and Pantano,O., (1984), *Astr. and Astrophys.* 130,43.

Bonometto,S.A. and Pantano O., (1987), *Astron. Astrophys.* 174,L9.

Bonometto,S.A. and Sakellariadou,M., (1984), *Astrophys. J.* 282,370.

Bonometto,S.A. and Sokolowsky,L., (1985), *Phys. Lett.* 107A,210.

Borgs,C. and Seiler,E. (1983), *Nucl. Phys.* B215,125.

Brandenberger,R.H., (1985), *Rev. Mod. Phys.*57,1.

Carr,B.J. and Silk,J., (1983), *Astrophys. J.* 268,1.

Caswell,W.E., (1974), *Phys. Rev. Lett.* 33,244.

Çelik,T., Engels,J. and Satz.H., (1983), *Phys. Lett.* 125B,411.

Çelik,T., Engels,J. and Satz.H., (1985) *Nucl. Phys.* B256,670.

Chodos,A., Jaffe,R.L., Johnson,K., Thorn,C.B. and Weisskopf,V.F., (1974), *Phys. Rev. D* 9,3471.

Christ,N.M. and Terrano,A.E., (1986), *Phys Rev. Lett.* 56,111.

Cleymans,J., Gavai,R.V., and Suhonen,E., (1986a), *Phys. Rep.* 130,217.

Cleymans,J., Nykänen,E. and Suhonen,E., (1986b), *Phys. Rev. D* 33,2585.

Coleman,S., (1977), *Phys. Rev. D*15,2929.

Coleman,S. and De Luccia,F., (1980), *Phys. Rev. D* 21,3305.

Courant,R. and Friedrichs,K.O., (1948), *Supersonic flow and shock waves* (Springer-Verlag).

Crawford,M. and Schramm,D.N., (1982), *Nature* 298,538.

Croxton,C.A., (1980), *Statistical mechanics of liquid surfaces* (Wiley).

Danielewicz,P. and Ruuskanen,P.V., (1987), *Phys. Rev. D* 35, 344.

Danos,M. and Rafelski,J., (1983), *Phys. Rev. D* 27,671.

DeGrand,T. and Kajantie,K., (1984), *Phys. Lett.* 147B,273.

Frautschi,S., (1971), *Phys. Rev. D* 3,2821.

Fucito,F. and Solomon,S., (1985), *Phys. Rev. Lett.* 55,2641.

Fukugita,M. and Ukawa,A., (1986), *Phys.Rev. Lett.* 57,503.

Fukugita,M., Ohta,S., Oyanagi,Y. and Ukawa,A., (1987), Preprint KEK-86-104, *"Numerical evidence for a first order chiral phase transition in lattice QCD with two lattice fermions"*.

Gavai,R.V., Potvin,J. and Sanielevici,S., (1987), Preprint, BNL-39490 and TIFR/TH/87-2, *"Metastabilities in the flavour QCD at*

low quark masses".

Gell-Mann,M., (1962), *Phys. Rev.* 125,1067.

Gibbs,J.W., (1928), *Collected Works*, Vol. 1, Yale University Press.

Gottlieb,S.A., Kuti,J., Toussaint,D., Kennedy,A.D., Meyer,S., Pendleton,B.J. and Sugar,R.L., (1985), *Phys. Rev. Lett.*55,1958.

Gottlieb,S.A., Kuti,J., Toussaint,D., Kennedy,A.D., Meyer,S., Pendleton,B.J. and Sugar,R.L., (1987), preprint, UCSD-IOP10-271, *"The latent heat of pure gluon deconfinement"*.

Guggenheim,E.A., (1959), *Thermodynamics* (North-Holland).

Gunton,J.D., San Miguel,M. and Sahni,P.S. (1983) in *Phase transition and critical phenomena,* Vol.8, ed. Domb,C. and Lebowicz,J.L. (Academic Press).

Gupta,R., Guralnik,G., Kilcup,G.W., Patel.A. and Sharpe,S.R., (1986), *Phys. Rev. Lett.* 57,2621.

Guth,A.H., (1981), *Phys. Rev. D* 23,347.

Guth,A.H. and Weinberg,E.J., (1981), *Phys. Rev. D* 23,876.

Gyulassy,M., Kajantie,K., Kurki-Suonio,H. and McLerran,L., (1984), *Nucl. Phys. B* 237,477.

Hagedorn,R., (1965), *Suppl. Nuovo Cimento* 3,147.

Hagedorn,R., (1983), *Z. Phys. C* 17,265.

Hagedorn,R., (1985), CERN preprint, CERN-TH 4100/85, *"Miscellaneous elementary remarks about the phase transition from a hadron gas to a quark-gluon plasma"*.

Hagedorn,R., and Rafelski,J., (1981), in *Statistical mechanics of quarks and hadrons,* Bielefeld Symposium 1980, Ed. H. Satz (Noth-Holland).

Hawking,S.W., Moss,J.G. and Steward,J.M. (1982), *Phys. Rev. D* 26,2681.

Hedstrom,G.W., (1979), *J. Comput. Phys.* 30,222.

Henshaw,W.D., (1987), *J. Comput. Phys.* 68, 25.

Hetsroni,G., editor, (1982), *Handbook of Multiphase Systems* (McGraw-Hill).

Hogan,C.J. (1983), *Phys. Lett.* 133B,172.

Hoskin,N.E. (1963), in *Methods of Computational Physics* (Academic Press), Vol.3, pag.265.

Hsieh,D.Y. (1965), *J. Basic Eng.* 87,991.

Israel,W., (1966), *Il Nuovo Cimento* 44, 1.

Iso,K., Kodama,H. and Sato,K., (1986), *Phys. Lett.* 169B,337.

Jeffrey,J., (1976), *Quasi-linear hyperbolic systems and waves* (Pitman).

Kajantie,K. and Kurki-Suonio,H., (1986), *Phys. Rev. D* 34,1719.

Kalashnikov,O.K. and Klimov,V.V., (1979), *Phys. Lett.*88B,328.

Kapusta,J.I., (1979), *Nucl.Phys.* A148,461.

Kapusta,J.I., (1981), *Phys. Rev. D* 23,2444.

Kapusta,J.I., (1982), *Nucl. Phys.* B196,1.

Kapusta,J.I. and Olive,K.A., (1982), *Nucl. Phys.* A408,478.

Karsch,F. and Satz,H., (1980), *Phys. Rev. D* 21,1168.

Keller,H.B., Levine,D.A., Whitham,G.B. (1960) *J. Fluid Meth.* 7,302.

Kogut,J., Matsuoka,H., Stone,M., Wyld,H.W., Shenker,S., Shigemitsu,J. and Sinclair,D.K., (1983), *Phys. Rev. Lett.* 51,869.

Kogut,J., Polony,J., Wyld,H.W., Shigemitsu,J. and Sinclair,D.K., (1985), *Nucl. Phys.* B251,311.

Kovacs,E.V., Sinclair,D.K. and Kogut,J.B., (1987), *Phys.Rev. Lett.* 58,751.

Kurki-Suonio,H., (1985), *Nucl. Phys. B*255,231.

Laguna-Castillo,P. and Matzner,R.A. (1986), *Phys. Rev.D* 34,2913.

Lake,K., (1984), *Phys. Rev. D* 29,1861.

Landau,L.D. and Lifshitz,E.M., (1959), *Fluid Mechanics* (Pergamon)

Landau,L.D. and Lifshitz,E.M,. (1980), *Statistical Physics* (Pergamon).

Lichnerowicz,A., (1955), *Théories Relativistic de la Gravitation and de l'Electromagnétisme* (Masson).

Lifshitz,E.M. and Pitaevskii,L.P., (1981), *Physical Kinetics* (Pergamon), pag. 475.

Linde,H.D., (1977), *Phys. Lett.* 70*B*,306.

Lodenquai,J. and Dixit,V., (1983), *Phys. Lett.* 133B,77.

Madsen,J., Heilselberg,H. and Riisager,K., (1986), *Phys. Rev. D* 34, 2947.

Maeda,K., (1986), *GRG* 18,931.

Maeda,K. and Sato,H., (1983), *Prog, Theor. Phys.* 70,772.

Marciano,W. and Pagels,H. (1978), *Phys. Rep.* C36,137.

May,M.M. and White,R.H., (1967), *Methods in Computational Physics* (Academic Press), Vol.7, pag.219.

McKee,C.R. and Colgate,S.A., (1973), *Astrophys. J.* 181,903.

McLerran,L., (1986), *Rev. Mod. Phys.* 58,1021.

Mihalas,D. and Mihalas,B.W., (1984), *"Fondations of radiation*

hydrodynamics", Oxford University Press.

Miller,J.C. and Pantano,O., (1986), in *7th Italian Conference on General Relativity and Gravitational Physics*, eds. U.Bruzzo, R.Cianci and E.Massa (World Scientific), pag 357.

Misner,C.W., (1968), in *Brandeis University Summer Institute in Theoretical Physics*, pag.168.

Montvay,J. and Pietarinen,E. (1982), *Phys. Lett.* 115B,151.

Müller,B., (1985), in *Lecture notes in physics* 225 (Springer-Verlag).

Müller,B. and Eisemberg,J.M., (1985), *Nucl. Phys.* A435,791.

Ostriker,J.P. and Cowie,L.L., (1981), *Astrophys. J.* 243,L127.

Pantano,O. and Miller,J.C., (1986), in *7th Italian Conference on General Relativity and Gravitational Physics*, eds. U.Bruzzo, R.Cianci and E.Massa (World Scientific), pag 411.

Plesset,M.S. and Prosperetti,A., (1977), *Ann. Rev. Fluid Mech.* 9,145.

Plesset,M.S. and Zwick,S.A., (1952) *J. Applied Phys.* 23,95.

Plesset,M.S. and Zwick,S.A., (1954) *J. Applied Phys.* 23,493.

Potter,D., (1973), *Computational Physics* (Wiley).

Press,W.H., Flannery,B.P., Teukovsky,S.A. and Vetterling,W.T. (1986), *Numerical Recipes* (Cambridge Academic Press).

Prosperetti, A., (1982), *Phys. Fluids* 25,409.

Rayleigh,Lord (1917), *Phil. Mag.* 34,95.

Richtmyer,R.D. and Morton,K.W., (1967), *Difference methods for initial-value problems* (Wiley-Interscience).

Roache,P.J. (1976) *Computational fluid dynamics* (Albuquerqe: Hermosa).

Sale,K.E. and Mathews,G.J., (1986), *Astrophys. J.* 309,L1.

Sato,H., (1986), *Prog. of Theor. Phys.* 76,1250.

Seibert,D., (1985), *Phys. Rev. D* 32,2812.

Seibert,D., (1987), *Phys. Rev. D* 35,2013.

Steinhardt,P.J., (1982), *Phys. Rev. D* 25,2074.

Suhonen,E., (1982),*Phys. Lett.* 119B,81.

Svetisky,B., (1986), *Proceedings of the 5th International Conference on Ultra Relativistic Nucleus-Nulceus Collision, "Qark Matter 86"*, Asilomar.

Svetiski,B. and Fucito,F. (1983), *Phys. Lett.*131B,165.

Synge,J.L., (1960), *Relativity, the general theory*, Noth-Holland.

Theofanus,T.G., Biasi,L., Isbin,H.S. and Fauske,H.K., (1969), *Chem. Eng.*

Sc. 24,885.

Thompson,K.W., (1987), *J. Comput. Phys*. 68,1.

Toimela,T., (1985), *Int. J. Theor. Phys*. 24,901.

Touschek,B., (1968), *Il Nuovo Cimento, B* 58, 295.

Toussaint,D., (1987), preprint, UCSD-PTH 87/03, *"Supercomputations in QCD"*.

Van Hove,L., (1983), *Z. Phys. C* 21,93.

Van Hove,L., (1984), CERN preprint, CERN-TH 4055/84, *"Nuclei matter under extreme conditions and the early universe"*.

Van Hove,L., (1986), CERN preprint, CERN-TH 4450/86, *"Prospect for production and detection of quark-gluon plasma"*.

Voloshin,M.B., Kobzarev,I.Yu., and Okun,L.B., (1975), *Sov. J. Phys*. 20,644.

Weinberg,S. (1972), *Gravitation and Cosmology* (Wiley & Sons).

Witham,C.B., (1974), *Linear and non-linear waves* (Wiley).

Witten,E., (1984), *Phys. Rev D* 30,272.

Zel'dovich,Ya.B. and Raiser,Yu.P., (1967), *Physics of shock waves and high temperature hydrodynamics phenomena* (Academic Press).